REPUBLIC OF TÜRKİYE

ALTINBAŞ UNIVERSITY

Institute of Graduate Studies

Electrical and Computer Engineering

MICROSTRIP ANTENNA DESIGN AND FABRICATION FOR SELF POWER MODERN WIRELESS SYSTEM

Hayder Hassan Mohammed AL-KHAYLANI

Doctor of Philosophy

Supervisor

Asst. Prof. Dr. Abdullahi Abdu IBRAHIM

Istanbul, 2022

MICROSTRIP ANTENNA DESIGN AND FABRICATION FOR SELF POWER MODERN WIRELESS SYSTEM

Hayder Hassan Mohammed AL-KHAYLANI

Electrical and Computer Engineering

Doctor of Philosophy

ALTINBAŞ UNIVERSITY

2022

The dissertation titled MICROSTRIP ANTENNA DESIGN AND FABRICATION FOR SELF POWER MODERN WIRELESS SYSTEM prepared by HAYDER HASSAN MOHAMMED AL-KHAYLANI and submitted on 16/12/2022 has been **accepted unanimously** for the degree of PhD in Electrical and Computer Engineering.

_____

Asst. Prof. Dr. Abdullahi Abdu IBRAHIM

the Supervisor

Thesis Defense Committee Members:

Asst. Prof. Dr.Abdullahi Abdu IBRAHIM	Department of Computer Engineering Altınbaş University	_____
Asst. Prof. Dr. Sefer KURNAZ	Department of Computer Engineering Altınbaş University	_____
Asst. Prof. Dr. Ayça KURNAZ TÜRKBEN	Department of Software Engineering Altınbaş University	_____
Asst. Prof. Dr. Serdar KARGIN	Department of Biomedical Engineering Arel University	_____
Assoc. Prof. Dr. Taha ELWI	Department of Communication Engineering Al-Ma'moon University	_____

I hereby declare that this thesis meets all format and submission requirements of a PhD dissertation.

Accepted by Altınbaş University Institute of Graduate Studies on the following date: 17/ 2 /2023

I hereby declare that all information presented in this graduation project has been obtained in full accordance with academic rules and ethical conduct. I also declare all unoriginal materials and conclusions have been cited in the text and all references mentioned in the Reference List have been cited in the text, and vice versa as required by the abovementioned rules and conduct.

Hayder Hassan Mohammed AL-KHAYLANI

Signature

DEDICATION

Firstly, I would like to express my thanks to Allah for letting me able to surpass all difficulties. I would like to acknowledge and give my warmest thanks to my supervisor (Assist. Prof. Dr. Abdullahi A. Ibrahim) to support me along PhD studies. his guidance and advance curried me through all the stages of writing my project. I would like to thank my committee members for letting my defense be an enjoyable moment and for brilliant comments and suggestion.

I express deeply thanks for all Electric and Computer Engineering Department-Altinbas University members for their supporting.

I would like to present a special thanks and appreciation to my Co-advisor (Prof. Dr. Taha A. Elwi) who made this work is possible to guide and support me through all the stages of accomplish my project.

It is impossible to extend enough thanks to my family, especially my greatest parents and my wife, I would like to dedicate this success to my father's soul who is a first and most supported me. Special thanks to my mother to give me the encouragement I needed throughout this process. I would like to give a special thanks to my wife for supporting, encouragement and understanding during my study journey and writing my project.

Warmest thanks to my lovely "sons" (Alhassan and Jad). Thank you to (my dear aunt , my wife parents, my brothers and my sister) for supporting. Finally, thank you to my friends and everyone who prayed for my success and completion of PhD in shaa Allah.

ABSTRACT

MICROSTRIP ANTENNA DESIGN AND FABRICATION FOR SELF POWER MODERN WIRELESS SYSTEM

Al-khaylani, Hayder Hassan Mohammed

PhD, Electrical and Computer Engineering, Altınbaş University,

Supervisor: Asst. Prof. Dr. Abdullahi Abdu IBRAHIM

Date: 12/2022

Pages: 145

Due to the urgent need for modern antenna technology to fit the recent applications including 5G systems, IoT terminals, and space satellite communication systems. However, the antenna technology still rarely relaxed due to the antenna size and passive performance limitations. This involves many advances to include self-powered systems based on green energy based on solar and radio frequency resources. Therefore, novel-reconfigurable sub-6 GHz microstrip patch antenna operating on three resonant frequencies 3.6, 3.9, and 4.9 GHz is designed for 5G applications. The proposed antenna is structured from metamaterial (MTM) array with matching circuit printed around a printed strip line. Antenna is excited with a coplanar waveguide to achieve an excellent matching over a wide frequency band. The suggested antenna shows excellent performance in expression of S11, gain, and radiation pattern that are controlled by two photo resistances. Suggested antenna shows various operating frequencies and radiation patterns after changing the photo-resistance cases. The main antenna novelty is realized by splitting the main lobe which tracks more users on same operating frequency. Nevertheless, major radiation lobe can be steered to required location by controlling the surface current motion utilizing two varactor diodes on the matching circuit. Next, the proposed design is developed to 3D array geometry for 5G applications. The suggested antenna array provides wideband with excellent matching impedance, S11≤-10dB, from 3.1GHz to 5.75GHz. The suggested MIMO array is constructed

from four elements arranged on cubical structure to provide low mutual coupling, less than -20dB, over all interested frequency bands. Each element is excited with coplanar waveguide (CPW). The radiation patterns are controlled by two optical switches of Light Dependent Resistors (LDRs). The suggested array shows excellent response to LDR statue changes in terms of directivity. The proposed antenna frequency band is found to be insignificantly affected with respect to LDR switching statues. The suggested array is fabricated and tested experimentally on expressions of S-parameters, gain and radiation patterns at 3.6GHz, 3.9GHz, and 4.9GHz. The maximum gain is found to be 3.6dBi, 4.2 dBi, and 4.1dBi at 3.6GHz, 3.9GHz, and 4.9GHz, respectively. Nevertheless, it is found that the suggested array achieved a significant beam steering about ±30o, ±40o, and ±45o at 3.6GHz, 3.9GHz, and 4.9GHz, respectively, after changing LDR switching statues. Such technique ensures the antenna beam controlling without need for biasing circuits. Next, RF energy harvesting system is proposed for self-powered system with solar panel integration. At the end, the antenna array is designed and fabricated, the simulation is done by using CST Studio software. It is found that the experimental results of fabrication are agreed very well with those obtained from simulations.

Keyword: IoT, Self-Powered, MTM, MIMO, LDR.

TABLE OF CONTENTS

Pages

ABSTRACT…….....vi

LIST OF TABLES …….....xiii

LIST OF FIGURES …….....xiv

ABBREVIATIONS …….....xviii

LIST OF SYMBOLS …….....xx

1. INTRODUCTION …….....1

1.1 OVERVIEW AND BACKGROUND …….....1

1.2 THESIS OBJECTIVES …….....2

1.3 MOTIVATION …….....3

1.4 PROBLEM STATEMENT …….....3

1.5 PROPOSAL DESIGN STRUCTURE ……4

1.6 THE DISSERTATION NOVELTY …….....6

1.7 CONSIDERATIONS …….....6

1.8 DESIGN AND GOALS …….....7

1.9 THESIS STRUCTURE …….....7

2. CHAPTER TWO…….....9

2.1 MTM THEORY AND CLASSIFICATIONS ……9

2.1.1 MTMs and LH- MTM Definitions ……..10

2.1.2 The Difference Between Backward Waves and LH- MTM…….....12

2.1.3 Composite Right/Left-Hand (CRLH) MTMs …….....14

2.1.4 Metamaterial Applications …….....15

2.2 ANTENNA THEORY …….....16

2.2.1 Maxwell's Equations …….....19

2.2.2 Fundamental Parameters of Antenna …….....20

2.2.2.1 Radiation pattern ……20

2.2.2.2 Radiation pattern lobes …….....21

2.2.2.3 Isotropic radiation …….....23
2.2.2.4 Beam width ……23
2.2.2.5 Directivity of antenna ……..……..24
2.2.2.6 Antenna efficiency …….....25
2.2.2.7 Antenna gain …….....27
2.2.2.8 Return loss (S11) ……..…….…27
2.2.2.9 Band width ……..……...28
2.2.2.10 Polarization …….....29
2.2.3 Antenna Types for 5G and Modern Applications ……..……..29
2.2.4 Antenna Reconfiguration Methods ……..……....32
2.2.4.1 Frequency reconfiguration …….....33
2.2.4.2 Polarization reconfiguration …….....33
2.2.4.3 Radiation-pattern reconfiguration ……..……....34
2.2.4.4 Compound reconfiguration …….....34
2.3.5 Antenna Reconfiguration Techniques …….....35
2.3 GENERAL STRUCTURE OF MICROSTRIP PATCH ANTENNA……...37
2.3.1 Flame Retardant (FR4) Substrate……..... 39
3.1.1.1 FR4 characteristics ……..... 40
3.1.1.2 FR4 applications ……..... 40
2.3.2 Feeding Techniques ……..…41
2.3.2.1 Coaxial probe cable …….……..41
2.3.2.2 Microstrip feed line …….....42
2.3.2.3 Proximity-coupling feed…….....43
2.3.2.4 Aperture-coupling feed …….....44
2.3.2.5 Coplanar waveguide……...44
2.3.3 Effective Parameters …….....45
2.3.4 Fractal Geometry ……47
2.3.4.1 Moore fractal geometry ……48
2.3.5 Microstrip Antenna Advantages and Disadvantages…….....49
2.3.6 Microstrip Antenna Applications …….....50

2.4 ANTENNA ARRAY ……51
2.4.1 Broadside Array ……52
2.4.2 End Fire Array……53
2.4.3 Collinear Array ……54
2.4.4 Parasitic Array...……55
2.5 MIMO BASED ANTENNA ARRAY ……56
3. CHAPTER THREE ……58
3.1 OVERVIEW OF RFEH SYSTEM ……58
3.2 RFEH SYSTEM DESCRIPTION ……59
3.3 IMPEDANCE MATCHING TECHNIQUES ……60
3.3.1 Matching Network with Quarter Wave Transformer ……61
3.3.2 Lumped Element Matching Network……61
3.3.3 Single-Stub Tuning ……64
3.3.3.1 Shunt stub matching ……64
3.3.3.2 Series stub matching ……65
3.4 RECTIFIER CIRCUITS ……67
3.4.1 (HWR) Half-Wave Rectifier ……68
3.4.2 Full-Wave Rectifier-(FWR) ……68
3.4.3 Voltage Doubler Rectifier ……68
3.4.4 Multistage Rectifier ……70
3.4.5 Schottky Diode (Ideal) ……71
3.5 DC. PASS FILTER ……72
3.6 RFEH SYSTEM APPLICATIONS ……72
3.7 SOLAR PV CELL ……75
3.8 CONSTRUCTION OF SOLAR CELL ……76
3.8.1 Photovoltaic Phenomenon in P-N Junction ……78
3.9 SOLAR CELL CHARACTERISTICS ……79
3.10 ANTENNA INTEGRATED WITH SOLAR CELL ……80
3.11 NEGATIVE EFFECTS OF SOLAR CELL ……80
3.12 ADVANTAGES OF SOLAR PV CELL ……81

3.13 DISADVANTAGES OF SOLAR PV CELL …….....81
3.14 APPLICATIONS OF INTEGRATED SYSTEM …….....82
3.15 PROPOSED INTEGRATED SYSTEM STRUCTURE…….....83
4. CHAPTER FOUR……...……...84
4.1 UNIT ELEMENT GEOMETRICAL DETAILS …….....84
4.2 UNIT ELEMENT DESIGN METHODOLOGY ……..……85
4.2.1 Transmission Line Design …….....86
4.2.2 Unit Cell Effects …….……87
4.2.3 T- Junction Effects …….……89
4.2.4 Gap Effects …….……91
4.2.5 Matching Circuit Effects …….……91
4.3 RADIATION PATTERN-DIRECTION AND BEAM SPLITTING…..……...94
4.4 ANTENNA EQUIVALENT CIRCUIT MODEL …….……98
4.5 EXPERIMENTAL VALIDATION ……..……...100
4.6 COMPARISON WITH OTHER REFERENCES ……..……..104
4.7 ARRAY DESIGN AND GEOMETRICAL DETAILS ……..……104
4.7.1 Antenna Array Parametric Study ……..……105
4.7.1.1 Return loss and mutual coupling ……..……105
4.7.1.2 Gain spectra …….....107
4.7.2 Antenna Array Correlation and Diversity ……..……107
4.7.3 Results Validation …….....109
4.8 SOLAR CELL EFFECT ……..…….114
4.8.1 Experimental Validation ……..……...116
4.9 SOLAR CELL HARVESTING …….…….....121
4.9.1 Properties …….…….....121
4.9.2 Solar Energy Harvesting …….……...121
4.10 RECTENNA-ARRAY STRUCTURE …….……122
4.11 PROJECT RFEH MODULE (RFD102A) …….……123
4.11.1 Electrical Properties……..……124
4.12 PROCEDURE OF INTEGRATED SYSTEM STRUCTURE……..……..127

4.13 SUMMARY …….…….129
5. CHAPTER FIVE …….131
5.1 CONCLUSION …….…….....131
5.2 FUTURE WORK…….…….....132
REFERENCES ……...134

LIST OF TABLES

Pages

Table 2.1: Maxwell's equations…….....19

Table 2.2: Comparison study of different types of 5G antennas …….……31

Table 2.3: Comparison table between reconfiguration techniques …….....34

Table 2.4: Advantages and disadvantages of reconfigurable techniques.……..….....36

Table 4.1: Antenna performance respect to varying of photo resistors states.……...….....91

Table 4.2: Antenna performance with different cases of photo resistors …….…...……92

Table 4.3: Antenna main lobe direction with varying the varactor diodes at 3.6GHz…….92

Table 4.4: Antenna main lobe direction with varying the varactor diodes at 3.9GHz…..…...93

Table 4.5: Antenna main lobe direction with varying the varactor diodes at 4.9GHz….....93

Table 4.6: Comparison between this work performance and other published results..……..104

Table 4.7: Output voltage of RFD102A module……...124

Table 4.8: Measured of DC output voltage of RFD102A module…….126

LIST OF FIGURES

Pages

Figure 1.1: Microstrip patch antenna …….....4
Figure 1.2: Integrate microstrip antenna with solar cell …….....5
Figure 1.3: Block diagram of RFEH system …….……6
Figure 2.1: Electromagnetic wave refraction at the media interface ……..10
Figure 2.2: The (ε, μ) diagram ……..12
Figure 2.3: Circuit model for backward wave line …….....12
Figure 2.4: CRLH-MTMs characteristic ……....15
Figure 2.5: Thevenin equivalent-antenna transmission line……17
Figure 2.6: Antenna as a transference device …….....18
Figure 2.7: Antenna analysis-coordinate system …..…….....21
Figure 2.8: 3D-radiation lobes and beam width …….....22
Figure 2.9: 2D-radiation lobes and beam width.…….....23
Figure 2.10: Antenna reference terminal…….....25
Figure 2.11: Losses of antenna …….....25
Figure 2.12: Band width on S11-plot.…….....28
Figure 2.13: Antenna polarization types ……29
Figure 2.14: 5G bands …….....31
Figure 2.15: Types of reconfigurable antennas.……..33
Figure 2.16: Reconfiguration techniques of reconfigurable antennas …….....35
Figure 2.17: Microstrip-antenna structure……...37
Figure 2.18: The current distribution on the patch surface …….……39
Figure 2.19: FR4 structure…….....40
Figure 2.20: The coaxial probe feed for rectangular microstrip patch ……...42
Figure 2.21: General view of microstrip feed line technique……..43
Figure 2.22: The proximity coupling feeding technique general view.…….....43
Figure 2.23: The aperture coupling feeding technique general view …….....44

Figure 2.24: Co-planer waveguide ……...…….....45
Figure 2.25: Different shapes of fractal geometry……...……...48
Figure 2.26: Moore fractal geometry curve …….....49
Figure 2.27: Antenna broadside geometry array ……..….....53
Figure 2.28: End fire antenna array …….....53
Figure 2.29: Collinear antenna array …….....54
Figure 2.30: Point to point MIMO …….....56
Figure 2.31: Multiuser MIMO ……56
Figure 2.32: 5G massive MIMO …….....57
Figure 3.1: Block diagram RFEH system ……..59
Figure 3.2: Impedance matching network …….....60
Figure 3.3: Relation between load resistance and delivered power …….....60
Figure 3.4: Quarter-wave transformer impedance matching ……..61
Figure 3.5: L-section matching networks ……...62
Figure 3.6: Shunt single-stub tuning circuits …….....64
Figure 3.7: Series stub tuning circuit …….....66
Figure 3.8: Transforms (AC) alternating current into (DC) direct current …….....67
Figure 3.9: Radio frequency half-wave rectifier…….....68
Figure 3.10: Full-wave rectification ……...68
Figure 3.11: Voltage doubler rectifier ……69
Figure 3.12: Rectifier at case of RF signal is positive ……69
Figure 3.13: Rectifier at case of RF signal is negative ……...70
Figure 3.14: N-stage multistage rectifier …….....71
Figure 3.15: Power requirements of small electronic products ……..…...73
Figure 3.16: RF energy harvesting applications …….....74
Figure 3.17: Structure of solar cell …….....76
Figure 3.18: Silicon solar cell; (a) monocrystalline, (b) polycrystalline ……77
Figure 3.19: I-V and P-V curves of solar cell/module …….....79
Figure 4.1: Single element of microstrip antenna ……...85
Figure 4.2: S11and gain spectra at different T.L. length ……86

Figure 4.3: Moore fractal effect …….....87
Figure 4.4: S11and gain spectra at one and two moore unit cells …….....88
Figure 4.5: Relative permeability of the unity cell …….....88
Figure 4.6: Relative permittivity of the unity cell …….....89
Figure 4.7: The motion current of MTM antenna element (2 moore cells) …….....89
Figure 4.8: MTM antenna after adding T-stub …….....90
Figure 4.9: S11and gain spectra after adding T-stub ……..90
Figure 4.10: S11 parameter with varying photo resistors conditions …….....91
Figure 4.11: S11 parameter for antenna design with varying LDR conditions …….....93
Figure 4.12: Radiation pattern of 3.6GHz cases …….....95
Figure 4.13: Radiation pattern of 3.9GHz cases …….....96
Figure 4.14: Radiation pattern of 4.9GHz cases …….....97
Figure 4.15: Antenna beam splitting …….....98
Figure 4.16: Equivalent circuit model …….....99
Figure 4.17: Antenna performance validations …….....101
Figure 4.18: Measured and simulated of radiation patterns ……..103
Figure 4.19: Cubic antenna array ……..105
Figure 4.20: S-parameters in different value of (S) ……..107
Figure 4.21: Gain of antenna array in various value of S …….....107
Figure 4.22: Correlation and diversity ……..108
Figure 4.23: Fabricated prototype of (MIMO) antenna ……109
Figure 4.24: S-parameter for simulated and measured antenna when all LDRs are off.…...110
Figure 4.25: Measured and simulated radiation patterns when all LDRs are off..…....111
Figure 4.26: S-parameter for simulated and measured antenna when all LDRs on.....112
Figure 4.27: Measured and simulated radiation patterns in state of all LDRs are on..……..113
Figure 4.28: Antenna performance with and without solar panel introduction…….116
Figure 4.29: Simulated and measured antenna performance with solar panel …….....118
Figure 4.30: Measured and simulated radiation patterns in state of all LDRs are off……...119
Figure 4.31: Measured and simulated radiation patterns in state of all LDRs are on……....120
Figure 4.32: Solar PV panel performance after mounted on array structure ……...122

Figure 4.33: Rectenna array structure (antenna+RFEH module) …….123
Figure 4.34: RFD102A-RFEH module…….....123
Figure 4.35: RFD102A-RFEH board……....124
Figure 4.36: Top view of RFD102A module…….....125
Figure 4.37: Input power vs output voltage of RFD102A …….....126
Figure 4.38: Steps of measurement results of proposed work ……..129

ABBREVIATIONS

MTM	:	Metamaterial
MIMO	:	Multi Input Multi Output
RF	:	Radio Frequency
RFEH	:	Radio Frequency Energy Harvesting
LDR	:	Light Dependent Resistor
RFDI	:	Radio Frequency Identification
5G	:	Mobile Fifth Generation
FR4	:	Flame Retardant Substrate
RHR	:	Right-Handed Rule
LHR	:	Left Hand Rule
CRLH	:	Composite Right Left-Handed
EM	:	Electro Magnetic
EBG	:	Electronic Band Gap
HPBW	:	Half Power Beam Width
FNBW	:	First Null Beam Width
VSWR	:	Voltage Standing Wave Ratio
LTE	:	Long Term Evaluation

IoT	:	Internet of Things
PCB	:	Printed Circuit Boards
FSS	:	Frequency Selective Surface
GPS	:	Global Positioning System
PV	:	Photovoltaics
WSN	:	Wireless Sensor Networks
WPT	:	Wireless Power Transfer
HWR	:	Half-wave rectifier
FWR	:	Full-wave rectifier
AAC	:	Antenna Array Correlation
AAD	:	Antenna Array Diversity
CST	:	Computer Simulation Technology
HF	:	High Frequency
VNA	:	Vector Network Analyzer
PNA	:	Professional Network Analyzer
SMA	:	Surface Mount Adhesive-Solder Impact

LIST OF SYMBOLS

λ	:	Wavelength
ε	:	Permittivity
μ	:	Permeability
ε_r	:	Relative Permittivity
Γ	:	Voltage Reflection Coefficient
E	:	Electric Field Intensity
H	:	Magnetic Fields Intensity
J	:	Current Density
D	:	Electric Flux Density
B	:	Magnetic Flux Density
$\boldsymbol{\rho}$	:	Charge Density
U	:	Radiation Intensity
P_{rad}	:	Total Radiated Power

1. INTRODUCTION

1.1 OVERVIEW AND BACKGROUND

(5G) is sophisticated technology of mobile broad-band communication that is planned to use after 2020. There are two frequency spectrum ranges of 5G system, sub-6 GHz that is including (1 GHz -to- 6 GHz) and above-6 GHz according to study of physical properties [1]. Different 5G antenna designs were reviewed, the authors attempted to produce the exhaustive review that covered vary important antenna designs and its parameters and performances enhancement such as gain, bandwidth and radiation pattern [2]. Since exploring the concepts of Metamaterial (MTM) structures in the last century; they have received big attentions by different industrial and scientific foundations [3]. This because, their nontraditional features and unique properties to realize especial devices for many modern applications [4]. So, MTM structures were introduced to various antennas for achieving novel deigns with enhanced performance in [3]-[5]. For example, in [3], the author applied the use of MTM defects between the antenna elements for MIMO applications by decrease the coupling between the antenna array elements. Other design was published in [4] based MTM patch structures for cylindrical antenna design for gain-bandwidth product enhancements. MTM structure was published in [5] for wearable applications; in this work the authors applied the use of MTM inclusions to minimize the effects of electromagnetic felid absorption by the human body. A monopole antenna array design based on fractal-geometry was suggested for MIMO applications, this array provides the broadside radiation pattern this property as the result of fractal geometry adding, high Mutual Coupling reduction was achieved [6]. A novel multiband fractal sub-6 GHz microstrip antenna utilizing circle and triangle fractals for different wireless applications [7]. The authors demonstrated the effect of loading Koch-fractal on square microstrip antenna edges to get good performances [8]. Multiband Reconfigurable Antenna of (Sub-6 GHz) 5G Wireless Communication is designed. Antenna reconfigured based on (ON, OFF) states of pin diode [9]. A reconfigurable microstrip patch antenna to operate at two frequencies is designed. The concept of switching the lumping element pin diode between (ON) and (OFF) state, to energy saving and power consumption reduction is introduced [10]. In another concept, the introduction of the solar panel to the modern antenna designs has become the most urgent for the self-powered wireless systems [11]. For this, the MTM based antennas were integrated with solar panels in different publications [12]-[15]. For instance, the authors in [12] proposed an antenna

design based on MTM for gain enhancements by integration their antenna design with the solar panel as a substrate. Furthermore, another design was suggested in [13] to integrate the solar panel a reflector for a Vivaldi antenna based corrugated grating patch with MTM. In [14], a design of MTM structure based on plasmonic antenna array for modern applications; in that design, the authors printed their antenna array on flexible solar panel. Design of an antenna based MTM in [15] was introduced for self power wireless system by attaching the antenna ground plane with solar panel. Later, the researchers explored another technique to harvest the green energy from an arterial resource based on RF energy bands [16]. In such technology, the antenna design was introduced with certain specifications such as: high gain-bandwidth products to improve reception efficiency [17], unidirectional radiation patterns to ensure the locus independency [18], and size reduction to ensure system embedding and compatibility with miniaturized electronic circuits [19]. Nonetheless, a matching impedance between antenna and the rectifier-circuit is a significant issue to ensure the rectification efficiency of the resulted structure [20].

1.2 THESIS OBJECTIVES

The objectives of this work, design and fabricate reconfigurable microstrip antenna array based on Solar cell and RFEH with following features:

a. Design a microstrip antenna of a miniaturized size to suite the application of a 5G network.
b. The proposed antenna should be resonant during the Sub-6 GHz bands with in frequency from 2.5GHz to 6GHz.
c. The Microstrip antenna array would be integrated with Radio Frequency Energy Harvesting (RFEH) and a solar panel to provide a self-power wireless system that is very suitable in modern applications.
d. To maintain the antenna array performance such as stable gain, good radiation coverage direction and low cross polarization levels.
e. The antenna elements performance would be configured with LDR photo resistances to control their performance inside multipath reflection environments.
f. Metamaterials could be introduced for this design to decrease the coupling between the array elements in MIMO array system.

1.3 MOTIVATION

a. Due to the feature of microstrip antennas technology which includes low profile, lower weight, easy to manufacture and easy to be integrated with portable electronic devices; the author is motivated to design of miniaturize microstrip antennas that are applicable to the 5G requirements at sub-6GHz.
b. Moreover, such antenna can be integrated into RFEH and solar panel to resource power wireless system that is very suitable for many modern applications including the 5G network.
c. They are applicable to different high-speed antenna devices including pin diode characters that may be used later to reconfigure the antenna performance.
d. Their structure can be engineer by using metamaterial to realize unusual properties of enhanced been and frequency bandwidth.

1.4 PROBLEM STATEMENT

To overcome the limitations in previous studies such as degrades the gain , transmission losses especially in high frequency, and power losses because solar cell nature at attaching the solar cell to ground plane by integrated antenna with solar cell [11]. Bad shadowing effect which prevents the light rays from fall on solar cells [14] . low power produced by of RFEH system and the other base challenges of (RFEH) system is to progress the efficiency of rectennas by improving the collecting of individual energy and transformation ability of every source [17].

Therefore, this work proposed new design of Self Power Wireless System by introduced the integrated system of sub-6 GHz rectenna microstrip array with solar cell that able to offer efficient power to load through solar cell and Radio Frequency Energy Harvesting (RFEH), this leading to reduce the cost, as well as improved the gain of antenna and efficiency of RFEH system with low cross polarization levels and good radiation performance.

1.5 PROPOSAL DESIGN STRUCTURE

Microstrip antenna have many features and properties. It lighter weight, small volume, costly, lower profile, smaller dimensions and easy of fabrication. Microstrip antenna consists of very thin metallic patch placed on dielectric material as a substrate that placed on ground surface, as be clarified in figure (1.1). When antenna is working, the generated waves through the dielectric

suffers reflections and the energy is radiated from patch edges**.** Microstrip antenna is utilized many applications such as RFID (radio frequency identification), WSN, and biomedical and healthcare.

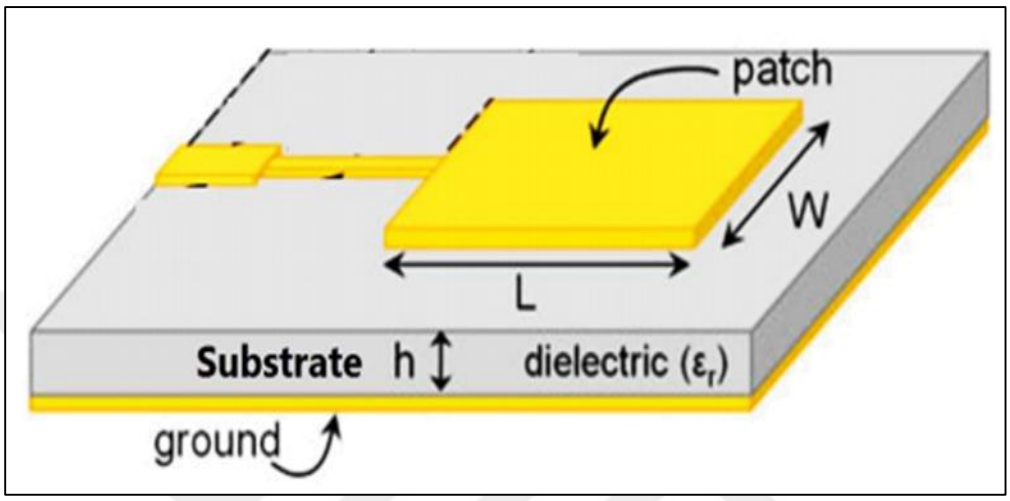

Figure 1.1: Microstrip patch antenna [15].

Modern applications of wireless communication need antennas that designed based on new researches that aims to use green-energy harvesting [1]. Due to, most of these applications based on batteries that affected by overheat and charging loss which leads to decline the charge and discharge time [2]. For these reasons, most of previous works presented the integrated antenna with solar cell by utilizing the transparent antenna which consists of patch that design to allow flow the light through it, such as meshed structure, where the light rays can flow through the mesh openings and the conductor remain represents as valid radiator of (MWF) microwave frequencies. Transparent substrate and meshed ground where all these three layers allow to arrive light to solar cell which used to generate electric power to the load, for example, figure (1.2) as be shown below.

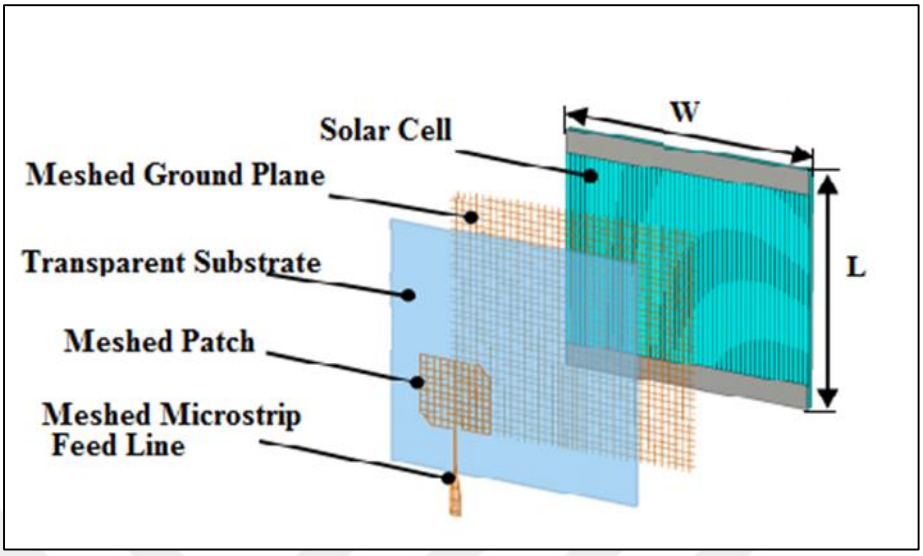

Figure 1.2: Integrate microstrip antenna with solar cell.

But these designs have more limitations [21] such as degrades the gain, transmission loss especially at high frequency and electromagnetic radiation losses because nature of solar.

the proposed system is integrated the sub-6 GHz microstrip antenna array with solar cell and Radio Frequency Energy Harvesting system. Where the solar panel would be located perpendicular to antenna array axis to avoid the shadow effect of array structure and allow to arrive 100% of sunlight directly to solar cell without obstacles**.**

Radio Frequency Energy Harvesting (RFEH) system consists of four parts as be shown below in figure (1.3), where first part is an Impedance matching circuit, second part is a rectifier circuit which utilizes to convert (RF) signal wave to (DC) power, third part is Dc low pass filter and finally is a load. Where the system represents a microstrip rectenna integrated with solar cell**.**

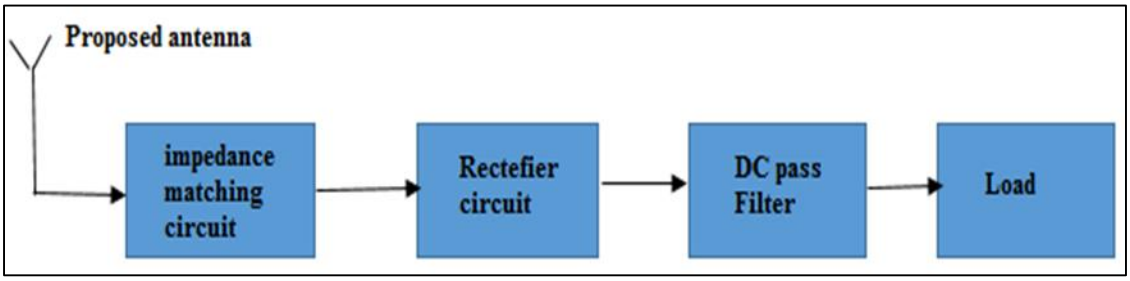

Figure 1.3: Block diagram RFEH system.

1.6 THE DISSERTATION CONTRIBUTION

a. The main novelty is realized by splitting the major radiation lobe to more users on same operating frequency.
b. Steering a main lobe for desired destination via utilizing two varactor diodes.
c. A miniaturized low-profile metamaterial-based antenna would be proposed for 5G applications.
d. The antenna would be fabricated on FR4 substrate to be integrated to solar panels and RFEH system for self-powered applications.
e. The proposed antenna would be applicable for sub-six bands with almost stable gain during broad range of frequencies.
f. Antenna could be subjected to MIMO systems based on array structure.
g. To maintain the antenna array performance, the solar panel would be located perpendicular to the antenna array axis.
h. Antenna reconfiguration by using two LDRs and two varactor diodes would be applied for suggested antenna to control of array performance**.**

1.7 CONSIDERATIONS

a. Introduced the usage of green energy resources in the wireless communication systems.
b. Design and fabricate a novel reconfigurable antenna array for modern wireless communication systems.
c. Improved the performances of the wireless communication systems through proposed novel antenna array.
d. Construct all above considerations in one suitable integrated system for modern 5G applications.

1.8 DESIGN AND GOALS

a. Miniaturized the antenna size.
b. Enhanced and improved the antenna parameters.

c. Reduced the negative impacts of mutual-coupling between the array elements.

d. Negative effects reduction of solar cell on antenna array performances.

1.9 THESIS STRUCTURE

a. Chapter Two (MTM and Antenna Theory): It discusses the properties of metamaterial and its applications and antenna theory (antenna parameters, different types of antennas and antenna reconfigurable).
b. Chapter Three (Microstrip Antenna Theory): It displayed particularities and details of microstrip antennas with the use of multiple feeding technique. Also, it covers three popular procedures for the microstrip antennas analysis
c. Chapter Four (Renewable Energy Resources -RFEH): it studies the details of Radio Frequency Energy Harvesting system construction and its applications.
d. Chapter Five (Renewable Energy Resources -Solar cell): it studies the structure and the physical properties of solar Photovoltaic cell as well as its effect on antenna radiation and its advantages and disadvantages in proposed integrated system.
e. Chapter Six (Results and Discussion " Reconfigurable Antenna Array"): It designs integrated system that consists of a reconfigurable Microstrip antenna array by using CST Simulation and compared the simulation results with the prototype fabrication model results.
f. Chapter Seven (Results and Discussion" Effect of solar cell and RFEH on Antenna array): its analysis all the results and compared the result of CST simulation with the prototype fabrication model results.
g. Chapter eight (Conclusion and Future Work): Finally, conclusion of this dissertation and Future work are displayed in this chapter.

2. CHAPTER TWO

In this chapter, the theory of metamaterial, antenna concept, microstrip antenna, and MIMO based antenna array are discussed. This chapter is divided of following sections:

2.1 MTM THEORY AND CLASSIFICATIONS

Metamaterials (MTM) have more features and properties that different the properties of naturally materials. The term "meta" means beyond nature in the Greek word, in other word, these materials are built with an appointed- specifications to achieve the desired performance. The structure of this materials is caused their properties, where it does not dependents on physical synthesis [22]. In other word, Metamaterials defined as the material that obtains its electromagnetic magnetic properties from the material structure not from the material nature. If the structure is designed accurately can be gained a negative refractive index at certain frequencies. For this reason, these materials are not dependent on (RHR) right-handed rule and hence, named (left -handed MTM) [23]. Meaning of negative refractive index does not mean the standing movement of the signal, but means bending the electromagnetic waves opposite direction at the rays traveled from a (RH-side) to a (LH-side) as be clarified below in figure (2.1) [24].

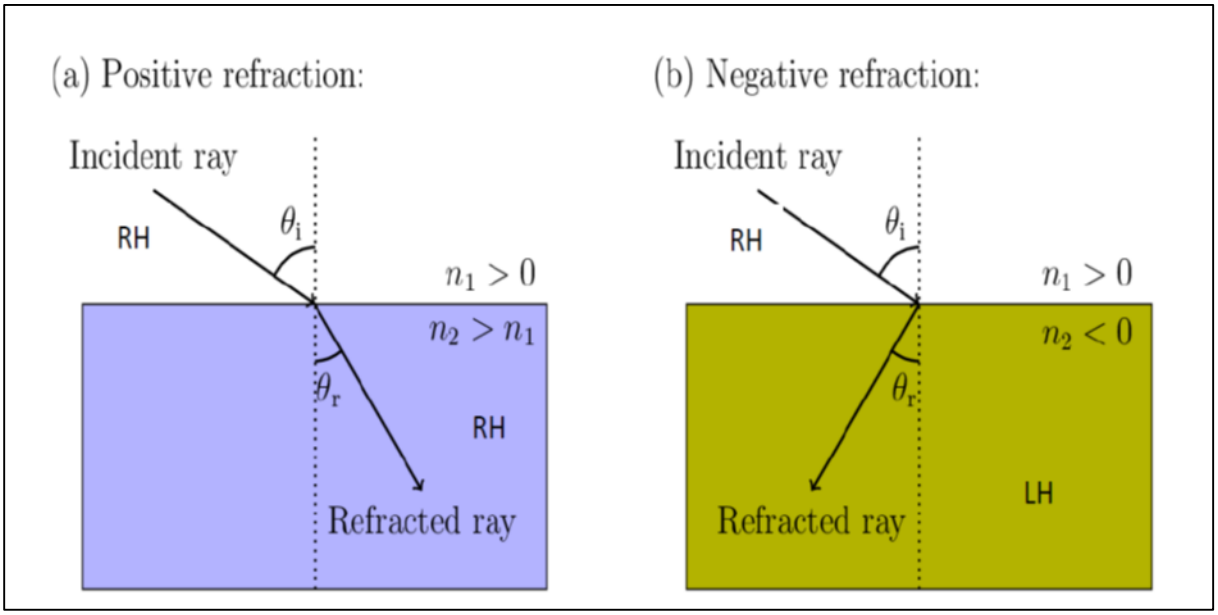

Figure 2.1: Electromagnetic wave refraction at the media interface (a) two mediums of similar handedness (positive refraction) (b) two mediums of opposite handedness (negative refraction).

The metamaterials MTMs widely used in researchers and scientific research to involve broad domain of frequencies, starting from radio frequencies into the visible frequencies. Now, these materials used to the microwave (MWF) frequency band (1-100 GHz), MTM applications can be shown in in section (2.1.4).

2.1.1 MTMs and LH- MTM Definitions

One of definitions of the metamaterials is an efficient homogeneous synthetic material with properties, features and characteristics not found in other material [23]. The efficient homogeneous structure means the size of material cell size (p) is much small compared with guided wavelength λg. For this object, in average the cell volume must be less than a quarter of wavelength $p < \lambda g/4$. To ensure the refraction domination on the scattering / diffraction over the electromagnetic wave propagation inside a MTM. ($p = \lambda g/4$) will be considered as material effective homogeneity condition [21]. The ($\varepsilon r\ \mu r$) parameters depend on unit cell properties of the structure to be a real material in the state of effective homogeneity, as the result the structure is considered to be uniform electromagnetic field in the propagation direction. The refractive constant (n) can be determined by the equation (2.1), that shows the relation between (n) constant and permittivity (ε) and permeability (μ) parameters: -

$$n = \pm\sqrt{\varepsilon r\ \mu r} \tag{2.1}$$

(εr), (μr) are permittivity and permeability of free space relative, given by ($\varepsilon o = \varepsilon / \varepsilon r = 8.854 * 10^{-12}$), ($\mu o = \mu/\mu r = 4\pi * 10^{-7}$).

Figure (2.2) show the (ε, μ) diagram, that shows the combinations sign of (ε,μ) pair . it arranged as (+,+), (−,+), (+,−), and (−,−),Where the first three pairs are represents the conventional materials, but the last group acts a new type, that acts LH- materials [20]. The negative sign of the (ε,μ) parameters, the LH-MTM has anti phase and group velocities. Based on the last definition, LH materials represents metamaterials because its constructs by human and effective homogeneous where $(p < \lambda g/4)$, as well as, it has the unique properties ($\varepsilon r , \mu r < 0$). although MTM in references utilize to refer to (LH-materials), but it includes wide scope. where LH-materials are considered most common type of metamaterials because their special properties with a negative refractive index. Section (2.1.3) shows this type of MTM and the composite right/left-handed CRLH metamaterials.

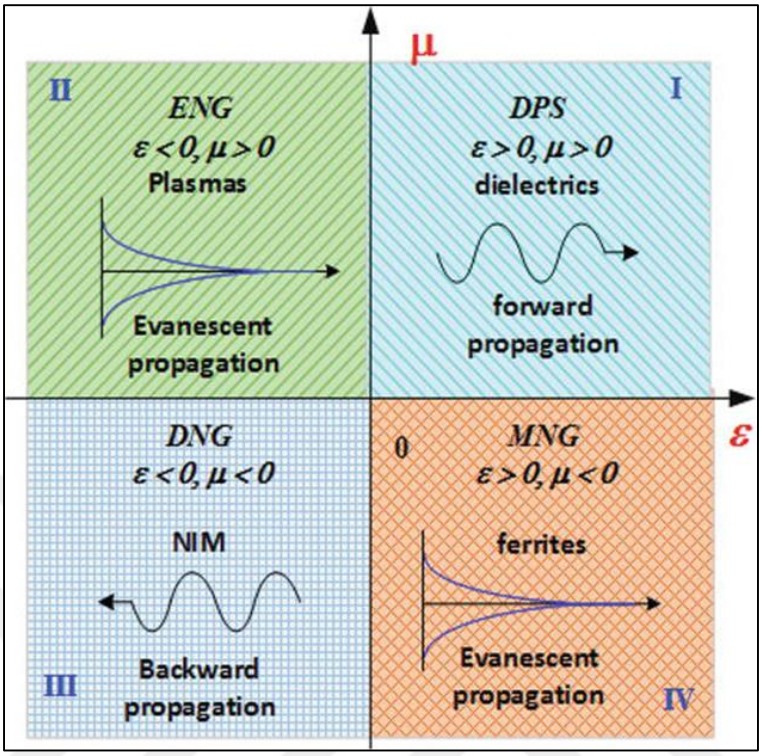

Figure 2.2: The (ε , μ) diagram.

2.1.2 The Difference Between Backward Waves and LH-MTM

Antiparallel phase and group velocity propagation is unresent theory. backward waves are the signals have special characteristics of its propagation where that represents the (CRLH) model. Brillouin and Pierce were used the circuit model that shown in figure (2.3) below, to show CRLH and its uses [21].

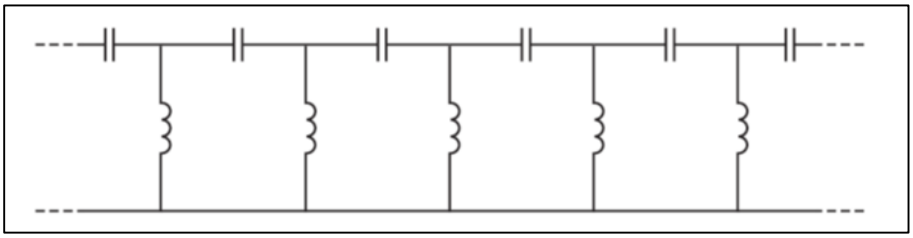

Figure 2.3: Circuit model for backward wave line.

Backward waves have been related with the reverse amplification phenomenon that occurs in traveling wave tubes, many references that shows the backward waves details, for all background waves states excepting the magneto static backward volume waves, where that occurs in space harmonics or in higher modes. Therefore, in structure, the cell size of this type at wave propagates, must be approximately equal ($p \approx \lambda g/2$) or multiple these size ($p \approx n\lambda g/2$) within the higher modes.

As a result, for described these waves cannot be used (ε) and μ parameters because that waves propagate suffers from the diffraction and scattering [25]. Consequently, the real structures electromagnetic behavior is not present, for instance, the refraction property that subjects to Snell law. moreover, LH-MTM works at the fundamental mode, effective homogenous structure at cell size ($p< \lambda g/4$), at this state, can be identified the parameters and the structure behave and work as real material. In reality, when the cell size ($p < \lambda g/4$,) the difference between left-handed (LH-MTM) structures and dielectric materials to be only quantitative.

The structural units introduced in particular the permittivity value in dielectric materials are molecules according of angstrom order, while the volume in modern left- handed materials are centimeters in the microwave band. The electric unit structure size equal ($p/\lambda g$) $\approx 10^{-9}$ at L-X of microwave bands for the first state and equal ($p/\lambda g$) $\approx 10^{-1} - 10^{-2}$ for the second case. But, LH-MTMs display a similar quality of refractive phenomena to the classic dielectrics. This means LH-MTMs behaves similarly to dielectrics, thus the metamaterials is called on this material in spite of with negative properties. Because it has effective homogeneity and may be expand to covered 2D and 3D structures.

2.1.3 Composite Right/Left-Hand (CRLH) MTMs

Caloz proposed the idea of CRLH-MTM, which represents the broader case of (LH-MTMs) and gives a brief description of its core. TL-model illustrated in figure (2.4) are made up of series capacitors (CL) and shunt (stub) inductors (LL), which are meant to give left-handedness from the preceding section's clarifications. However, currents and voltages produce parasitic effects when they pass through the material [3]. When current is passed through the capacitor CL, a magnetic field is generated, resulting in a series inductance L_R; moreover, voltage gradients occur between the upper conductors and the ground surface, resulting in a shunt capacitance (C_R). As a result, even in limited frequency range, a pure LH (PLH) structure is not completely present, because a true LH structure must incorporate (L_R,C_R) and (LL,CL) reactance. This fact is the basis for the use of the name CRLH to explain the properties and nature of actual left handed- MTM [22]. The basic features of a CRLH may be deduced from an examination of the analogous model shown in Figure (2.4). (a), L_R and C_R are short and open at low frequency range, therefore the circuit become pure LH-structure due it has antiparallel phase and group velocities, this LH structure is high pass circuit, so an LH stopband is present below a certain cutoff. While at high frequency range CL and

LL are short and open. The circuit become purely RH- structure with parallel phase and group velocities, this RH- structure is low-pass circuit, so an RH stopband is present above a particular cutoff. Generally, when series and parallel resonances are unequal, a gap is existing between the LH and RH structures.

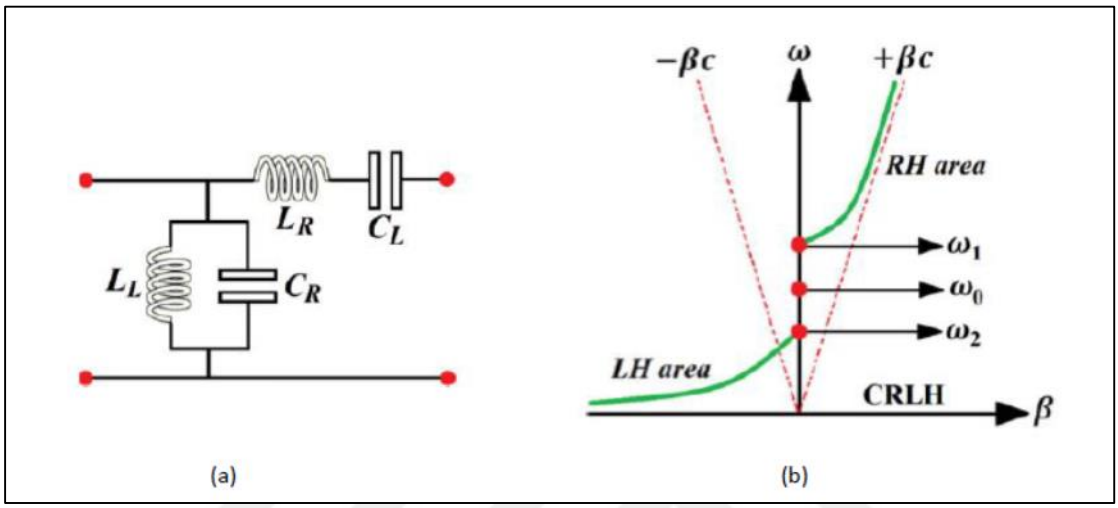

Figure 2.4: CRLH- MTMs characteristic (a) unit cell structure (b) diagram Dispersion. (LR = CR = 0 at LH circuit), (LL = CL =∞ at RH circuit) mentioned for comparison purposes.

In this diagram (ωse < ωsh) , the opposite can be applied also depending on the LC values. If the resonances are balanced, the gap is completely disappearing, and an infinite-wavelength propagation ($\lambda g = 2\pi/|\beta|$) at the transition frequency ω_o is obtained. In spite of the filter feature, The (CRLH) operates only at the transition frequency where the condition of effective homogeneity is satisfied ($p < \lambda g/4$), it never operates at borders of the Brillouin-zone, where($p \approx \lambda g/2$). The dispersion curve of CRLH containing LH and RH effects is quite different from the pure LH/ RH structures due to the combined effect of the structures at all frequencies.

2.1.4 Metamaterial Applications

Metamaterials (MTM) introduced different view as a result of their unnatural interactions with the electromagnetic waves to overcome the traditional and developed technology limitations, due to it have more features and properties that different the properties of naturally materials. These features made it utilized in many applications such as:

a. Discover the novel characteristics of (EM) electromagnetic materials.

MTM is considered as the materials that have a negative refractive index and very low or high value of negative permeability or permittivity [20].

b. Used in RF components manufacturing

MTM have the important influence on sensor technology, where These elements basically consist of (active power amplifiers and couplers, power dividers, and bandpass filters (BPFs) as passive circuits) [24].

c. Overcoming the limitation of conventional materials

(MTM -TLs) are artificial lines of reactive materials which have larger degree of freedom than conventional lines and setting the dispersion and the impedance characteristic [22].

d. Improved the capability of current devices

MTMs have been validly utilized to rise the performance of previous components such as the microwave components designs or to produce the novel devices theoretically as invisibility cloaks, transformation electromagnetic devices and optical Nanocircuits [26].

2.2 ANTENNA THEORY

One of definitions of Antenna is a special transducer which converts the electromagnetic fields into AC alternating current or Inversely side converter [28].There are two types of antenna , transmitting antenna and receiving antenna ,the first type works to convert AC power into Electric-Magnetic field for transmitted and the second antenna type used to convert Electric-Magnetic energy into AC power for utilizing by electronic circuit. At any case, it designed to work in allocated frequency band and refuse any signal of another frequency bands [29].

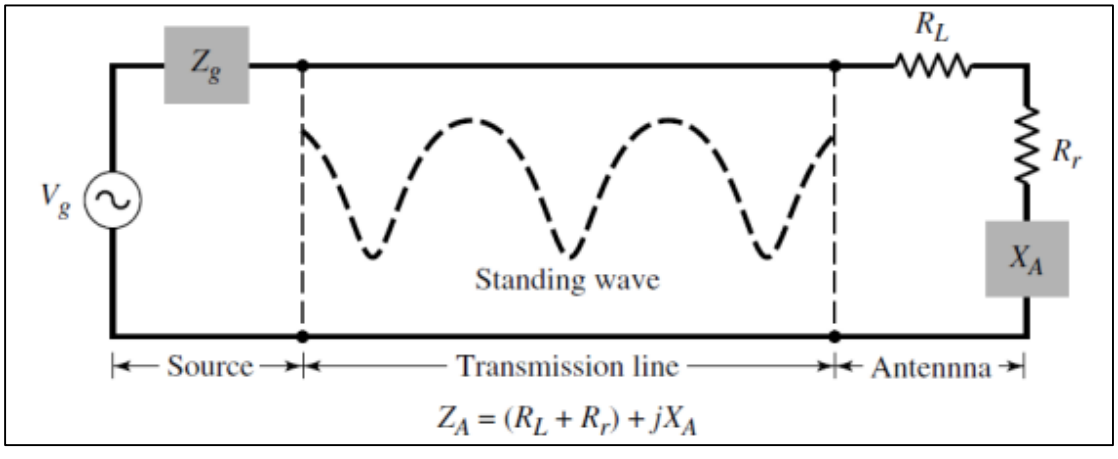

Figure 2.5: Thevenin equivalent-antenna transmission line [29].

Antenna is considered a transceiver device, where it is possible to utilize as sender or receiver. Antenna can be represented and constructed at transmitting mode by Thevenin-equivalent circuit as be clarified in figure (2.5). The source is considered as ideal-generator, transmission line represents as line that has Z_A impedance, finally, the load is represented as ($Z_A = (R_L + R_r) + jX_A$) connects with transmission line to represent antenna. The load resistance (R_L) refers to a dielectric resistance and conductor losses that placed side by side with antenna structure and Rr acts the radiate resistance, which uses to represent the radiation of antenna. X_A) is reactance that represents an imaginary part of impedance, it links with radiation resistance and concerned with radiation of antenna [27]. IEEE antenna definition introduced in [28] according to the following concept "That part of a transmitting or receiving system that is designed to radiate or receive electromagnetic waves", it is displayed in figure (2.6) below.

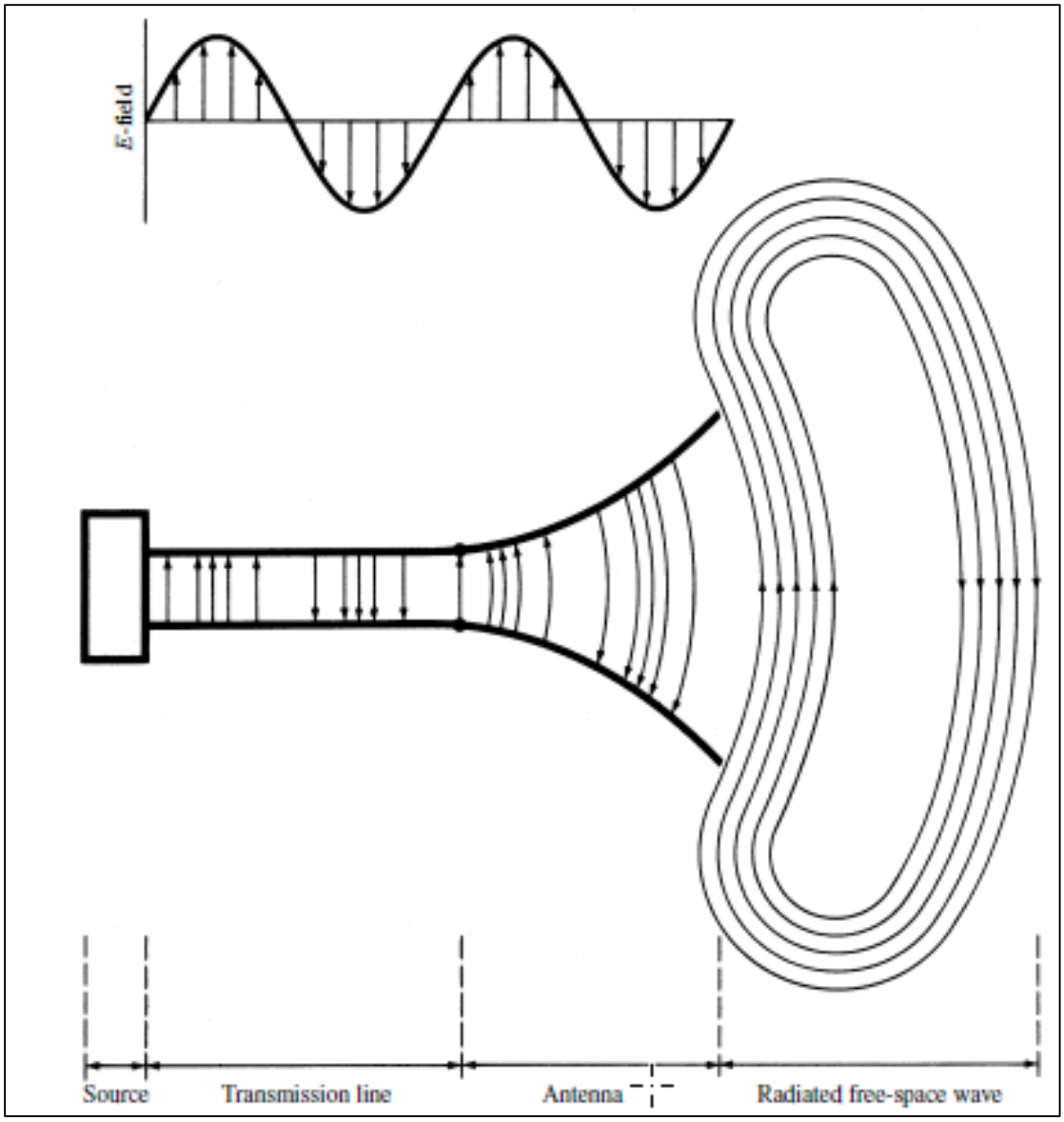

Figure 2.6: Antenna as a transference device [29].

2.2.1 Maxwell Equations

Maxwell equations are four complex equations which describes arising magnetic and electric fields of electric charges distributions and currents, and how different with time. It can be shown these equations in table (2.1). It is group of partial differential and integral equations which works at same time with Lorentz force law, form of basis of quantum theory, classic electromagnetics theory, classic optics and electric circuits. Their created basis of all importance technologies such as (magnetic, electric, optics and radio) as well as involving power generation [28], TV, WCS, computers etc. These equations explain how magnetic and electric fields generate the currents and

charges and how to changes each other. One important result of these equations which explains how the oscillating electric and magnetic fields can propagate in same light speed. This known the electromagnetic radiation waves, these waves generate in different wavelengths to generate a frequency spectrum of (RF) radio frequency waves. The name of this equations is taken from name of scientist of mathematics and physics (James Clerk Maxwell) to be named the Maxwell equations. the first form of this equations published during 1861 - 1862 and a first scientist was described that the light is an electromagnetic shape is Thidé [29].

Table 2.1: Maxwell equations.

Name	Differential equation	Integral equation
Guess's Law	$\nabla .\ D = \rho_V$	$\oint D.ds = \oint \rho_v.dv$
Guess's Law for magnetism	$\nabla .\ B = 0$	$\oint B.ds = 0$
Maxwell-Faraday equation	$\nabla \times E = -\frac{\partial B}{\partial t}$	$\oint E.dl = -\frac{\partial}{\partial t} \oint B.ds$
Ampere circuital Law	$\nabla \times H = J - \frac{\partial D}{\partial t}$	$\oint H.dl = \oint (J + \frac{\partial D}{\partial t}).ds$

"These equations explain the relationship between Electric Field Intensity E ($V\ /m$), magnetic fields Intensity H (A/m), electric density charge ($\boldsymbol{\rho}$) ($coulomb/m3$) , and current density (J)

($ampere/m2$). quantities (D) is electric flux density ($coulomb/m2$) and B is magnetic flux density ($weber/m2$), or ($Tesla$)".

2.2.2 Main Antenna Parameters

Antenna performance could be clarified by using group of parameters that affecting at antennas designing and measuring. These parameters can be into two types, first type is based on the field view point that including the radiate pattern, beam width, directivity, gain, polarization and band width. second type, based circuit-view point that containing input impedance, radiate resistance, reflection coefficient, return loss and (VSWR) [30].

2.2.2.1 Radiation-pattern

Antenna radiation-pattern is known a graphical representation or mathematical function of the antenna radiation properties such as function of space axis. It is specified mostly in far field region

and it represents as directional coordinates function. Radiation features including the radiation intensity, power flux density, directivity, field strength, polarization. The most importance of these property is (2D or 3D) energy radiation spatial distribution as surface function constant radius or position monitor along path. Figure (2.3) can be shown example of antenna coordinate analysis system [31].

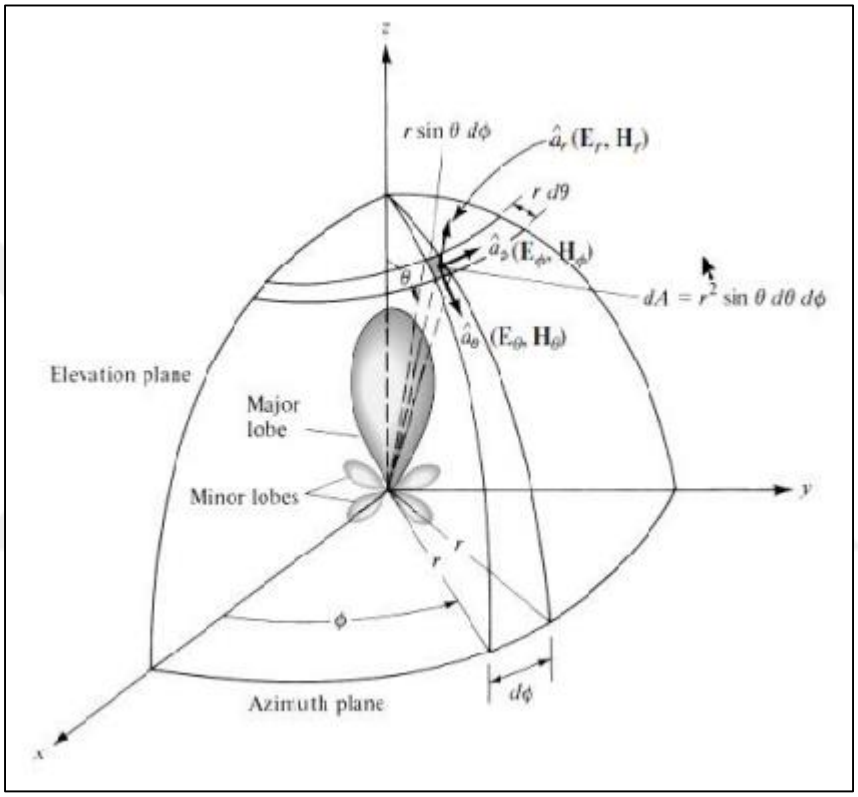

Figure 2.7: Antenna analysis-coordinate system [31].

The pattern amplitude field is chart of received electric and magnetic field in fixed radius and the pattern amplitude power is chart of power density alteration in constant radius. Power and field pattern are represented with maximum value. Power pattern is measured by (dB) in logarithmic scale.

2.2.2.2 Radiation-pattern lobes

Lobes of radiation pattern that could be organized into major lobe and minor lobes (main lobe, side lobes and back lobes) .

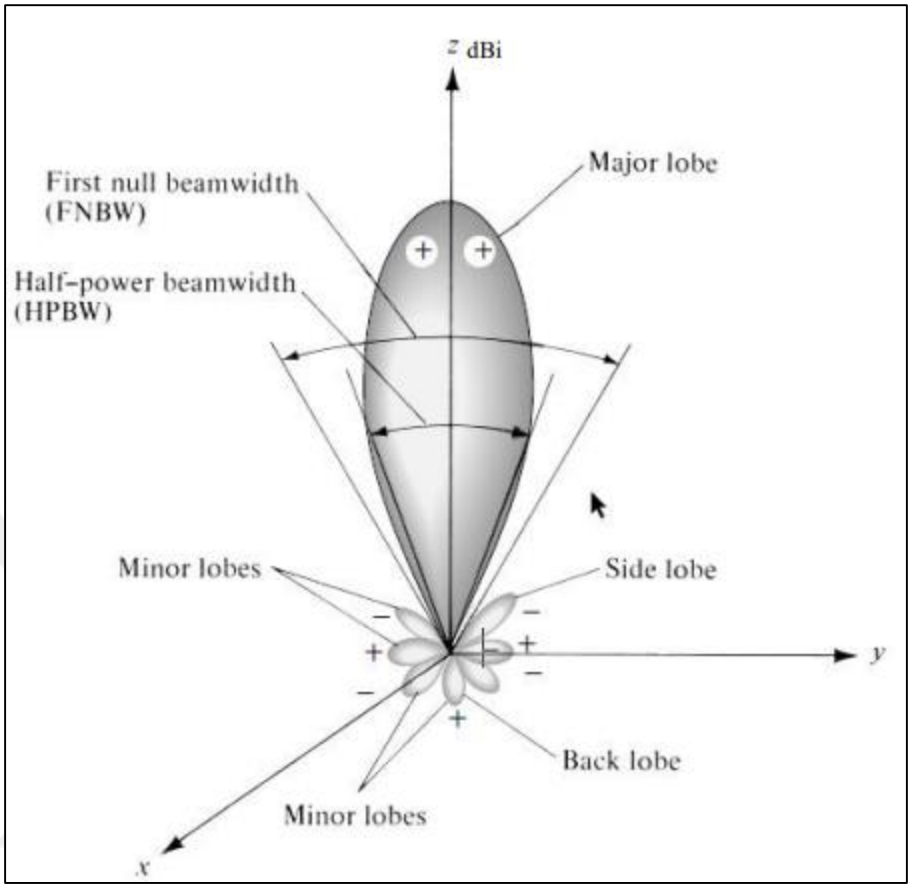

Figure 2.8: 3D-radiation lobes and beam width [31].

Radiation lobes can be identified as part of radiation pattern that bounded weak radiation intensity regions relatively [30]. Figure (2.8) presents a symmetric 3D- polar pattern involve set of lobes with vary radiate intensity that may be have different volumes. Figure (2.9), that shown the radiation lobes and beam width.

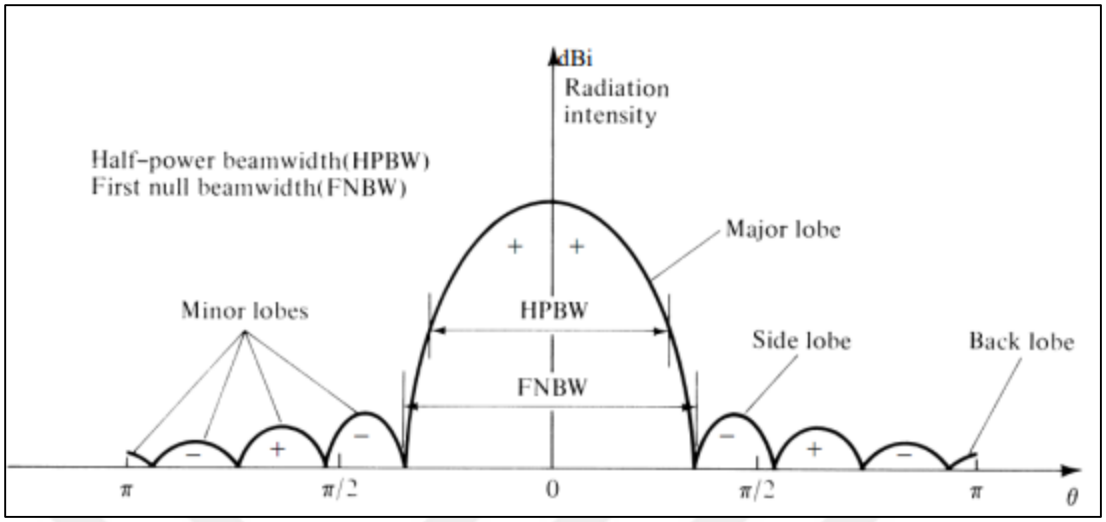

Figure 2.9: 2D-radiation Lobes and beam width.

2.2.2.3 Isotropic radiation

It can be occurred when the source radiates in all directions at same intensity. it considers an important factor for enhanced the antenna radiation pattern. In general, when radiation-intensity is equal for all space directions, it is called isotropic radiation [30].

2.2.2.4 Beam width

Beam width is one of very importance parameter of antenna, antenna is oftentimes utilized as a trade-off between beam width and side-lobes level. Beam width is also utilized to show the antenna capability to recognize between two adjacent radiate elements, sources or targets [33]. It founds many of beam widths types in antenna radiation pattern. (HPBW) Half Power Beam width is considered most importance, which defines in IEEE “In a plane containing the direction of the maximum of a beam, the angle between the two directions in which the radiation intensity is one-half value of the beam”. (FNBW) First Null Beam width is defined as the angular separation between the pattern first null beam width. Both types (HPBW and FNBW) can be clarified above in figure (2.8) and (2.9) that clarifies 2D and 3D radiation lobes and beam width [31].

2.2.2.5 Antenna directivity

It is defined in IEEE definitions standard as "ratio of the radiation intensity in a given direction from the antenna to the radiation intensity averaged over all directions". Rate of isotropic radiation

intensity is equal to whole antenna radiated power divided by (4π). If not set the radiation intensity directional, then its direction toward of maximum radiation. In other word, directivity of non-isotropic antenna is equal to ratio of radiation intensity at given direction over radiation intensity of isotropic antenna. Its equation can be expressed Mathematically in below [31]:

$$D = \frac{U}{U_o} = \frac{4\pi U}{P_{rad}} \tag{2.2}$$

$$D = D_O = \frac{U_{max}}{U_o} = \frac{4\pi U_{max}}{P_{rad}} \tag{2.3}$$

where:

D = antenna directivity (dimensionless)

Do =$Dmax$: maximum directivity

U = radiation intensity (W/unit solid angle) it calculated by multiplying radiation density ($Wrad$) with square of distance (r^2). $U = r^2 Wrad$.

$Umax$= maximum radiation intensity (W/unit solid angle)

Uo= radiation intensity of isotropic source (W/unit solid angle)

P_{rad}= total radiated power (W)

2.2.2.6 Antenna efficiency

Antenna Efficiency term including many of efficiencies are related with antenna design. The equivalent efficiency is clarified in figure (2.11), where (e_o) is the total efficiency is used with considered the losses on antenna input terminals and its structure. These losses may be occurring when the reflections happened because a mismatch between antenna and T.L., and losses that happened due to nature of dielectric and conductor material, it can be computation via eq. :($P=I^2 R$). Figures (2.10) and (2.11) shown the antenna terminals and antenna losses respectively [31].

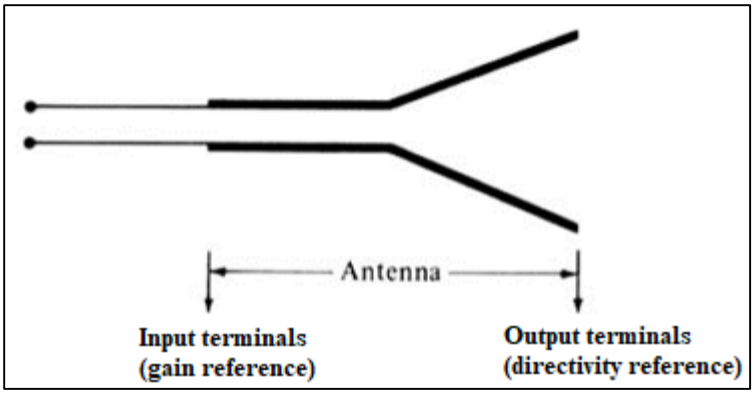

Figure 2.10: Antenna reference terminal.

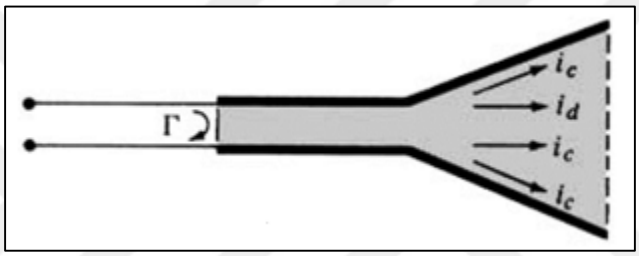

Figure 2.11: Losses of antenna.

The mathematical expression of total efficiency shown below:

$$e_o = e_r\, e_c\, e_d \tag{2.4}$$

Where:

e_o = total efficiency (dimensionless)

e_r = reflection efficiency (mismatch) = (1-|Γ| 2) dimensionless)

e_c = conduction efficiency (dimensionless)

e_d= dielectric efficiency (dimensionless)

Γ = voltage reflection coefficient on input terminals (constant)

$$\Gamma = \frac{\mathrm{Zin} - \mathrm{Z0}}{\mathrm{Zin} + \mathrm{Z0}} \tag{2.5}$$

Where:

Z_{in} = antenna input impedance.

Z_o = characteristic impedance of the transmission line.

VSWR = voltage standing wave ratio = $\frac{1+|\Gamma|}{1-|\Gamma|}$

In general, e_c and e_d can be calculated experimentally because difficult to compute it. Where cannot compute it by measurements, in general for more appropriate, equation (2.3) can be written as equation (2.6)

$$e_o = e_r e_{cd} = e_{cd} \left(1- |\Gamma|^2 \right) \quad (2.6)$$

Where, $e_{cd} = e_c\, e_d$ = antenna radiation efficiency, which represents the relation between the gain and directivity [29].

2.2.2.7 Antenna gain

Gain is considered one of most importance of antenna parameters and one of most parameters that announced in specialized antenna research. Antenna gain is closely connected to directivity, where it takes into account the antenna efficiency and directional capabilities. Antenna Gain could be defined as "ratio of the radiate intensity in certain direction to the total input power that accepted by antenna that radiated isotopically")[31]. gain can be expressed as be shown below, In equation (2.7):

$$\text{Gain} = 4\pi \frac{radiation\ intensity}{total\ input\ (accepted)\ power} = 4\pi \frac{U_{(\theta,\emptyset)}}{P_{in}} \quad (2.7)$$

Antenna gain can be expressed by multiple antenna radiation efficiency (e_{cd}) and antenna directivity $D\ (\theta, \phi)$ in equation (2.8)

$$G(\theta, \emptyset) = e_{cd}\ D(\theta, \emptyset) \quad (2.8)$$

2.2.2.8 Return loss (S11)

Return loss or S11 is identified as 'ratio of the antenna incident power P_{inc} to power reflected back from the source antenna P_{ref}'. It tells us amount of input signal power reflected. In other word, it can be showed difference between transmitted power signal to reflected power that happened due to variations of links and channel impedance [33].It is negative reflection coefficient measured in decibels (dB) and in terms of the voltage, is Voltage Standing Wave Ratio (VSWR). It can be express in equation (2.9) [30-31].

$$R= 10 \log_{10} \frac{Pin}{Pref} = 20 \log_{10} \left| \frac{VSWR+1}{VSWR-1} \right| = -20 \log_{10} |\Gamma| \quad (2.9)$$

2.2.2.9 Band width

In IEEE standard is defined as "the range of frequencies within which the performance of the antenna, with respect to some characteristic, conforms to a specified standard" [30-31]. B.W is range of frequencies on each side of center frequency, value of center frequency must be acceptable and appropriable of antenna characteristics such as (beam width, pattern, matching impedance, polarization, gain, side lobes, radiation efficiency, beam direction). Almost, B.W is calculating on or nearest (-10 dB) as (S11) reflection coefficient factor as clarified in figure (2.9).

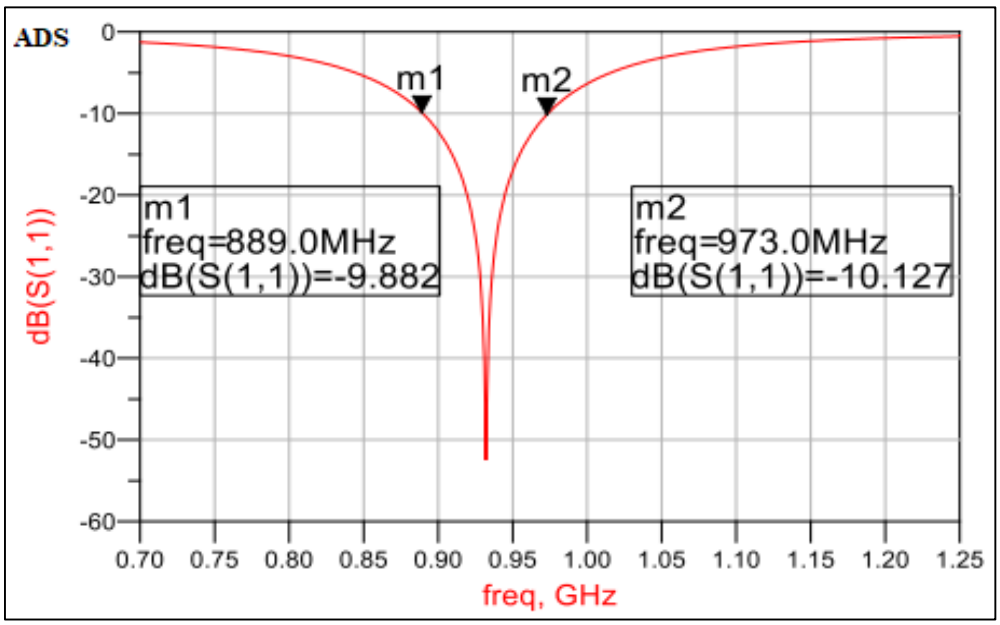

Figure 2.12: Band width on S11 plot.

We can observe from figure above the center frequency equal to 9.35 MHz and the frequency side m1=889 MHz , the frequency side m2 =973MHz where B.W= m2-m1= 84 MHz.

2.2.2.10 Polarization

Polarization is defined "property of electromagnetic wave describing the time-varying direction and relative magnitude of electric-field vector" [31]. there are three types of radiate polarization are linear polarization, circular polarization and Elliptical polarization as be clarified in figure (2.13). radio wave initial polarization is determined by the antenna. The brief definitions of these types of radio wave initial polarization are

a. Linear polarization is occurred when vector (E) that represents the electric field at a point in space as function of time, in directions on a long line.
b. Elliptical polarization is generated if the (E) vector traces as ellipse shape.
c. Circular polarization is occurred if (E) vector has fixed length but rotates around. the rotation perhaps in right or left side.

Any type of polarization to be available and can be chosen by (RF) system designer.

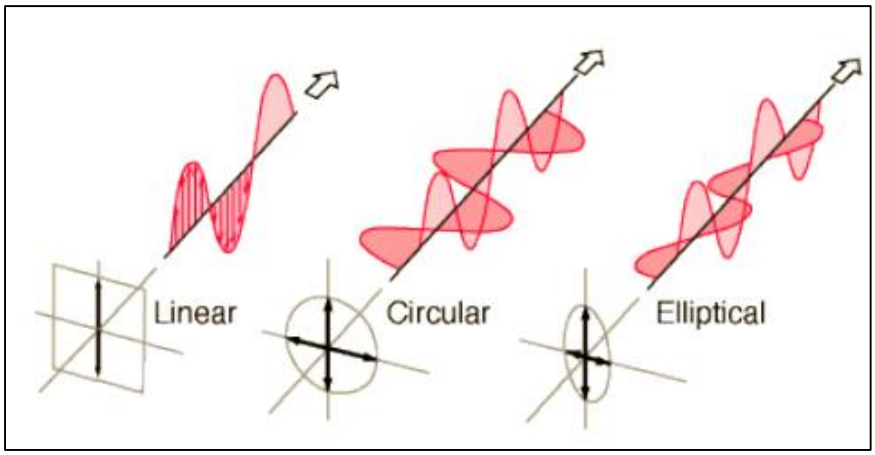

Figure 2.13: Antenna polarization types.

2.2.3 Antenna Types for 5G and Modern Applications

Telecommunication system providers were investing in mobile communication networks to increase coverage capacity, improve services, and entice more users, from the first mobile phones introduced in 1980. Mobile phone calls were started when (1G) first generation networks was built, in spite of limited mobile network coverage and capacity. Providers built second generation (2G)

second generation of mobile communication networks, it is including voice calls and SMS services, followed then third generation (3G) and fourth generation (4G-LTE) networks to support video calls and to solve these limitations [1]. Each generation added faster speeds, high capacity, new properties and new services. However, fifth generation (5G) was began build in 2018 by Telecommunications companies to meet the growing demand for data from consumers and companies. 5G networks allow the providers to support more consumer services and requirements such as virtual reality applications , supporting the smart devices that needs to connect by internet (like health care and monitoring system devices), supports a modern industrial uses (like sensors and monitoring systems), implements the advanced data analysis, in addition, allow to use the sophisticated technologies like (smart cities and autonomous vehicles). Spectrum is one of important elements that support 5G system. The electromagnetic spectrum is utilized for all wireless communication technologies [32-33]. The radio frequency band is very important band that utilized in wireless communication system. Multiple spectrum bands are utilized for 5G such as Low-band frequency (less than 1 GHz), Mid-band frequency or that called sub-6 GHz (from 1 GHz to 6 GHz), and high-band frequency (above 6 GHz - mmW). In order to provide ultra-fast services in crowded cites, 5G networks requires (mmW) as high band spectrum to existing user benefits from 5G technologies implemented for mid-band spectrum that offered high speed, capacity, faster service and more extra features. Many of (IoT) applications need wide-spread coverage, which can deliver in 5G that used low band [34]. Moreover, most mobile devices (cell phones) are using (sub -6 GHz) frequencies because this band are very suitable for wireless communications where it have good properties such as it can travel for long distance , large areas coverage and it can easily to breach through different obstacles. For these features, more users are utilizing the mobile devices wide range of modern applications [35]. All researchers which works to develop 5G technology acknowledge that 5G spectrum consists of three main frequency ranges as be explained below:

a. First band is (Sub-1 GHz) is used for metropolitan area network, suburbia and rural settings, and in addition, in buildings coverage that using IoT devices and services.
b. Sub-6 GHz band (1-6 GHz) that used to increase bandwidth, stable gain and it contain (3.3 to 3.8 GHz) band which expects to be basis for many 5G services.
c. Above (6 GHz) that includes (mmW) which uses for provide Ultra-high wideband speeds.

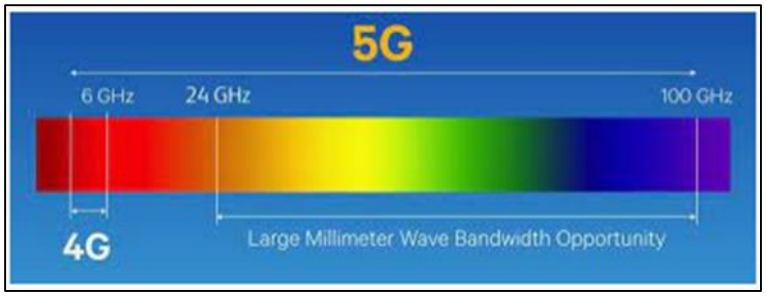

Figure 2.14: 5G bands.

One of most important elements of 5G mobile technology is antenna design. This section discussed a comparison study that shown in Table (2.2). This table compare the advantages and disadvantages between the different antenna types for the 5G mobile communication and modern applications. Where, the comparison table is discussed a single element antenna or array configuration and antenna performance in different terms such as; Frequency, gain, and bandwidth are discussed. as well as, a comparison included the antenna design complexity and the ability of antenna to integrate with small electronic devices [29-31].

Table 2.2: Comparison study of different types of 5G antennas. “tables continued” for the table overflowing to page 32.

Antenna Type	Advantages	Disadvantages
Monopole	• Simple to design and fabricate • In multi element monopole antenna design it can easy to rotate in any direction	• Less gain • Required large area of ground • Given poor response in bad weather condition
dipole	• Simple to design and fabricate • Receive balanced signal	• Less gain • Cannot use for long distance • Low bandwidth
Megneto-electro dipol	• High front to back ratio • Low side lobe and back lobe level • Wide band width • Low cross polarization	• Complex and high cost design and fabrication •
Antipodal Vivaldi Antenna (AVA)	• Gain Enhancement • Provide wide bandwidth • Stable radiation pattern	• Required large space • Low gain and low frequency

Table 2.2: Comparison study of different types of 5G antennas. “tables continued” for the table overflowing to page 32 ‘Tables Continued’.

Fractal	• Miniaturize antenna size • Wide bandwidth • Good impedance matching • Provides consistent antenna performance over the operating range	• Complex design • Limitation on repetition of fractal design
Planar Inverted F Antenna	• Low profile • Good impedance matching • Enhanced front to back ratio	• Narrow bandwidth • Low gain
Inverted F Antenna	• Small size • Good impedance matching due to intermediate feeding	• Narrow bandwidth • Low gain
Microstrip Patch Antenna	• Low profile • Low cost • Linear and circular polarization • Easy to fabricate • Easy to integrate with other circuits.	• Narrow bandwidth • Low or Moderate gain

2.2.4 Antenna Reconfiguration Methods

Reconfigurable antenna is one of most important properties that should be considered to design 5G antennas to convert the classical antenna to smart antenna by using some electronic devices such as PIN diodes, varactor diodes and optical switches. This section produced a study for classify antenna reconfiguration into four types: frequency, polarization, radiation pattern (beam forming) and compound reconfiguration [36]. These reconfigurable classifications based on features of reconfiguration methods as be shown in Figure (2.15). As well as, this section explained the applied reconfigurable techniques.

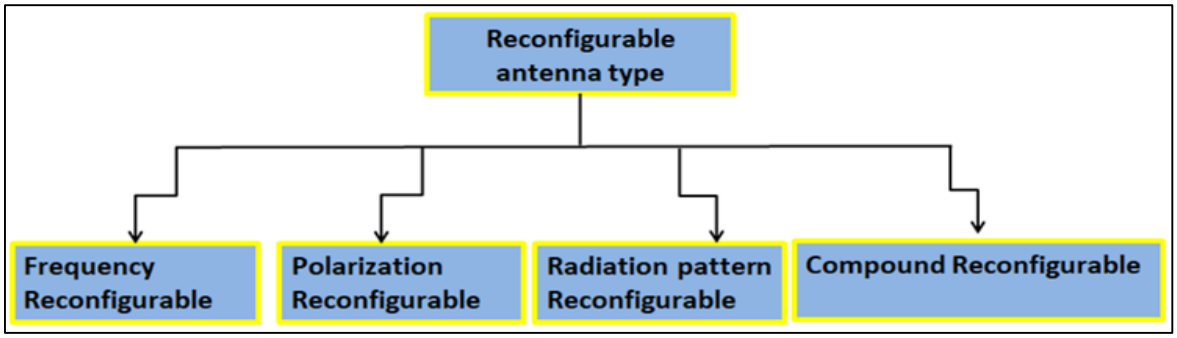

Figure 2.15: Types of reconfigurable antennas.

2.2.4.1 Frequency reconfiguration

In modern communication systems, users can benefit from different situations especially at communication system operates in multiple frequency bands. Where that can show when a transceiver transmits the signal at one frequency and receives signal on another. In this state, must be use different antennas for each band but this state is considered costly and led to increase the system design complexity and increase the constructed area of the system. For these reasons, the new communication system proposed to use a frequency-reconfigurable antenna that caused to reduce the cost and reduced the system complexity and it considered most important aim is to guide antenna target frequency [37].

2.2.4.2 Polarization reconfiguration

In this type of antenna reconfigurability, antennas can modify their polarization situation with survival frequency and radiation pattern are constant. The desirable type of reconfigurable antenna on MIMO systems is a different polarization scheme. These are achieved by adjusting the antenna surface structure to change the electric field direction. theoretically, the losses power by communication between a circularly polarized and linearly polarized among 3 dB.

Antenna that is called vertically polarized is offer well protected from the surroundings. This antenna radiation pattern is distinguished by supporting the coverage of ground level from horizon to horizon. Reconfigurable polarization antennas enhanced the radio connection budges by providing an excellent line-of-sight property without path mismatching [38].

2.2.4.3 Radiation-pattern reconfiguration

This reconfiguration is another important and attractive topic of smart antennas. It refers to beam-steering techniques (main lobe direction) and antenna gain management in both azimuth and elevation planes. The reconfigurable of antenna radiation pattern supports the link quality improvement by concentrating the signal in desired direction. This type achieved an excellent control of antenna gain within coverage area and guide the radiation into certain direction [37][39].

2.2.4.4 Compound reconfiguration

Compound reconfigurable is one of most important type of reconfigurable, where it contains more reconfigurable types. Compound reconfigurable antennas can be operating with a variety characteristic. It suitable to change of frequency, polarization phase and the different forms of their radiation pattern, the frequency or polarization altering to create multiple processes of reconfiguration. multiple antenna characteristics configurations are discussed [37][40].

Table (2.3) represents the comparison between reconfiguration techniques where is shown the advantages and disadvantages of these four techniques.

Table 2.3: Comparison table between reconfiguration techniques. “tables continued” for the table overflowing to page 35.

Reconfigurable Technique Type	Advantages	Disadvantages
Electrical	• Ease of Implementation • Low Cost	• Complex structure • Requires biasing system
Optical	• No Need the use of bias lines • No intermodulation distortion	• Lossy behavior • Complex activation mechanism
Mechanical	• No need active elements • No need of biasing system	• Slow response • Requires power source
Smart Materials based Reconfigurable	• Low profile • Lighter weight	• Low frequency • Limited application

2.2.5 Antenna Reconfiguration Techniques

To obtain the required reconfiguration functionality must be choose one of a reconfigurable technique which led to get the desired results of functionality or characteristic. There are four global methodologies are utilized with antenna to realize the reconfiguration. In other word, to convert the classical antenna to smart antenna in order to adapt antenna for a practical wireless communication activity which needs an adaptive RF frontend. figure (2.16) is been shown these four categories techniques.

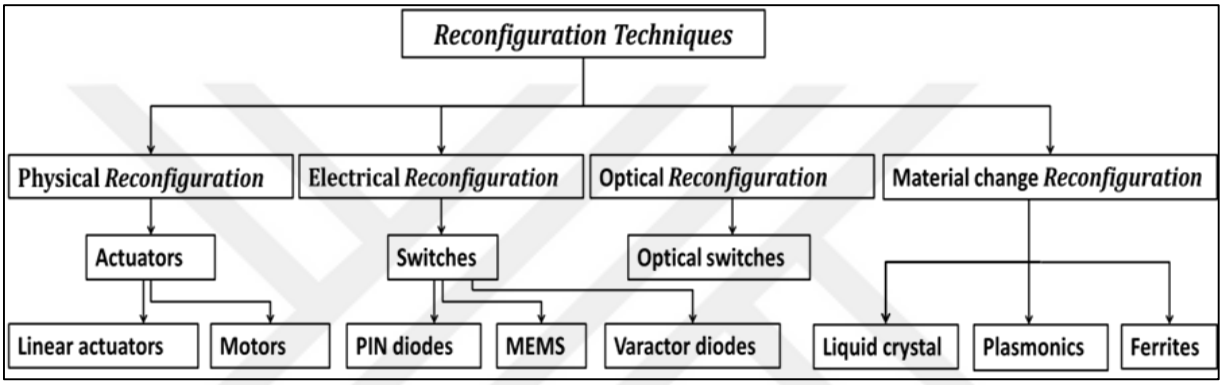

Figure 2.16: Reconfiguration techniques of reconfigurable antennas.

a. Physical reconfiguration

The best example of physical reconfigurable is a mechanical reconfiguration approaches that used the linear actuators and motors for build this type of reconfiguration. It does not need biasing networks such that in electrical reconfiguration techniques, but it does require the rotation mechanisms such as servo motor [41].

b. Electrical reconfiguration

This reconfigurability technique can be achieved by different types of switching techniques like image silicon, varactor diodes [42], PIN diodes [10], RF MEMS.

c. Optical reconfiguration

The photo detector switches (such as photo resistor) turn into conductive when expose it by light (such as laser beam) on antenna structure [43].

d. Material change reconfiguration

This type of reconfigurable techniques can be done by using Magnetic ferrites. Material modification is considered one of important factor to get the reconfigurable strategy such as Smart materials harmonized and liquid crystals [44].

Table (2.4) is shown the advantages and disadvantages of different reconfigurable techniques:

Table 2.4: Advantages and disadvantages of reconfigurable techniques. "tables continued" for the table overflowing to page 37.

Reconfigurable Technique	Advantages	Disadvantages
Varactor	Continuous tuning is produced and it Uses very nonlinear and also have A small less energy than other method	Very nonlinear and also have a small less energy than other methods. Dynamic range
physical	There are no biasing circuits required in the Slow responsiveness, high cost , high physical, which eliminates interference, power needs, large bulk, and difficult losses, and radiation pattern distortion	Slow response, High cost, High power need, large bulk
RF PIN	Less necessary driving voltage, higher on linear, it requires a high DC bias voltage tuning speed & power handling capabilities, and wastes a lot of energy In its ON low cost, and great reliability due to the state. Poor quality attributes tuning by lack of a moving portion.	On linear, it requires a high DC bias Voltage tuning speed & power handling Capabilities and wastes a lot of energy in cost, And great reliability due to the state Poor quality.
Optical	Linear Properties, High reliability, requires Complex, Loss behavior, activation with no biasing circuits	Complex, Loss behavior, active mechanism
RF MEMS	Insertion loss is low, isolation is good, linearity is great, power loss is low, and a DC supply is not utilized	High control voltage (50-100 V), low Switching velocity, poor dependability , short lifespan and discrete tweaking are all required
Smart	Size as it has high relative permittivity and permeability	Low efficiency

2.3 GENERAL STRUCTURE OF A MICROSTRIP PATCH ANTENNA

The microstrip antenna consists of very thin metallic surface as (patch), dielectric material as a substrate has a dielectric constant placed on a ground plane [45-46], as be clarified in figure (2.17).

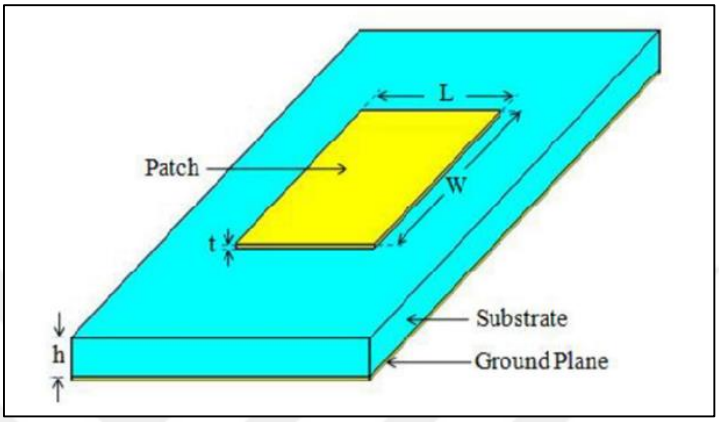

Figure 2.17: Microstrip antenna structure.

ground surface and patch are constructed of conductive materials like copper and gold that are engraved using different techniques. further, the patch can be designed of any geometric shape, regular or irregular.

It is important to mention the patch shape and dimensions, substrate thickness, feed line location, the dielectric constant, the microstrip antenna performances such as gain, bandwidth, resonate frequency and efficiency. For example, patch length (L) about ($0.3333\lambda g < L < 0.5\lambda g$) where λg presented the guided-wavelength of substrate plane. patch layer thickness is very thin compared with the ($t << \lambda g$). Numbers of substrates could be utilized to the microstrip patch antenna design that are either rigid or flexible. The height (h) of antenna substrate is generally calculated ($0.003\lambda g \leq h \leq 0.05\lambda g$). One of an important antenna parameter that affected on the antenna performances is a substrate dielectric constant (ε_r) that is about ($2.2 \leq \varepsilon_r \leq 12$) [47].

In general, the Microstrip antenna works in master mode, when its feed line is located in center of patch width (W) and in the end of patch length nearly (L). The correct position is achieved by electromagnetic field division in the antenna patch. Figure (2.18) is shown The difference for the electric field axis (voltage axis) and magnetic field axis (current axis) through antenna patch , it is clear the top value of current located at the patch center and lesser value located on left and right side, on other hand, voltage value is zero in the patch center, max value indicated on the left side and the minimum value indicated on right side.

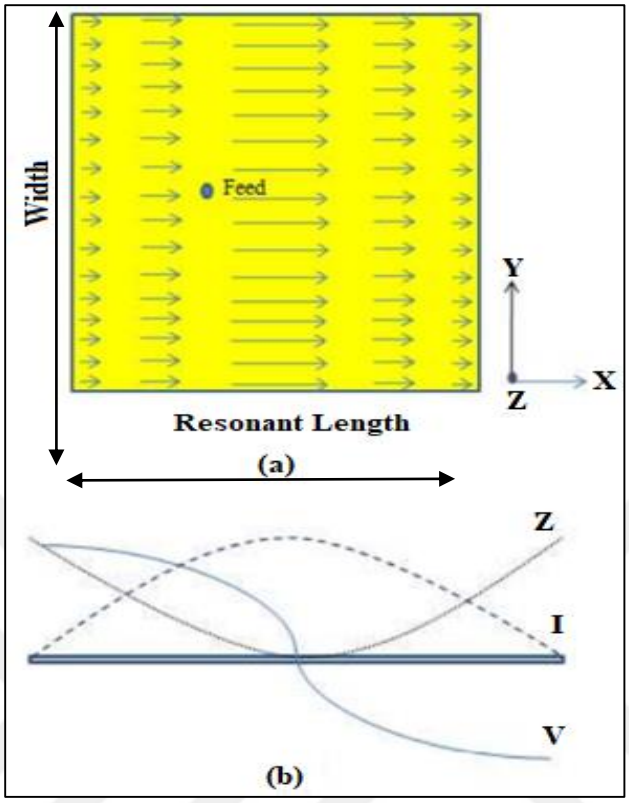

Figure 2.18: V-I-Z patch distribution (a) patch surface current distribution (b) the voltage (V), current (I) and impedance (Z) distribution along patch.

Where, Theoretically, the gain will be (0 zero) as the minimum value in t center of the patch surface and it equal to (infinite) as the maximum value in the patch edges. 50 possibly located somewhere along the antenna length where the antenna has to be fed.

2.3.1 Flame Retardant-(FR4) Substrate

FR-4 or FR4 is one of important microstrip antenna substrate type, where it is a glass reinforced epoxy plate material. It is composite material, consists of woven-fiberglass rag with epoxy-resin envelope which is flame-resistor in other word self-extinguishing. FR4 substrate is the preferred material for most printed circuit board PCB application. it has more advantages such as a good resistance-weight ratio, water absorption immunity, high mechanical strength and good insulating capacity in different environments whether its dry or humid, as well as, it has low cost and variable material that make it as main standard for production of PCBs or electronic prototyping fabrication [48]-[50]. FR4 layer are an electrical insulator with high dielectric constant, where it has the dielectric constant (ε_r)=4.4.

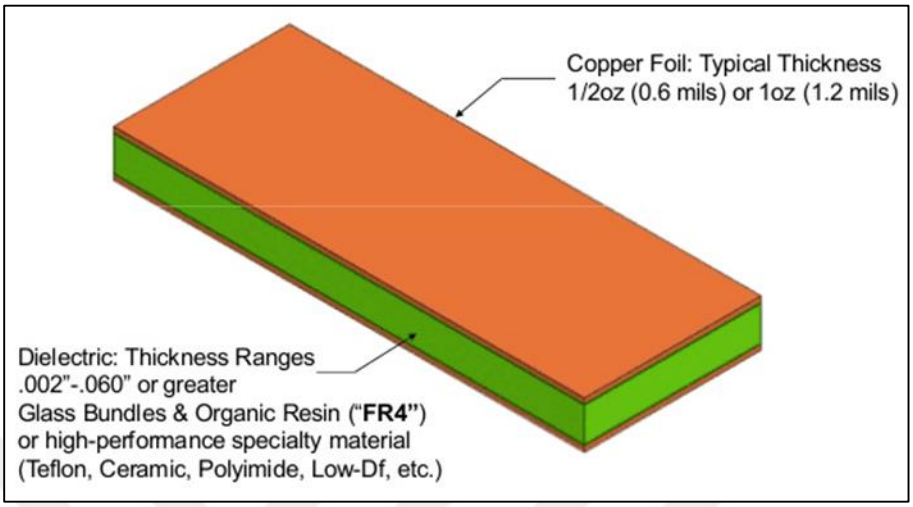

Figure 2.19: FR4 structure.

2.3.1.1 FR4 characteristics

a. High mechanical strength and dielectric property.
b. Good resistance material to heat and humidity.
c. high mechanical processing property

2.3.1.2 FR4 applications

Due to the its insulation property, RF4 is used for industry equipment like transformer insulation boards, insulation parts of motors, grinding gears and electronic switch boards. It can show below the more popular its applications.

a. For machine parts such as insulation gasket, ships parts, lapping carrier.
b. For electronic requirements as lithium battery
c. The black type of FR4 for portable solar pane
d. For series of (PCB)Printed Circuit Boards
e. As a substrate surface of Microstrip Patch Antenna

2.3.2 Feeding Techniques

This section concentrates to list many techniques of feeding (RF) radio frequency power for microstrip antenna. In general, these techniques divided into two varieties, contacting and non-contacting type. In first type, (RF) power is feed instantly through a connection point between RF source and the patch as a microstrip line. In other hand, in second type an electromagnetic field work to transfer power between the radiation patch and RF source line [45]-[46]. there are five feed techniques that used widely; coaxial probe (contacting category), microstrip line, aperture coupling, proximity coupling (both non-contacting category) and coplanar waveguide. The most important role of feeding techniques is realized maximum coupling, which leads to a maximum achieved gain. in other side, the undesired radiations, wave losses, faked radiation, and side lobes will be caused the gain decreasing [30],[47].

2.3.2.1 Coaxial probe cable

This feeding is shown in figure (2.20). Is a simplest feeding technique of microstrip patch which the inside jointer of a coaxial cable is welded to antenna radiation patch while the outer of jointer is linked to a ground surface [30]. this technique has many advantages as be list below:

a. Easy of fabrication.
b. Easy to matching.
c. Low fake radiation.

In other side it has numbers of limitations such as:

d. narrow bandwidth.
e. complex design especially at heavy substrate due the hole that drilled in substrate.
f. Mismatched problem at rising substrate thickness where the input impedance to be high inductive.

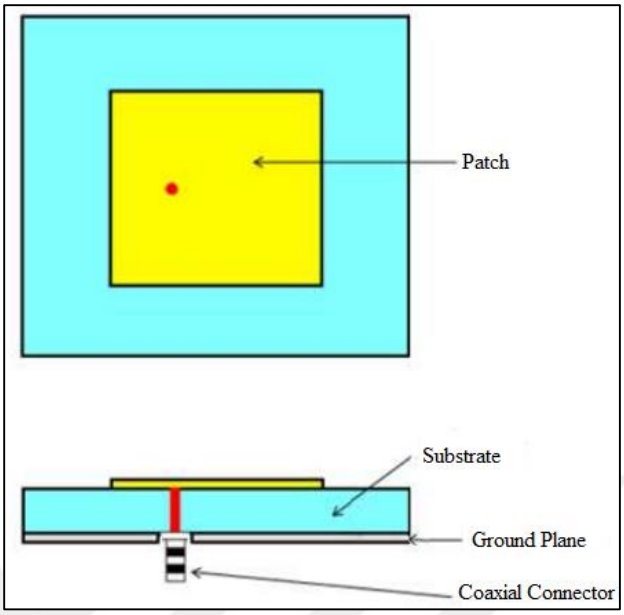

Figure 2.20: Coaxial probe feed for rectangular microstrip patch.

2.3.2.2 Microstrip feed line

Second simple feeding technique of microstrip patch antenna is a microstrip line. This type is connected directly to the patch surface on the substrate layer which allow planar structure, as be clarified in figure (2.21). it is possible to realize the matching between the feed-line and patch [30]. This feed technique has more advantages such as:

a. Easy of fabrication.
b. Simple model.
c. Has Impedance matching

And it has some of Limitations such as:

a. Feed line radiation.
b. in thicker substrate the surface waves are increased which limits the (B.W) of antenna radiation.

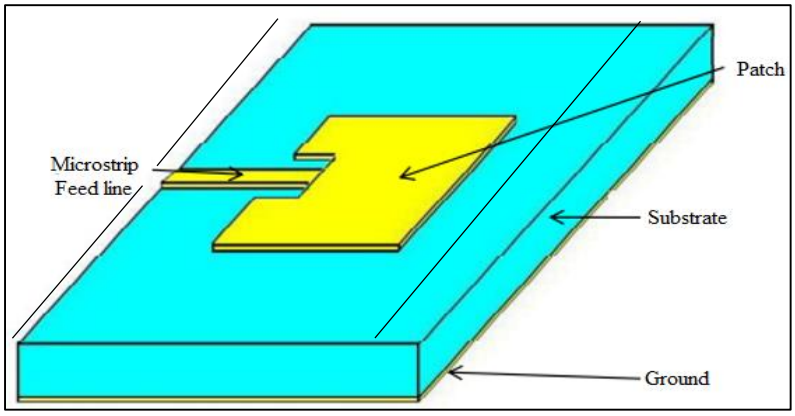

Figure 2.21: General view of microstrip feed line technique.

2.3.2.3 Proximity-coupling feed

Is a non-contacting feeding technique as can be shown in figure (2.22), this feed method builds by located a feeding line between two dielectric-substrate while remain patch position above upper substrate [30]. its benefits are listed below:

a. Eliminated the spurious feed radiation,

b. Provide very high B.W (increased by 13%)

c. Matching is completed easily because it can control to antenna patch width-to-length ratio and feed line length.

While, can be describe the limitations of it as listed below:

a. Difficult of fabrication because the two dielectric substrates need proper bias.

b. Increasing the antenna thickness.

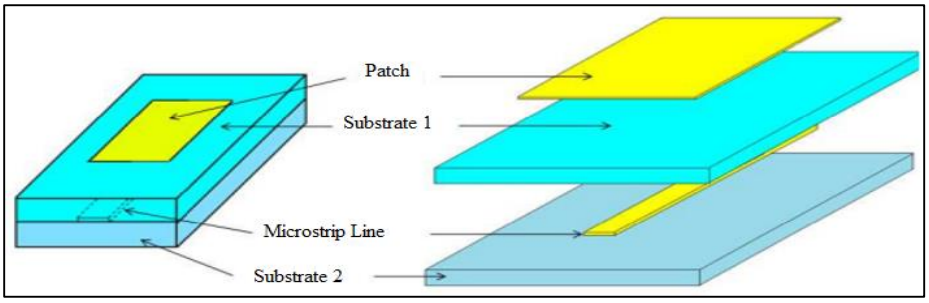

Figure 2.22: Proximity coupling feeding technique general view [48].

2.3.2.4 Aperture-coupling feed

Is considered a non-connecting feed technique, in this type the feed line is discrete on microstrip patch by substrate1, ground and substrate2, as be clarified in figure (2.23) [47], the ground layer is placed between two substrates, a bottom substrate use thick dielectric material while a top utilize lower thick dielectric material to realize the patch radiation [30]. generally, patch surface is located on the top layer. The ground layer includes a (slot- coupling) positioned down the patch middle for top coupling direction to reducer cross gathering due to arranging symmetry. Size, shape and aperture position are specified the rate of patch coupling into the feed line. Advantages of this feed technique are listed below:

a. Decreasing the false radiation because a ground surface is separating antenna feed line and patch surface.

   in other side, some limitations such as:

a. Difficult fabrication because it consists of several layers, which cased in result the high antenna thickness.
b. Bandwidth is narrow.

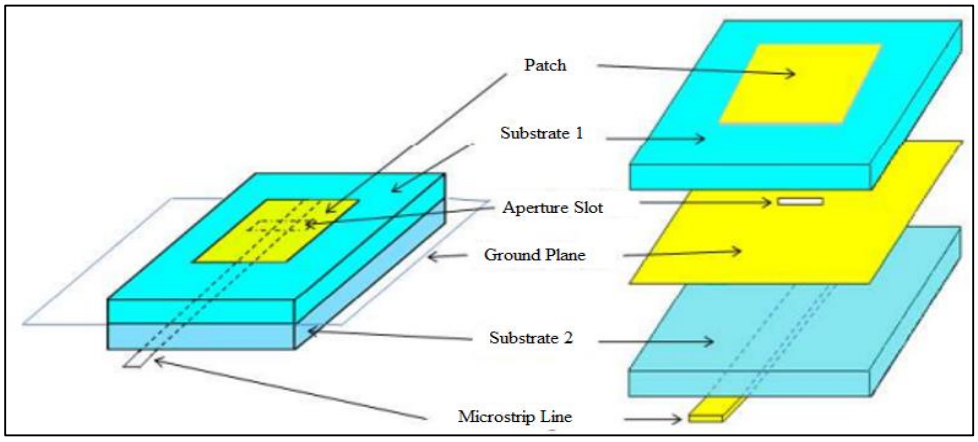

Figure 2.23: Aperture coupling feeding technique general view.

2.3.2.5 Coplanar-waveguide

It was invented in 1969 by Cheng P. W [51], firstly, as a way of incorporating non-mutual components and isolators to transmission line. classical coplanar waveguide is simple design, that designed to printed the patch feedline on dielectric substrate and locate the two divisions of conductor ground plane above of substrate (one division on each side),

this technique can be seen in figure (2.24).where all three conductors are coplanar because they are on the same dielectric substrate.

This technique is considered one of electrochemical planar transmission line forms, is made by utilizing circuit board technique and is utilized to transmit Microwave spectrum. This transmission lines are constructed in the monolithic microwave integrated switches with minimum size [51]. The advantages of this feeding technique listed below:

a. Low dispersion
b. Simple realization
c. Broadband performance

but the its disadvantages are listed below:

a. High cost fabrication
b. It is need thick substrate relatively.

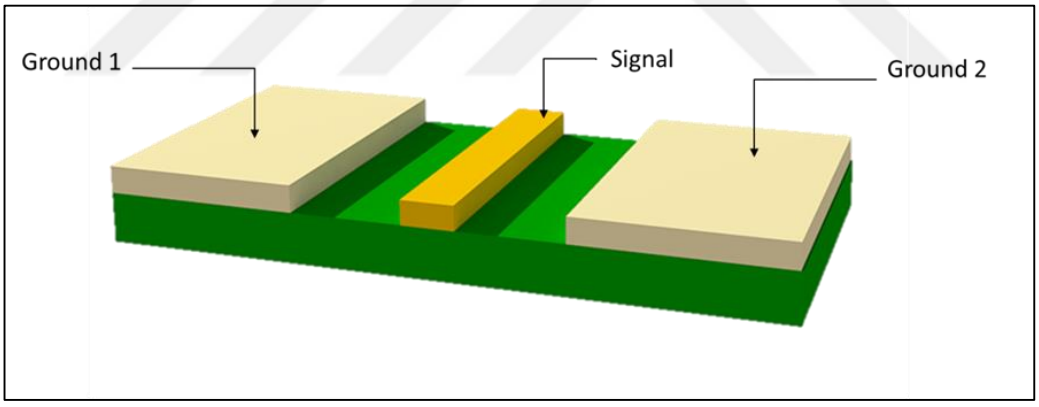

Figure 2.24: Co-planer waveguide.

2.3.3 Effective Parameters

First step of antenna design is guessing antenna length (L) and width (W) [45],[46]. patch length and width are computed by utilizing equation (2.10) as shown below.

$$W=\frac{C}{2f_r}\sqrt{\frac{2}{\epsilon_r+1}} \tag{2.10}$$

where c is the light velocity, ϵr is a relative permittivity and fr is a resonance frequency.

While, the effective parameters are (effective length, resonant frequency, and effective width) due to the fringing effects and the electrical features of patch are greater than its physical dimensions. To evaluate patch length must be calculate some parameters [47] such as $\epsilon_{r_{eff}}$:

$$\epsilon_{r_{eff}} = \frac{\epsilon_r + 1}{2} + \frac{\epsilon_r - 1}{2} \left(1 + 12 \frac{h}{W}\right)^{-0.5} \tag{2.11}$$

(ΔL) is an extension length (where it represents length increasing due fringing field) is can calculate by equation (2.12):

$$\frac{\Delta L}{h} = 0.412 \frac{(\epsilon_{r_{eff}} + 0.3)\left(\frac{W}{h} + 0.264\right)}{\left(\epsilon_{r_{eff}} - 0.258\right)\left(\frac{W}{h} + 0.8\right)} \tag{2.12}$$

mentioned to above equation, it can be calculating the patch actual length as be clarify in equation (2.13):

$$L = \frac{C}{2 * f_r * \sqrt{\epsilon_{r_{eff}}}} - 2\Delta L \tag{2.13}$$

Now, it can be compute the length and the width of antenna ground surface by benefits from equations (2.10) and (2.13) as be shown in equations (2.14) (2.15) that shown below:

$$L_g = 6h + L \tag{2.14}$$

$$W_g = 6h + W \tag{2.15}$$

2.3.4 Fractal Geometry

In modern life, wireless communication devices are converting into portable due to application requirements of new developed technologies. Antenna is the main element that needing in these devices. Hence, antenna miniaturization is an important topic for many latest researches [52]. To minimize Antenna-profile needing understand the relationship between physical antenna size and its operation wave-length. This relationship is a base factor that affected in antenna design. The antenna size is proportional with its operating frequency inversely but when antenna size is miniature, its electrical influence surface reduced with no change on operation frequency. As the antenna electric size is dependent on operating wavelength (λ) there is the antenna physical size can be expressed as half, quarter or any ratio of resonating (operational) wavelength [53].

Fractal geometries have more applications in different fields such as biology, geography and engineering. In engineering field, fractal geometry has been utilized on antenna design processes, design of (FSS)-frequency selective surface, digital image processing and bio medical signal processing, where theory concept of fractal antenna design is introduced modern research area. Due to various attracting features of fractal antennas, it is considered major attraction of recent research [54],[55].

The “fractal” is described by any geometric subject such a line or geometry shape that is regular or irregular. where it looks-like a broken shape in systematic and comprehensive method. In this geometry, original object is divided into several small parts, each small division be identical to original. This property is named (self-similar) which occurs on different manufacture stages. Original object is scaled with various dimensions that is named (scaling property). Usually the natural objects are (self-similar) that makes the fractal structures appropriate for miniaturized antenna design field [53].

(Space-filling) property results is electrically large size features, although the physical size is remained small. The (self-similar) property supports utilizing the iteration function system for similar shapes. The (self-scaling) enables the iteration function system to utilize similar shapes by multiple scales. These three properties enable fractal geometry to be efficient for using in small areas. where it allows to antenna miniaturization process to produces more curves that considered very long electrically with compact structured [56]. Due to the fractal properties which presented above, the fractal-geometries great utilizing in fractal antenna designs. When compared the fractal

antennas and traditional antennas, it is found that a fractal antennas have more advantages than conventional antenna such high B.W with very miniature antenna size and it have multiple resonant frequencies that caused multiband. All these properties make it suitable for modern wireless applications. Figure (2.25) clarified different shapes of fractal geometry.

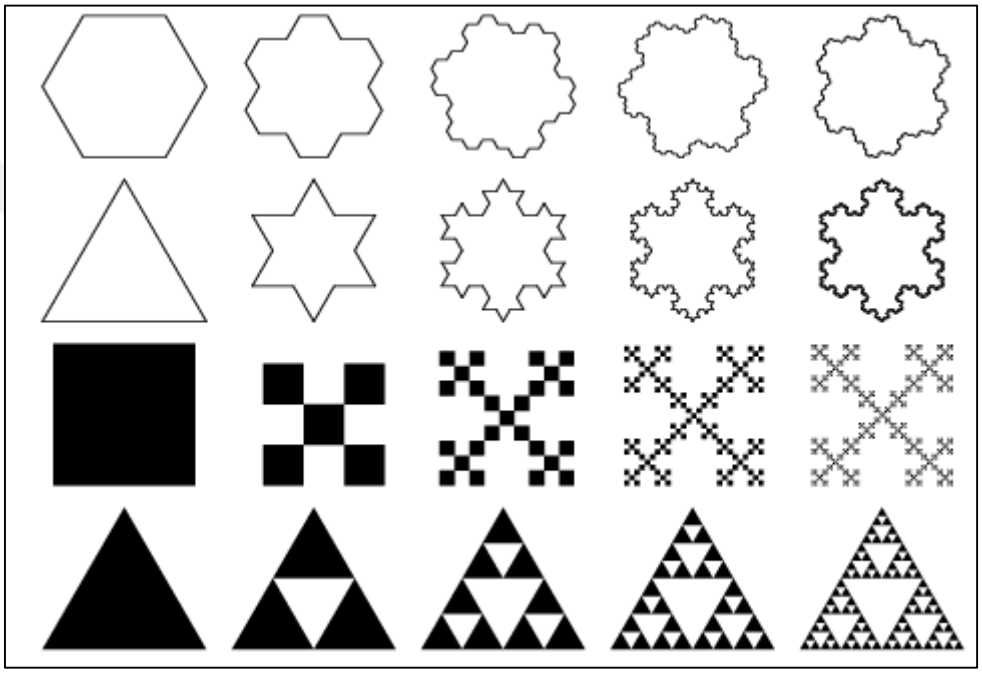

Figure 2.25: Various shapes of fractal geometry.

2.3.4.1 Moore fractal geometry

Moore structure is a form of a fractal geometry**.** Moore curve is a continuous fractal as (space-filling curve) that is vary of Hilbert curve, exactly it is considered the loop version of Hilbert curve and it may be describe as combination of four copies of Hilbert curves in certain method to make the endpoints are matching. Figure (2.26) presents a single cell of Moore fractal curve [57].

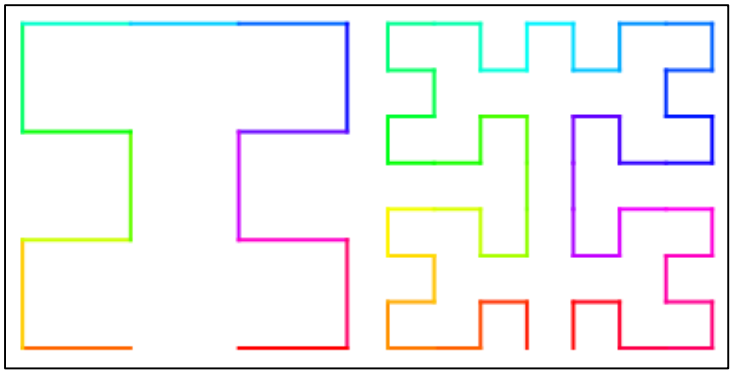

Figure 2.26: Unit cell of the moore fractal curve.

2.3.5 Microstrip Antenna Advantage and Disadvantages

Microstrip patch antenna has a low profile, less weight and is simple to fabrication, because these features its widely used in modern wireless devices like cell phones, pagers and other sophisticated communication systems that need good performance such as (satellite, , spacecraft etc). [58],[59] Some of microstrip antenna advantages are listed below:

a. Low cost
b. It is possible to Manufacture.
c. Reconfiguration ability.
d. Antenna design is easy with desirable polarization.
e. .High Mechanical performance such as shock Resistant.
f. Convenient to microwave spectrum.
g. Suitable to antenna array that has high gain and directivity.

Contrariwise, the microstrip antenna has number of limitations when compared with other types of antenna. Some of the major disadvantages are listed below:

a. Cross polarization.
b. non-efficient polarization parameter.
c. affected by faked feed-radiation
d. Narrow band width (5% - 10% without using any technique)
e. losses on dielectric and conductor material.
f. Sensible to environmental-conditions such as temperature.
g. Has surface wave which occurs at used high dielectric constant of substrate.

h. Low and moderate gain.

There are different methods to eliminate this limitation, microstrip antenna bandwidth could be increased by utilizing a special method such as (defected ground plane strategy, stacked Patches, slotted patches, parasitic patch) [60],[61]. Microstrip antenna gain and power handling capability could be enhanced by designing antenna array. Usage of (EBG) structure and (MTM) are support antenna characteristics improvement [62]-[64].

2.3.6 Microstrip Antenna Applications

Due to more advantages of microstrip antenna, it is used in different modern wireless communication applications. Microstrip patch antenna wide utilize in the military systems such as aircraft, satellites and rockets [58],[59]. In new life, the usage of microstrip antenna in commercial field is increasing due to its less cost and easy fabrication as well as its used in advanced printed circuit technology. because the development present researches of microstrip antenna design field, the expected in near future most of traditional antennas would be replaced by microstrip patch antenna. other main applications of microstrip antennas are listed below:

a. Mobile Communication [65].
b. Satellite Communication.
c. (GPS) Global Positioning System.
d. Direct Broadcast Satellite System.
e. In Radar Applications.
f. Medical applications [66].

2.4 ANTENNA-ARRAY

Study of one antenna element indicates that radiation is uniform-distributed and it can generate wide beamwidth but the directivity and gain are low relativity. For example, in dipole antenna, max-radiation occurs in the normal direction of its axis while reduce slowly at move towards antenna axis. This type of radiation form may be preferred for broadcast services due to its cover wide area but is not preferred on (point to point) communication service. Thus, for meet the needs of (point to point), the design of antenna must be offer narrow- beam and high directivity and radiation must be emitted to desired direction. Antenna size increasing is a simple way to realize this requirement, because an antenna large size leads to high directivity characteristics [67]. But

this way is inconvenient practically, because the antenna to be bulky and it is need wide area to instillation. Other way to enhance antenna performance, increasing gain value and high signal directivity but without antenna size increasing is proposed in [68] by arrange antennas in certain configuration, spaced and phased which supports the maximum gain to desired direction and neglected other directions. From this method, we can get high directive-gain. This arrangement of more than antenna is pointed to antenna array, each antenna arranged is known an element. Array elements are found at any type (dipole, slot, aperture, etc.). The antenna array benefits from interference phenomenon which occurs between radiations of different elements. where it is considered one of the ways to combinate the radiations that generated from multi radiators, thus the interference is occurred that be constructive in prefer direction and destructive others. Main task of array is to generate high gain-directive. Field is represented as vector in both magnitude and phase. Overall antenna array field at any point that far from its center is the field vectors sum that produced via the individual antennas. The phase field of each element field depends on the distance which separates between elements of array that in turn depends on the direction. In general, antenna array types can be classified into four classifications [30],[69] as be listed below:

a. Broadside array
b. End-fire array
c. Collinear array
d. Parasitic array

2.4.1 Broadside Array

This array type arranged the number elements in line which draws perpendicular to their radiation axes [69]. The spaced that separated between these elements are equal space and the fed current is equal in magnitude and in same phase. Feed technique is supported array to fire on broad-side direction that be vertical to array elements axis, it represents the maximum radiation while the small radiation on other direction. if the element pattern directional so, the array can be radiate maximum radiation in same direction. In figure (2.27) (a), it can be clarified the antenna array elements are arranged on horizontal-axis at equal space between their and the radiate direction is vertical to elements axis. in other elements arrangement, the array elements can be arranged in vertical-axis but in this state, the radiation direction will be horizontal. In conclusion, the geometry

arrangement of broadside-array is represented by arrange all array elements in one axis while the major lobe be vertical to these axis (the plane containing the array elements). Broadside-array radiation pattern is displayed in figure (2.27) (b). In broad side array the bidirectional pattern can be converted to uni-directional by placing identical array by distance equal to (λ/4) behind this array and the fed current is leading 90^{o} .

Figure 2.27: Broadside array (a) broadside Geometry (b) radiation pattern.

2.4.2 End Fir Array

This type of array is similar for broadside-array in view point of array elements arrangement but the basic variance appearance in direction of main lobe radiation. where trend of main lobe is vertical to array axis in broadside array; while its direction in along array axis in end fire-array [69],[70]. As be clarified in figure (2.28).

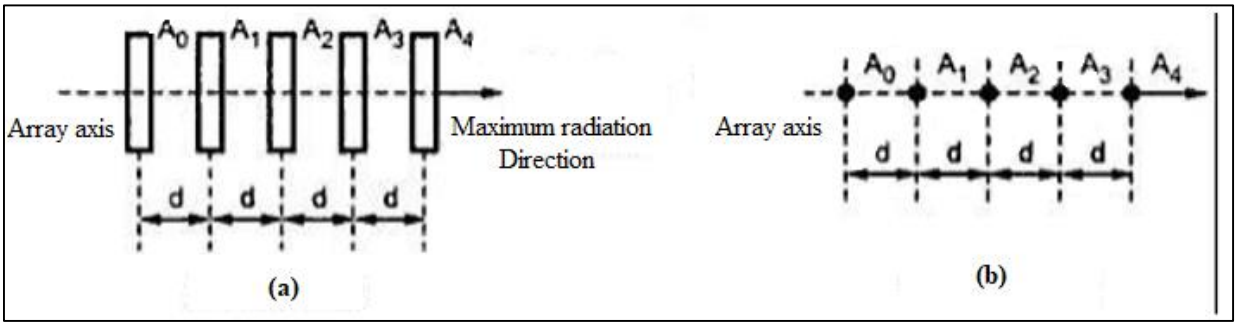

Figure 2.28: End fire array (a) top view (b) front view.

In end fire-array the number of elements is spaced by equal distance along array line. All elements are feeding individually with equal magnitude current but in different phases, gradually, the elements that arranges in same axis generate maximum radiation along array axis. Finally, this array can be defined is array which generates unidirectional max radiation that along array elements.

2.4.3 Collinear Array

In this type of array elements are arranged coaxially, so, elements are either arranged end to end form over one line or stacked one on other [69]. An array is same broadside array where the antennas are feeding through equally phase current. But its radiation pattern has circular symmetry and the major lobe anywhere is normal to major axis. For this reason, this array type is known a broadcast or Omni-directional. Simple collinear array includes two elements and it can have more than two antennas as be shown in Figure (2.29). the Collinear Array characteristics does not depend on elements number directly. For example, gain for array that contains (two, three, and four elements) is (2 dB), (3.2 dB) and (4.4 dB) respectively [30]. Gain ratio of (4.4 dB) acquired by array is a comparatively lesser than gain obtained through other arrays. Maximum gain can be obtained when the space between elements is arranged from (0.3λ to 0.5λ), but this much distance leads to difficulties structure and feeding. To operate the antennas must be arranged their ends much close and connected simply by insulator.

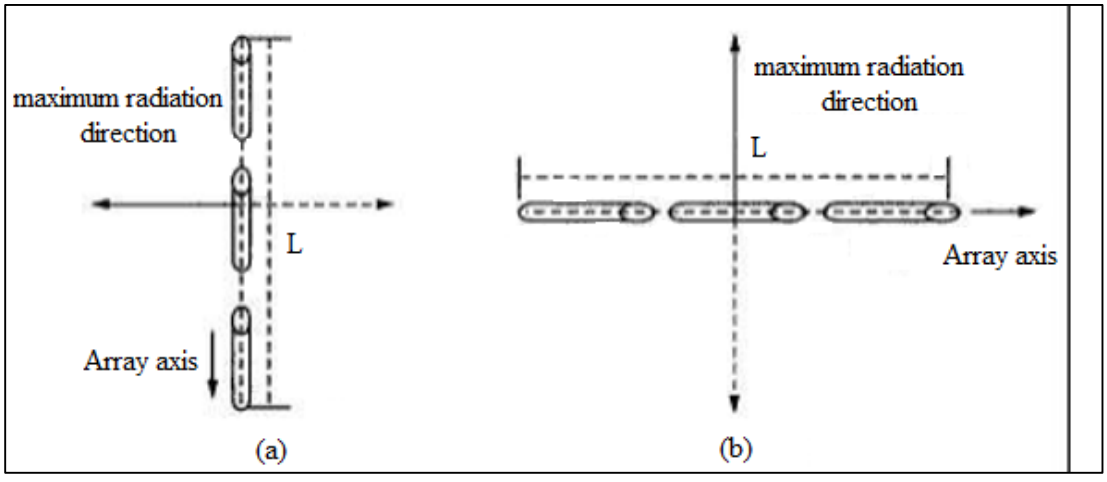

Figure 2.29: Collinear antenna array: (a) vertical-array (b) horizontal-array.

Increasing length of collinear-array leads to increase directivity, moreover, if elements number of single array more than (3 or 4), in order to keep these elements current in same phase, it is necessary to link a phasing-stub between neighbor elements. usually the collinear-array is coordinate on vertical axis for increase the total gain and directivity on horizontal direction. For example, Stack dipole antennas by increase its number to double with proper phase is produced increasing (3dB) of directive gain [67].

2.4.4 Parasitic Array

This array is somewhat similar broad side-array but only one antenna can feed directly from source while other elements are connected electromagnetically, due to their nearness from feeder element. A feeder element is called (driven element) whereas other elements are known (parasitic element) [69]. A parasitic element longer by (5%) to represent the driven element as reflector and another element shorted by (5%) represents a director. Reflector works to make direction of max radiation vertical to driven element which helps to make maximum radiation is vertical to next parasitic. Simple array has three elements: reflector, driven element and director. Where it can be shown this type of array in Yagi-Uda antenna array. Current phase and amplitude in parasitic element are depending upon it tuning, distance between antennas and driven element which connects with its. The difference of distance between the driven-element and parasitic-elements lead to change the relative phases so, it helps to make pattern as unidirectional. distance of ($\lambda/4$) and ($\pi/2$) radian phase difference offered a unidirectional-pattern. Proper design of parasitic array has distance (0.1λ-0.15λ) offers frequency band width of 2% order, gain about 8 dB and forward to back ratio (FBR) around 20 dB. It acts good practical example, especially on frequency band (100 - 150 MHz), Yagi-array utilized for TV reception. It can be constructed simplest array configuration by used two points sources have same polarization and discrete via finite-distance. The array construction concept can be extended by increase the elements number and isotropic array can be created. Depending on isotropic point sources conditions (amplitude and phase), can be classified this array into three types [68]:

a. Array of equal-amplitude and phases.
b. Array of equal-amplitude and opposite-phases.
c. Array of unequal-amplitude and opposite-phases.

2.5 MIMO BASED ANTENNA ARRAY

(MIMO) Multiple-Input Multiple-Output is very important wireless technology that utilizes multiple transmitters and receivers, it uses for transmitting more data rate at the same time and to treat the lack of data problem faced by conventional wireless communications techniques (SISO) under interference multipath conditions and signal fading [71]. MIMO technology is divided into three types that lists below:

a. Point to point MIMO: this type is presented in 1990 as a simple MIMO form that consists of base station supported by antenna array as source station so the various terminal is orthogonal multiplexed as be clarified in figure (2.30) [72].

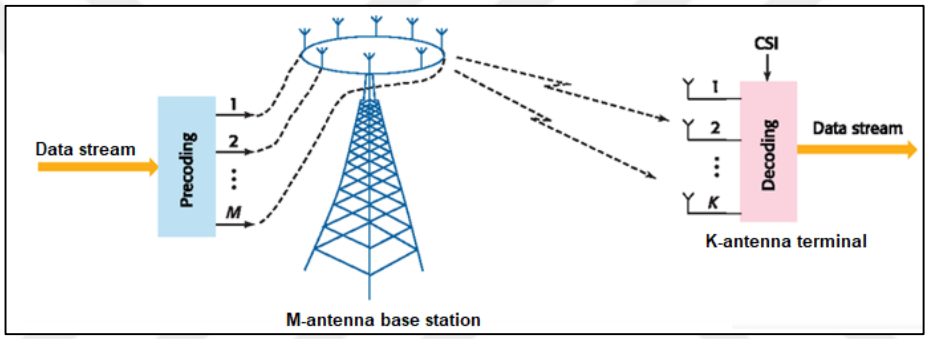

Figure 2.30: Point to point MIMO system.

b. Multiuser MIMO Second type, the idea of this type is that a single base station to serve a multiplicity terminal using the same time–frequency recourse and the multiuser MIMO is obtained from point-to-point setup by breaking number of antenna in terminal side as clarified in figure (2.31) [43],[72].

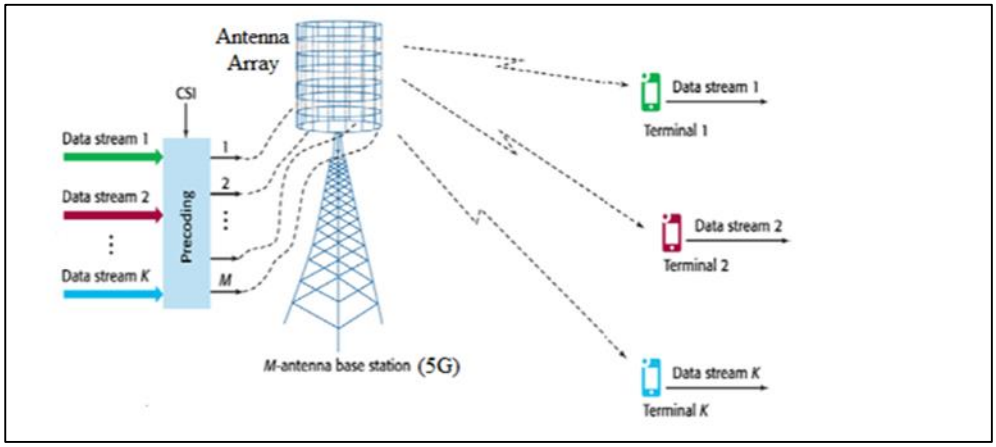

Figure 2.31: Multiuser MIMO.

c. At last Massive MIMO: Each base station is equipped with a large number of antenna terminals so in massive MIMO there is no Cooperation in among base stations that show in figure (2.32) [73].

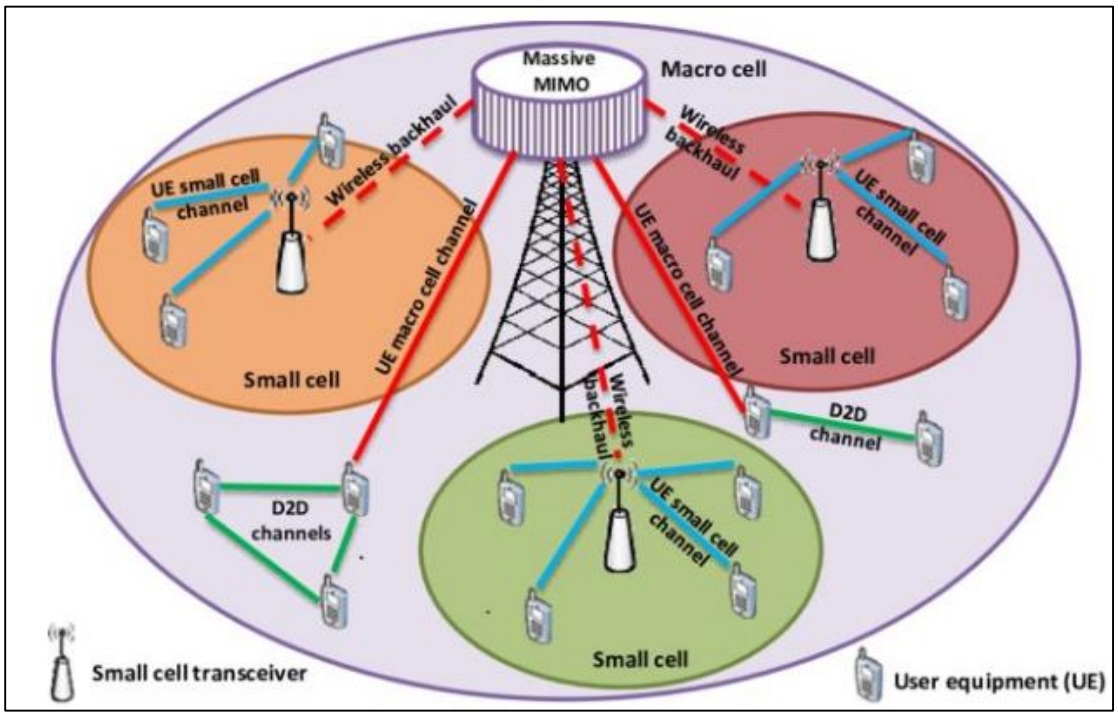

Figure 2.32: 5G massive MIMO.

5G antennas have several advantages as faster speed, lower latency, high capacity for large number of connected devices, less interference, and high efficiency. Antenna miniaturization for sub-6 GHz 5G is critical for increasing MIMO channels capacity in order to make the smartphones and other mobile terminals more ergonomic and multifunctional [71],[72].

3. CHAPTER THREE

In this chapter, the concept, structure, advantages, disadvantages and applications of renewable energy resources-RFEH system and solar PV cell are displayed as be following parts:

3.1 OVERVIEW ON RFEH SYSTEM

Harvesting energy is one of most important modern technique. most of surrounding energy sources are found as solar, thermal and physical movement [74], thermoelectric and kinetic-energy [75], respectively. But none all these sources can offer a continuous power because it nature. Collecting energy of RF is suitable E-harvesting way, where the power is offered until interrupt the source signal [19].

Radio Frequency Energy Harvesting-(RFEH) is modern technology due to it has many advantages over the more popular technologies. There are more methods that used to develop the effective of (RFEH) to generate enough power for operating urgent autonomous systems which needs low power such as WSN, IoT and RFID. [76].

Power could be transport via utilizing inductive-coupling for short distances, where the inductive-power carried to medium distances while (RF) power for long distances. Wireless Power Transfer-(WPT) is new technique can deliver power into wanted locations, especially, that are not accessible on classic energy harvesting methods. many ways to achieve wireless power- supply. (Near-field) inductive-coupling operates on some centimeters, however, it is featuring of high efficiency, this method is independent on radio wave propagation. It works on much short distances than wavelength of energy supply. This approach is used in consumer products that needs wireless charging of rechargeable battery like the electric shavers or toothbrushes [77]. it can transfer energy in near-field by effect of magnetic coupling between two components (usually happened at coils). This technology used huge transmitters and receivers and transfer energy over short ranges. The highest power efficiency occurs at close to optimal operating point. Transfer efficiency can be realized up to (70%) with considering losses between transmitter and receiver for distance not more than 1 meter, but, the whole system efficiency is below (20%). In other hand, energy can be transferred by utilizing high frequency field properties, high power (RF)-energy along one km-distance with more than 70% of power efficiencies. Same technique is used for

transfer power within distance range less than 10 m for high frequency-Radio Frequency Identification devices [76],[77].

3.2 RFEH SYSTEM DESCRIPTION

Components of RFEH technique are arranged into four parts [78]-[80].

a. Impedance matching circuit

b. Rectifier circuit

c. Dc- Pass filtering

d. load

It can be shown in figure (3.1). The load is represented DC energy storage tool like (battery, capacitor, etc.) or direct power device. In both states, load contents such as resistors and capacitors are not constant. Requirements of rectifier characteristics would be achieved by analyzed signals of antenna output or rectifier input and load input, when antenna integrated with RFEH system is called Rectenna [79].

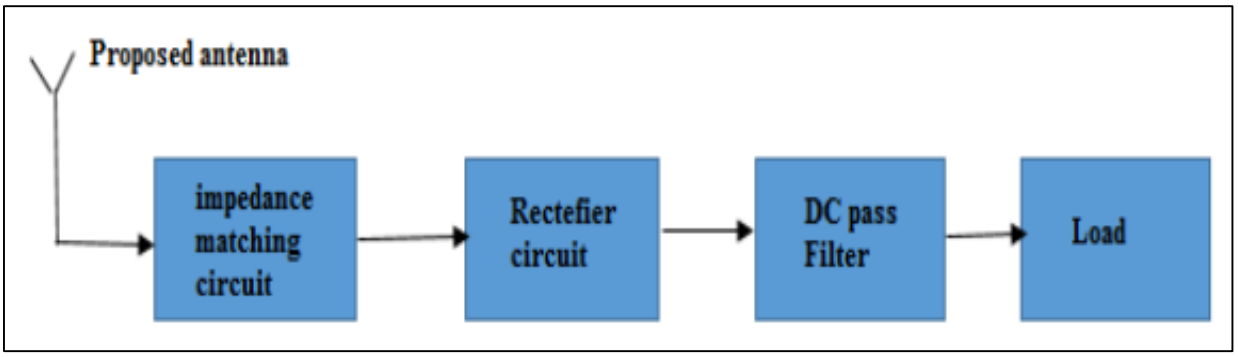

Figure 3.1: Block diagram RFEH system.

3.3 IMPEDANCE MATCHING TECHNIQUES

It is represented one of most importance parts of microwave system components. Simply, it is defined as process that making one terminal of impedance resemble another terminal. Oftentimes, it is very important to match load impedance and source impedance.

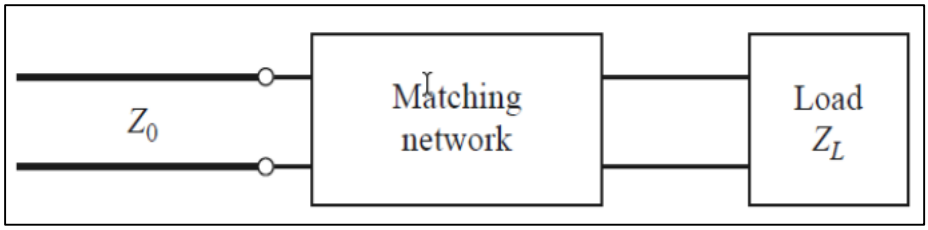

Figure 3.2: Impedance matching network.

It is located between load and (T.L.) as be clarified in figure (3.2). it realized on ($Z_0 = Z_L$) that satisfies maximum transferred power on this connect point as be clarified in figure (3.3), ideal matching-network is lossless for realize maximum delivered power of network. In matching circuit, reflections of T.L. will be rejected on left side of matching network, with consideration, there will be take place more reflections between load and matching circuit. There are many types circuits can be utilized for impedance matching [79]. This chapter will be explained the summarize of most rife impedance matching techniques.

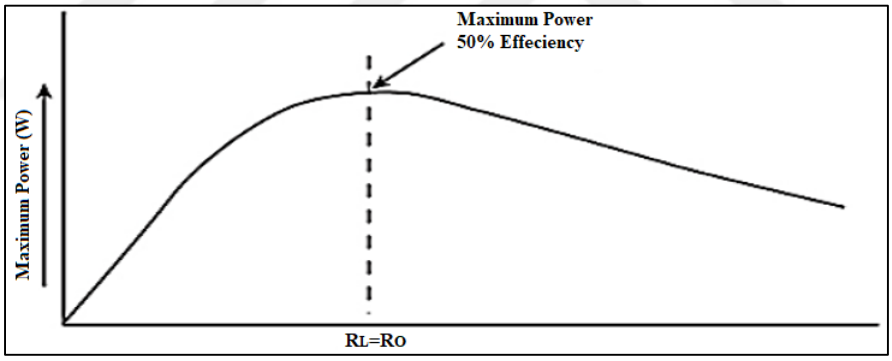

Figure 3.3: Relation between R_l and max delivered-power [79].

3.3.1 Quarter Wave Transformer-Matching Network

This type is simple matching technique, it is a transmission line that have length as quarter wavelength with characteristic impedance Z_1 which produces matching system when putting between the (R_L) and (T.L) impedance (Z_0). To calculate the Z_1value that required for matching, we use lossless equation (3.1):

$$Z_{in} = Z_1 + \frac{R_L + jZ_1 \tan \beta l}{Z_1 + jR_L \tan \beta l} \tag{3.1}$$

Where $\beta l = (\frac{2\pi}{\lambda})(\frac{\lambda}{4}) = \frac{\pi}{2}$ then $\tan \beta l = \infty$, $Z_{in} = \frac{{Z_1}^2}{R_L}$

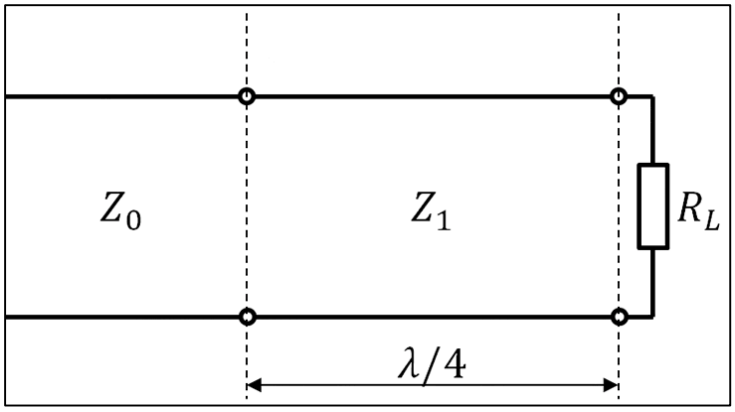

Figure 3.4: Quarter-wave transformer impedance matching.

To matching network, (Z_{in}) must be equal (Z_0), Hence**:**

$$Z_{in} = Z_1^{\,2}\, R_L = Z_0 \Rightarrow Z_1 = \sqrt{Z_0 R_L} \qquad (3.2)$$

3.3.2 Lumped Element-Matching Network

L-section with lumped elements are represented a simple form of impedance matching techniques, that used two lump elements for matching load impedance to (T.L) as be clarified in figure (4.5), this network has two ways for matching. First method by normalized impedance is ($Z_L = Z_L / Z_0$) inside $(1 + jX)$ circle on Smith chart, then should be used a circuit in figure (4.5) (a). Second way on Z_L is normalized form outside circle $(1 + jX)$ in chart, then we should utilize a circuit in figure (3.5) (b). The resistance of $(1 + jX)$ circle on chart ($\gamma = 1$) "where (γ) is the complex reflection coefficient" and the reactive elements are represented Ls or Cs [79],[80].

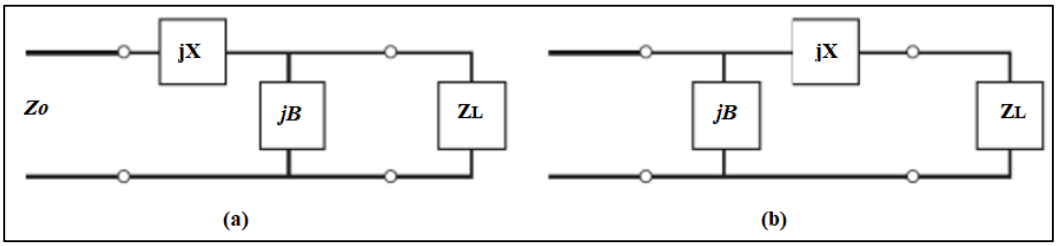

Figure 3.5: L-section matching network (a) normalized load impedance ($Z_L = Z_L / Z_0$) inside circle 1+JX (b) load impedance in normalized form $(Z_L = Z_L / Z_0)$ outside circle 1+JX [82].

In circuit (a) of figure (3.5), summation of total impedance of L-section and Z_L must be equal to Z_o, to meet matching so:

$$Z_0 = jX + \frac{1}{jB+1/R_L+jX_L} \tag{3.3}$$

After reorganized the equation (4.3) and breaking it into real and imaginary part, it can be obtained two equations of two unknowns (*X and B*):

$$B\,(XR_L - X_L\,Zo) = R_L - Zo \tag{3.4}$$

$$X\,(1 - BX_L) = BZo\,R_L - X_L \tag{3.5}$$

By solving the equation (3.4) for *X* and substitute in equation (3.5) produces quadratic equation of *B* in equation (3.6), there are two solutions of *(B* and *X*). It can achieve these two solutions physically by negative and positive values of either *X* or *B* (+*X* is inductor and -*X* is capacitor, while +*B* is capacitor and -*B* is inductor). Both solutions are clarified in equation (3.6) below.

$$B = X_L \pm \frac{\sqrt{R_L/Zo}\,\sqrt{R_L^2+X_L^2+ZoR_L}}{R_L^2+X_L^2} \tag{3.6}$$

The series reactance is found in equation (3.7), due to ($R_L > Z_o$), second square root is always positive.

$$X = \frac{1}{B} + \frac{X_L Zo}{R_L} - \frac{Zo}{BR_L} \tag{3.7}$$

If Z_L outside circle (1 + jX) in Smith chart, this means ($R_L < Zo$), we can use circuit (b) in figure (3.5), for an impedance matching condition, the acceptance must be equal (1/Zo), the load impedance is be seen in equation (3.8).

$$\frac{1}{Zo} = jB + \frac{1}{RL+j(X+X_L} \tag{3.8}$$

By arranging equation (3.8) and breaking it into imaginary and real part, produce two equations of B and X variables .

$$BZ_0 (X + X_L) = Z_O - R_L \tag{3.9}$$

$$(X + X_L) = BZ_O R_L \tag{3.10}$$

For solving the equations, the (X and B) gives:

$$X = \pm \sqrt{R_L (Z_0 + R_L)} - X_L \tag{3.11}$$

$$B = \pm \frac{\sqrt{(Z_0 - R_L)/R_L}}{Z_o} \tag{3.12}$$

Usually, the square roots value is positive due to ($RL < Z_O$). For notation, these two solutions are possible. For making match load to line impedance (Z_o), imaginary part should be 0, while real part value of input impedance equal (Z_o). that meaning, the general matching network has at least two solutions, where on L-section matching circuit these two solutions provided via two reactive components either L or C [79],[80].

3.3.3 Single-Stub Tuning

When the load is complex the stub-tuning is vastly utilized to match with T.L. Stub is including (shorted or opened) section on line, which connects to suitable point on line from load as parallel or series. In general, short-stubs is utilized for coaxial-cable applications, due to the open stub is working like antenna at their open ends. Most matching circuit are utilized a single-stub due to it can matching any load.

Stub reactance value effect is located by stub length as well as the distance from stub location to load (d), In single stub there are two influenced alterable parameters. Its length difference of short or open circuit, (equal ($\lambda/4$) for grant susceptance or reactance [79],[80].

3.3.3.1 Shunt-stub matching

In this state, first step selected (d) distance which satisfy an admittance value (Y_0), looking to line distance (d) of load like a form ($Y_0 + j\ B$). As illustrated in figure (3.6), then must be chosen ($-j\ B$) for a stub susceptance, the resulting on matching condition.

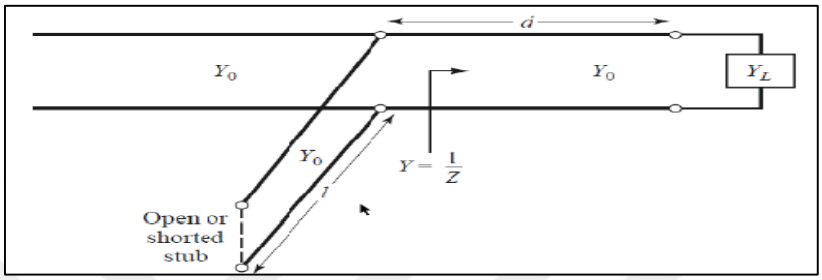

Figure 3.6: Shunt single-stub match circuits.

To gain the equations have variable (d and l), load impedance must be written such form ($Z_L = 1/Y_L = R_L + jX_L$). (Z) impedance can be gained below:

$$Z = Z_0 \frac{(RL+jXL)+jZo\ tan\beta d}{Zo+ j(RL+jXL)tan\beta d} \tag{3.13}$$

$$Y = G+JB = \frac{1}{Z} \tag{3.14}$$

$$G = \frac{R_L(1+(tan\beta d)^2)}{R_L^2+(X_L+ Z_o tan\beta d)^2} \tag{3.15}$$

$$G = \frac{R_L^2 tan\beta d-(Z_o-X_L\ tan\beta d)(X_L+Z_o\ tan\beta d)}{Z_o[R_L^2+(X_L+ Z_o tan\beta d)^2]} \tag{3.16}$$

If $RL = Z_0$, then tan $\beta d = -XL/2Z_0$. So, the two solutions for (d) are:tan^{-1}

$$\frac{d}{y} = \begin{cases} \frac{1}{2\pi} tan^{-1}\ tan\beta d & tan\beta d \geq 0 \\ \frac{1}{2\pi}(\pi + tan^{-1}\ tan\beta d) & tan\beta d < 0 \end{cases} \tag{3.17}$$

To get a desired stub length, find a stub susceptance, $Bs = -B$.

for open-circuited:

$$\frac{lo}{\lambda} = \frac{-1}{2\pi}\ tan^{-1}\ \frac{B}{Y_0} \tag{3.18}$$

and for short-circuited:

$$\frac{ls}{\lambda} = \frac{1}{2\pi}\ tan^{-1}\frac{Y_0}{B} \tag{3.19}$$

If the length given as negative value for eq. (3.18) or (3.19), then we can add (λ/2) to change the sign of results to be positive.

3.3.3.2 Series stub matching

In series stub state that clarified on figure (3.7), distance parameter (d) is define as a distance that at which an impedance (Z) from the load where (Z= Z_0+ $j\ X$). Then must be eliminate the reactance by using series stub with opposite sign ($-j\ X$), that will gain the match condition.

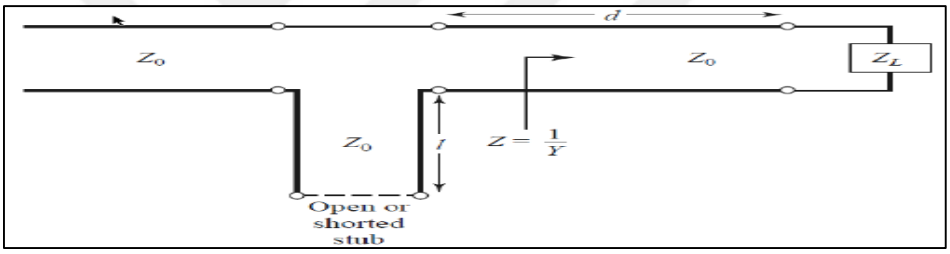

Figure 3.7: Series-stub match circuit.

To get the formulas of (d) and (l), an acceptable load is written (Y_L= 1/Z_L = G_L + jB_L). So, an acceptable (Y) can be written as below:

$$Y = Y_0\ \frac{(G_L+jB_L)+jY_0\tan\beta d}{Y_0+ j(G_L+jB_L)\tan\beta d} \tag{3.20}$$

$$Z = R + j\ X = \frac{1}{Y} \tag{3.21}$$

$$R=\frac{G_L(1+(tan\beta d)^2)}{G_L{}^2+(B_L+Y_0\tan\beta d)^2} \tag{3.22}$$

$$R=\frac{G_L{}^2\tan\beta d-(Y_0-B_L\tan\beta d)(B_L+Y_0\tan\beta d)}{Y_0[G_L{}^2+(B_L+Y_0\tan\beta d)^2\ ]} \tag{3.23}$$

If ($G_L = Y_0$), then (tanβd= $-B_L/2Y_0$) . So, there are two main solutions for (d):

$$\frac{d}{y}=\begin{cases}\frac{1}{2\pi}tan^{-1}\,tan\beta d & tan\beta d \geq 0\\ \frac{1}{2\pi}(\pi+tan^{-1}\,tan\beta d) & tan\beta d < 0\end{cases} \quad (3.24)$$

To calculate the length of stub, firstly, must be find the reactance value (X). Where it must be equal to value but negative sign to required stub reactance Xs.

For (short-circuited) stub:

$$\frac{ls}{\lambda}=\frac{-1}{2\pi}\,tan^{-1}\frac{X}{Z_o} \quad (3.25)$$

for (open-circuited):

$$\frac{lo}{\lambda}=\frac{1}{2\pi}\,tan^{-1}\,\frac{Z_o}{X} \quad (3.26)$$

if the length of eq. (3.25) or eq. (3.26) minus value, it can add (λ/2) to change the sign of results to be positive value [82].

3.4 RECTIFIER CIRCUITS

It is a second important part of RFEH system, it utilized to convert (AC) to (DC) voltage [81]. Rectenna system can harvest (RF) energy, where it consists of three main parts are antenna, matching circuit and rectifier circuit. Many modern applications are utilizing rectenna system for example, ((RFID), (WPT), WSN) systems. Efficiency of energy harvesting system depends on antenna and rectifier efficiency as well as, good matching connection between antenna and rectifier-circuit. A good matching is achieving by source-pull technique which offers best impedance for input and diode . Simply, rectifier circuit is defined as electric device including one or more diode to convert alternating-current into direct-current as be illustrated in figure (3.8). for H.W. Rectifier, the diode is working in one-way to allow flowing current on one direction. This process called the rectification [82].

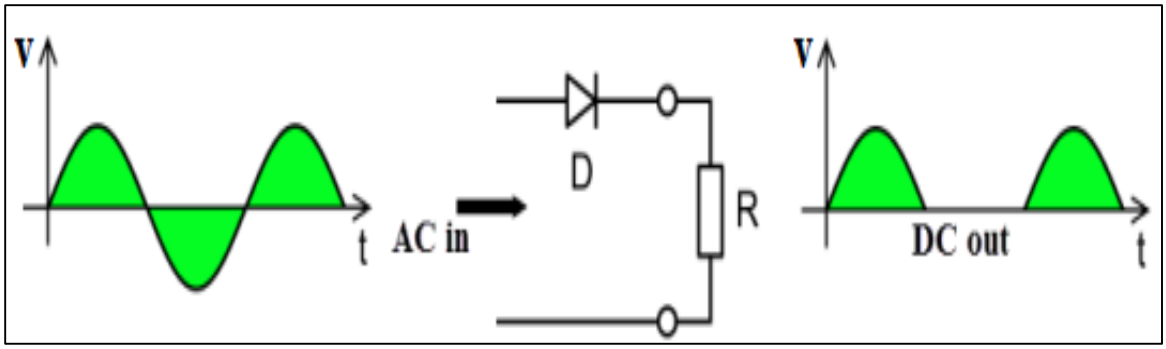

Figure 3.8: Rectification process.

3.4.1 Half-Wave Rectifier-(HWR)

It allows to negative or positive half wave of (AC) to pass through (HWR) circuit. For example, positive half wave in both figures (3.8) and (3.9) can pass throw rectifier circuit while the negative half cannot pass. This meaning, only one-half wave can reach to output [81].

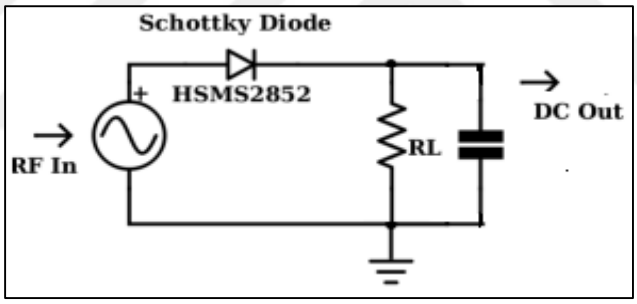

Figure 3.9: Radio frequency half-wave rectifier.

3.4.2 Full-Wave Rectifier-(FWR)

It allows both positive and negative half of AC-waves to pass through rectifier circuit to reach the output by utilizing two diodes that works as two valves, which lets us utilizing both halves of input wave to arrive for full-wave rectification as be clarified in figure (3.10). FWR is more rectification efficient than HWR.

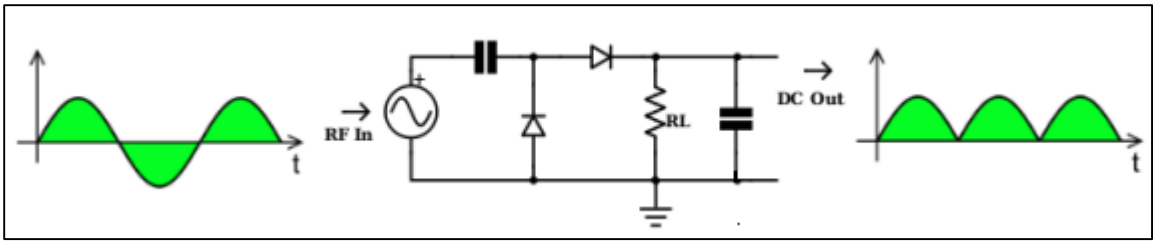

Figure 3.10: Full-wave rectification.

3.4.3 Voltage Doubler Rectifier

This rectifier type includes two diodes (D1 and D2) and two capacitors (C1 and C2), as be clarified in figure (3.11) where the forward current can pass just from ground to positive output voltage ($Vout$) by using D2 then D1. So, C1 prevent DC current to passing into source where C1 is stored a charge and allow to pass the source high frequency currents. But at the same case C2 is stored the resulting charge of ($Vout$) smoothing (ripple voltage). Essentially, this circuit operates like charge-pump design. C1 and D2 are represented dc-level shifter, while C2 and D1 make up a peak detector [81].

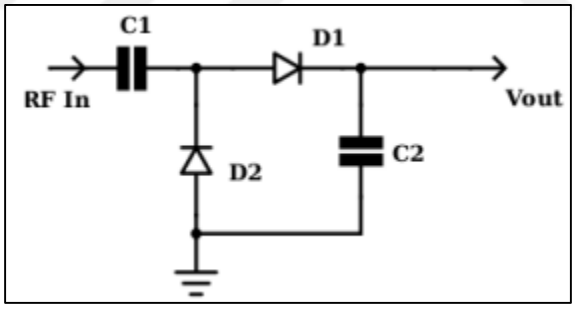

Figure 3.11: Voltage-doubler rectifier.

At RF-positive peak voltage greater than D1 voltage required, meaning of (D1 turn-on), on this state D2 work as open switch while D1 is turns on switch. as be clarified in figure (4.12).

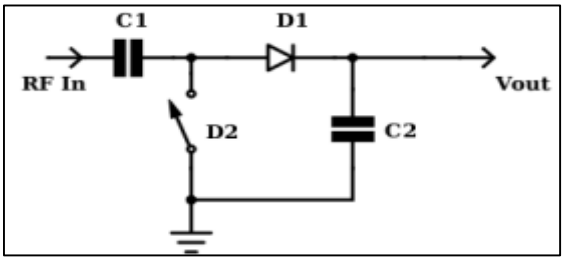

Figure 3.12: V.D.R on case of RF positive-Pulse.

In second state, at RF negative peak voltage greater than D2 voltage required (D2 turn-on), the current pass from ground through D2 and storing as charge on C1.

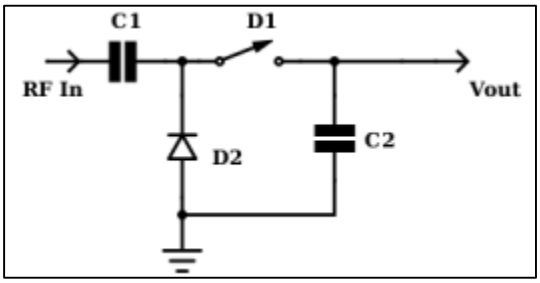

Figure 3.13: V.D.R on case of RF negative-pulse.

Voltage that storage C1 is calculated by difference between negative peak-voltage (Vpk) and diode turn-on voltage (Von) of (D2) at negative peak, as clarified on equation (3.27).

$$V_1 = V_{pk} - V_{on} \tag{3.27}$$

From figure (4.12) that clarified first state, it can be computed peak voltage of D1 by equation below:

$$V_{out} = V_1 + V_{pk} - V_{on} \tag{3.28}$$

$$V_{out} = 2(V_{pk} - V_{on}) \tag{3.29}$$

This meaning the (V_{out}) can be computed by summation voltage on C1 (V_1) and positive peak-voltage (V_{pk}) then subtract a turn-on voltage (V_{on}).

3.4.4 Multistage Rectifier

In general, one rectifier stage does not generate enough voltage for satisfied the E-harvesting application needs, the generated voltage equal to $2(V_{pk} - V_{on})$. For this reason, many of voltage doubler rectifiers must be utilized to build a multistage-rectifier. For example, figure (3.14) used four stages rectifier for producing the required voltage. Mathematically, it could be calculating a DC output voltage for numbers of stages (N-stage) rectifier by equation (4.30) that clarified below [81].

$$V_{out} = 2N(V_{pk} - V_{on}) \quad (3.30)$$

Multistage-rectifier is designed on figure (3.14) which clarifies a cascaded rectifier stages.

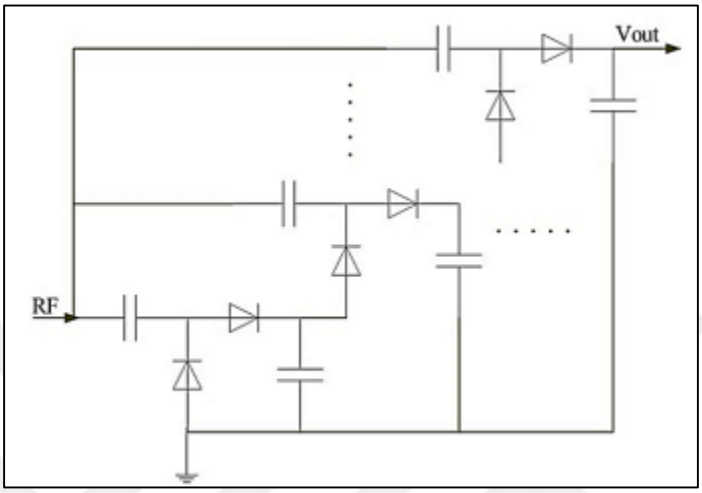

Figure 3.14: N-stage multistage rectifier.

3.4.5 Schottky Diode (Ideal Diode)

When calculated the (V_{out}) by using equation (3.29), it found best diode type could be achieve by choosing zero bias schottky-diode as (ideal diode) due to the output voltage (V_{out}) is increased by let diode voltage ($V_{turn-on}$) to be lowest as possible. (V_{out}) could be doubled peak voltage of RF input at ($V_{turn-on}$) is become very low and it could be ignored (equal to zero) as in theory, for this reason, V.D. Rectifier-circuit was called by its name. In noteworthy, V_{out} measured in practical field should be less than theoretical value due to it cannot ignored load resistance and a circuit is dose not able to pull all currents and charges which stored in Cs [81].

3.5 DC. PASS FILTER

A passive filter is one of an electronic filter sorts which is made from passive elements (inductors, capacitors and resistors).A passive filters are considered a popular form, due to does not need an external power supply where it depends just on (Ls, Cs and Rs) elements rather than active devices as transistors. The more complex passive filters may be involving the nonlinear components or more complex linear elements like the transmission lines [81].

In power system, a passive filter is utilized to suppress harmonic the currents and reduce the voltage distortion that appears in system sensitive parts.

3.6 RFEH SYSTEM APPLICATIONS

It can see the RFEH applications in many wireless communication devices like smart devices and WSN where the life growth rapidly within the last decades led to increase the wireless applications which requires to improve the power sources. Many of researchers are working to improve batteries efficiency [83]. The last great discovery to improve this field was 25 years ago, when Sony company utilized battery of lithium cobalt oxide cathode. the lithium-ion battery is considered the first rechargeable battery was discovered by combination with carbon anode [84]. But there are many limitations is found on batteries that influences negatively on autonomous systems needs such as: limited life, need constant recharging, costly due to battery replacement and contain different toxic chemicals.

(RFEH) may be considered a new technology to enable the wireless nodes for working to discrete time periods, to be a good alternative for batteries. Many autonomous devices have been worked successfully based on energy harvesting of microwave beams, this technique was suggested for different applications that utilized wireless-power like satellite [85]. RFEH- technology was first introduced on (1968) by P. Glaser. in (1976 to 1980), NASA encouraged the researchers to study in-depth of this concept by supporting conducted from U. S. Department of Energy [86]. Many parameters of such system are located through node power needs. Figure (3.15) showed many examples of nodes and its approximate power consumption.

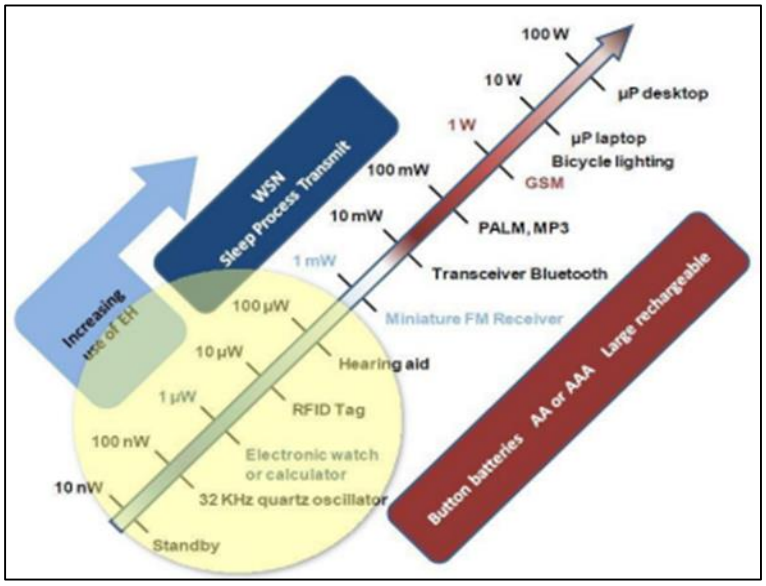

Figure 3.15: Power-needs for small electronic products.

Selected the working frequency band and rectenna kind is very importance for RFEH system which depends on aimed application where it may be critical due to its effect on autonomous system efficiency. In figure (3.16) can be clarified the highlight circle which covers the region of (RFEH) applicable, this area is possible to be widely based on energy source type. In addition, this figure illustrates the small electronic devices as wireless sensor network nodes.

In modern life, this technology became is very necessary to vary developed devices which needs low power for operating. It can be clarified the best examples for using this technology in figure (3.16).

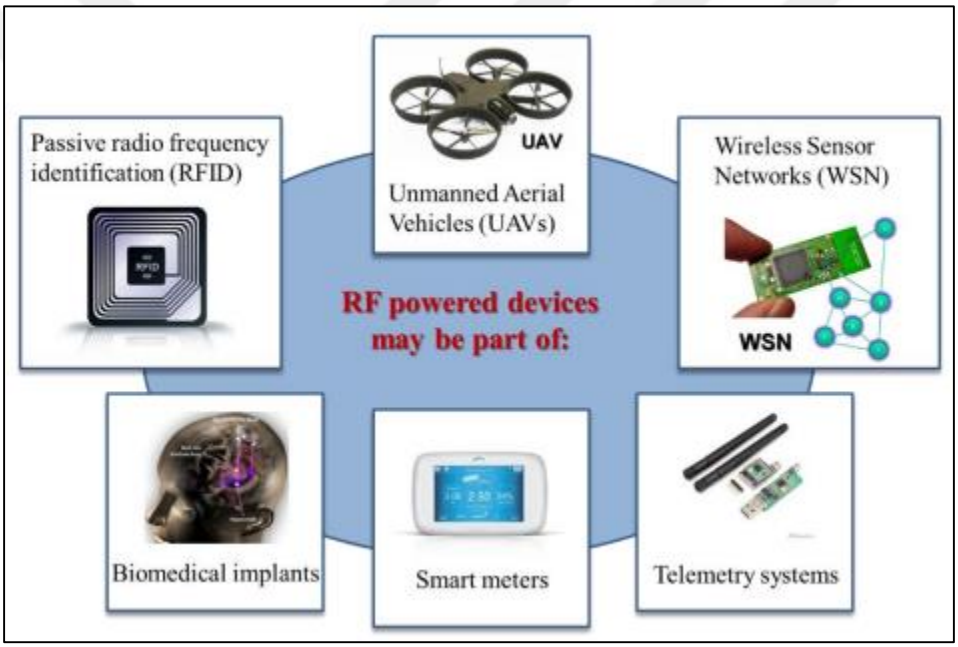

Figure 3.16: RFEH applications.

With the development of recent communications technologies, different RF is available on civilian environment for using in many different applications, that needs power for operating sensor nodes that utilized on autonomous systems. this situation paid to harvest the ambient RF energy to offer more power. This type of energy is very important for different application especially that related with human health like cardiac pacemakers, and prostheses .also, it uses in applications that required (high up-time) for working to avoid the risks by used batteries or other classical power source ,like environmental monitor system for example, the forest fire detection where difficult powered source maintenance and not available the wired power source as well

as,(RFEH) used by embedded sensors for example, it placed inside bridges asphalt where cannot install batteries or other traditional power sources[87]-[89].

from above information, it can be listed the different applications fields that uses (RFE harvesting) such as:

a. Health monitoring and biomedical devices.
b. RFID system.
c. Wireless sensor network (WSN).
d. Embedded in structures.

Finally, RF power harvesting is considered as alternative power sources. It could be used instead of batteries where it delivers independent energy source that offers maintenance decreasing and operation cost. Whole above features make it very important suitable alternative power source for smart systems and applications especially, that requires low operation power.

3.7 SOLAR PV CELL

In urgent life the greatest number of electronic devices are portable because it has more advances features than the traditional devices such as smaller size, lighter, using less power, used batteries as power supply. These advanced features allow for many electronic devices types to operate without wires connection in power lines grid or in communications networks [90]. Recently, the integrated system that structured from communication systems with photovoltaic (PV) technology is received much interest where it is offered low cost and independent applications. This system can offer compact, dependable and authoritative autonomous system that use to many applications [91]. the independent remote base station one of applications that using this technology but these devices are including the separate solar cells and antennas that needs large surface area, for this reason it is necessary a compromise the system in limited surface that implemented by integrated antennas with photovoltaic solar cells [74]. All previous studies that represents integrated antenna into solar cell by using a transparent antenna which consists of patch which designs (such as meshed structure) to allow to flow optical-signals through openings of mesh while the conductor still works as valid radiator of MW-frequencies. As well as, the transparent substrate layer and meshed ground surface are allowed to arrive the light to solar cell that used for provide the load by an electric power [11],[15].

A photovoltaic (PV) cell is used for facilitating operation without external power source. Thus, solar panels are provided the energy to device during day and night depending on light source. solar panel size is important factor to provide enough power to operating the communication system.

This work proposed a standalone self-powered communication system is integrated the (sub-6 GHz) microstrip antenna array with solar cell and Radio Frequency Energy Harvesting system. (PV) solar panel is mounted on top of array (vertical to an array axis) into avoid array shadow effects and permit to arrive of (100%) sunlight directly on solar cell without obstacles.

This self-power system is suitable for 5G and other modern applications such as portable electronic communication devices and sensor networks.

3.8 CONSTRUCTION OF SOLAR CELL

Solar cell is semiconductor device capable to convert the light-energy to electricity directly by photovoltaic (PV) effect. Basically, the important material that used for solar cell production is a silicon. Solar cell elements are shown figure (3.17) [92],[93]:

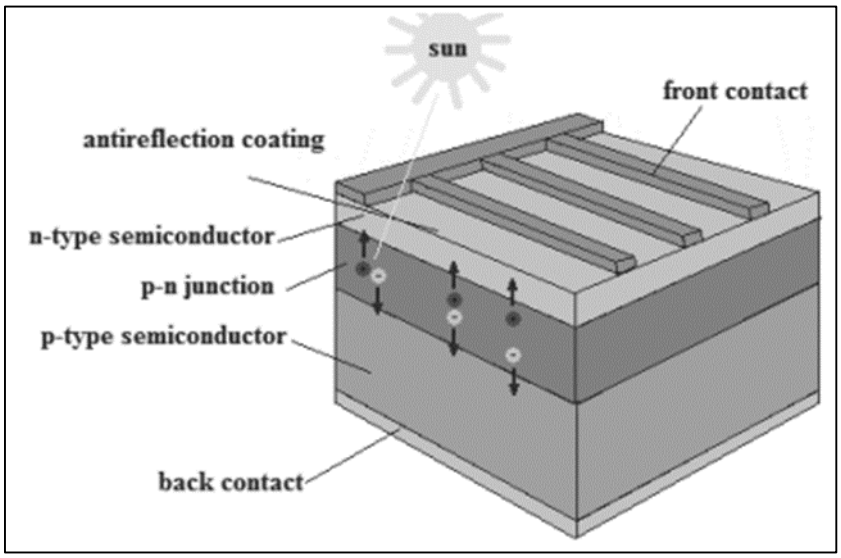

Figure 3.17: Structure of solar cell.

a. Silicon wafer of (mono or polycrystalline) with p-n junctions on surface.
b. Front-back contact, front contact should be constructed on proper shape to get most of incident rays.

c. Antireflection layer –is located as a cover on front surface.

In general, there are three main types of solar cells:

a. A monocrystal silicon is a (single-crystal) wafer cells made via (Czochralski) process with homogeneous structure. It is expensive due to the cells are cut of cylindrical ingots. The cutter wafer surface does not cover whole square module of solar cell without actual waste of burnished silicon [94]. These cells have about (0.3mm) as thickness. This type realizes high performances and long life. Figure (3.18) (a) is shown the monocrystalline silicon cells.

b. Polycrystal silicon cells consists of more small silicon cereals, it is produced by casting the ingots through melt large square block of silicon, neatly cooled to be solid. (Poly-Si) cells are less cost than (mono-Si) cells but less efficient [95]. These cells have thickness about (180 to 350 micrometer). Figure (3.18) (b) is shown the polycrystalline silicon cells.

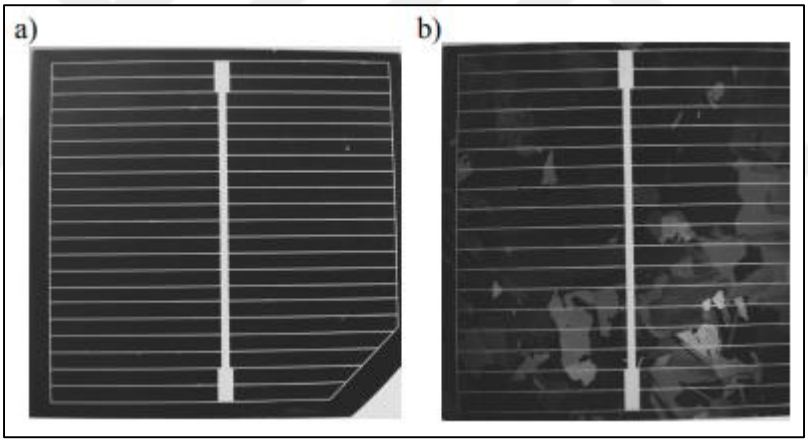

Figure 3.18: Silicon-solar cell (a) monocrystalline (b) polycrystalline.

c. Amorphous cells are produced by embedded few silicon layers on surface of other material such glass. where cannot distinguished individual cells. Usually, this type is utilized in small electronic-devices like calculators and watches [96].

Solar cells can make in the same techniques that be used for processing and manufacturing the other semiconductor devices. it is necessary to keep the strict requirements for cleaning and quality monitor for semiconductor fabrication. Usually, the (p-type) wafers are lightly, to create solar cell like this wafer, surface spread of (n-type) performed on wafer front-side. This form (p–n junction) placed at few-hundred nanometers under surface.

To rise amount of light arriving to (p-n junction) should be used anti-reflection coatings that connected with sola PV cell. Urgently, titanium dioxide was utilized for antireflection coatings, but now, silicon nitride is utilized mostly due to its super surface perfusion features.

Then the metal contact placed on back and the bus bars of metal contact are printed on front surface utilizing silver paste. Back contact is also representing screen-printing of metal paste, in usual using aluminum. Generally, this contact covers whole solar cell back surface. Then a metal paste is heated in several hundred degrees to produce the metal electrodes and after making metal contacts, solar cells are connected via wires or metal ribbons then are collected as the shape of solar panels.

3.8.1 Photovoltaic Phenomenon in P-N Junction

When light beam falls on (p-n junction) [97], the photon needs large energy to produce (electron-hole) pairs. The collection of new generated electric charge-carriers in most, produce heat. (PV) creation condition is disconnected these pairs before recombination, this needs to existence an internal electric field which be found in (p-n junction) because a spatial-cargo. In (E) electrons are moving from (p-type) into (n-type) at same time the holes are moving from (n-type) into (p-type), the result is generated (electron-hole) pairs. Where the minority-carriers on one connector side are separated to become a majority carrier but with less lifetime on other side, this lead to create solar cell voltage (VPH) and current (JPH). Its noting, not the whole light photons are been as part of (PV) conversion because the reflection effect on the surface. R (λ) is a light reflection constant for cell while the (1 - R (λ)) is a light-photon which passes to cells which includes (PV) conversion. The reflection work to reduce the power which is obtained where it depends surface-polishing. to improve the reflected light reduction the solar cells are wrapped by anti-reflection coating.

when the photons stream incident to semiconductor surface, surface absorbed only (1 - R (λ)) photons part. These photons can permeate semiconductor but due to its low thickness, some of photons guide through it until arrive through back surface [92],[93].

3.9 SOLAR CELL CHARACTERISTICS

Number of solar cells are collected into panels and the panels collected to build modules. Solar cell properties are represented by (current-voltage) characteristics. Where the electric current intensity depends of vary values of radiation. If the resistance of current-flow is removed, the panel output current is to be multiple of single cell current and is attached to cells and modules parallel connections. In similar the module output voltage depends on number of series connections cells [98]. PV solar cell can produce the electricity just at it is illuminated and the electricity is not storage. Figure (3.19) shown the PV solar cell characteristics.

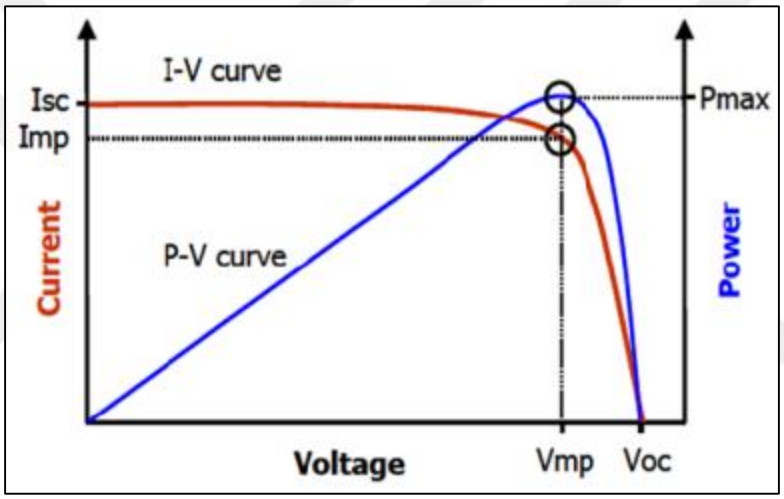

Figure 3.19: Solar cell/module of (I-V) and (P-V) curves.

3.10 ANTENNA INTEGRATED WITH SOLAR CELL

This section describes the different constructions of antenna and solar cell integration such as:

a. Integrated the solar cell and transparent antenna, is used for achieve a self-powered system by attaching transparent antenna on solar cell. The transparent antenna should have good optical transparency to allow to arrive the light photons to solar cell in order to it can to generate the electricity. at same time the antenna also should have good radiation efficiency to avoid the negative impact of photovoltaic generation on its performances [11],[15].
b. Integrated the solar cell with antenna has patch and ground metal-meshed structure, this type of integrated system is discussed in more previous studies where the antenna with contains a patch that design to allow for light photons flowing through its openings, while the conductor

is remained a valid radiator. The layers (mesh patch, transparent substrate and meshed ground) allow to arrive the optics light to solar cell that uses to produce the electric power [12].

c. another design was suggested in [13] to integrate the solar panel a reflector for a Vivaldi antenna based corrugated grating patch with MTM.
d. In [14], In [14], researchers suggested a new design of plasmonic antenna array by printed it on flexible solar panel, this design based MTM.
e. This work proposed integrated sub-6 GHz microstrip rectenna array with solar panel as the external part, where solar panel are mounted perpendicular to elements array axis (above array structure) in order to avoid the antennas structure shadowing and allowing to (100%) of light photons arrival directly to solar cells without obstacles.

3.11 NEGATIVE EFFECTS OF SOLAR CELL ON ELECTROMAGNETIC FIELD

The light feeding of solar cell includes solar source and non-solar source of light for this reason the cell is named as photovoltaic (PV) cell. The thin amorphous silicon development that used in polymer-substrate of solar cell technology make it is easy to solar cell cutting as appropriate for different shapes of antennas like slot antennas, that leading to optimal using of available area without affected on antenna radiation characteristics [95]. This work proposed another solution to avoid the disadvantages of solar PV cell on antenna radiation parameters by located the solar panel perpendicularly to antenna array axis (as separated part located above antenna array). It can be shown the negative effects of solar PV cell on antenna parameters bellow (when used the traditional (PV) cell) [13], [99].

a. Radiation losses because the nature material of solar cell .
b. Sometimes caused antenna gain Reduction
c. Reflected and scattering of the radiation
d. Noise and distortion of radiation rays.
e. Generated heating

3.12 ADVANTAGES OF SOLAR PV CELL

a. It produced power without pollution
b. Dependence reduction on other power resources such as foreign oil and fossil fuels.

c. Available clean power resource which is every day even at low light intensity.
d. Less cost, in future investment where no need electric payment bills.
e. Solar panel need less maintenance.
f. It can be Used batteries for storing extra power.
g. It considered more Safety than conventional electric resources.
h. Improvement the electric Efficiency where the efficiency of same solar cell will become more efficient in other time.

3.13 DISADVANTAGES OF SOLAR PV CELL

a. Needs large space in order to achieve high efficiency.
b. It is not used in dark places.
c. Efficiency depends on location, direction and light source intensity.
d. It affected by shadowing effect where it could not produce enough power at finding the obstacles along light direction.
e. Negative impacting on antenna radiating characteristics.
f. It cannot produce enough power at night so, it needs good quality of batteries storage.

3.14 APPLICATIONS OF INTEGRATED ANTENNA WITH SOLAR PV CELL

a. space vehicle and satellite: The needing of directivity, frequency wide bands and compact antennas in order to earth and space communications observation, needs advanced solutions for integrated design that uses for modern small satellites like CubeSat standard [100].The design has maximize solar panel surface that is important to get efficient solar power to operate a space vehicles for long time Therefore, the shadowing eliminating caused by obstructions of incident light to solar cells is essential but without reduced the antenna performances In last decades, more studies have been improved to design high-performance antennas of small satellites and place a transparent patch over solar panels surface [13] [85].
b. Sensor network: in spite of development of battery technology and less demands of electronics power, but more (WSNs) nodes are installed in places that can not to obtained the electric power, it may be impossible to provide enough power for this application as well as the battery alteration is expensive and not practical. these reasons paid to the design the self-powered

sensor nodes which gets the electrical energy from surrounding sources such as light photons by using solar (PV) cell [101]. Main aim of this work is to realize self- powered system without used batteries that needs periodical maintenance, replacement or recharging.

c. Biomedical devices: biomedical devices which used solar PV cell can be classified into two type first one represented the external usage devices, in general these devices used out of human body such as devices of measured blood pressure or heart rate where it could operate by using power that generates by PV cell. Second type is representing the implanted devices inside human body instead of that used in implanted traditional devices to evade batteries usage that needs surgical for replacement [102]. Energy harvesters rely on piezoelectricity, thermoelectricity, and solar electricity to operate an implantable device. but most of these (EH) sources suffered from different limitations such as low power generation, large size relatively, poor efficiency. The studies focus on solar photovoltaic cells due to their high efficiency but it affected by tissue absorption losses therefore the researchers proposed implanting devices in hypodermis to obtain a stable power output [103].

3.15 THE PROPOSAL INTEGRATED SYSTEM STRUCTURE DESCRIPTION

In this section, we described the final work design, this integrated system that structured by integrated sub-6 GHz microstrip antenna array with solar cell and Radio Frequency Energy Harvesting system. Where solar panel is located above array structure on a vertical to antenna array axis (as separated part) to avoid shadowing effect of rectenna array and to allow about (100%) of sunlight to arrive directly to solar (PV) cell without obstacles and to avoid the negative effect of solar (PV) cell on antenna radiation characteristics due to it material nature if it located in parallel as part of antenna array . This integrated system has ability to power generation for rectenna array ,power is represents the collection of (RFEH) low power and good amount of power by solar (PV) cell as well as is supporting a good radiation performance, gain and efficiency with low cross polarization levels ,where it realizes balance between electromagnetic radiation and power-generation.

4. CHAPTER FOUR

5G is a sophisticated technology for mobile broadband communication. 5G is technology is aimed to offer high data rates, high data speed, fast connections, high capacity and other more properties and features than other wireless networks. 5G frequency spectrum is involved two ranges, (sub-6 GHz) which includes range (from1 GHz into 6 GHz) and above (6 GHz) according to physical properties [1]. One of the most essential elements of 5G is antenna designed where it should be suitable for 5G applications [2].

This chapter is introduced design of 3D antenna array based solar (PV) panel and (RFEH) RFD102A module integration to self-powered applications for 5G and modern wireless networks. Such integration is used to realize a self-powered node. The results are implemented by using CST-software simulation and compared with HFSS simulation and measurement results.

4.1 UNIT ELEMENT-RECONFIGURABLE ANTENNA GEOMETRICAL DETAILS

Single antenna design structure has (four (4) Moore fractal patches with coplanar-waveguide feeding technique, Transmission line, load matching circuit and T-stub) is clarified on figure (4.1) (a). Moore-Fractals are utilized to increase efficiency of antenna size reduction and multiband performances as well as that gives a good gain with small size where it allow to flow the maximum current in long electrical path structure in small area [57].Coplanar-waveguide feed is utilized to avert a capacitive-coupling between antenna components, increasing the bandwidth and to maintain the other surface without any printed circuit that would be very useful technology for impeding the busing system and other relative electronic circuit [51].

T. L. is designed of (0.6) as width to relies (50 Ohm) matching-circuit and allow to flow surface currents into Moor-structures [31] [104]. Gaps on T. L. are utilized to paid the current motion to Moore-fractals cells as explained in [105]. Matching-circuit is presented to avert the surface-waves retardation which creates in opposite interference and to avoid an inductive-losses because utilize T. L.-junction which could be removed via capacitive-effect on matching-circuit [31]. T junction is presented to repress the surface waves of structure ages which effects badly on radiation efficiency [106].

Proposed antenna has dimensions (62*40) engraved on a (FR4)-substrate without ground layer. Substrate has good dielectric index about (4.3) and (1.6mm) as height. Two Light dependent

Resistor (LDR) as photo resistance utilized in antenna structure for getting various operate frequencies of (sub-6 GHz) band and good radiation patterns by change the states of (LDR) as (On/Off) for. These cases represented (00,01,10,11) [37],[107].

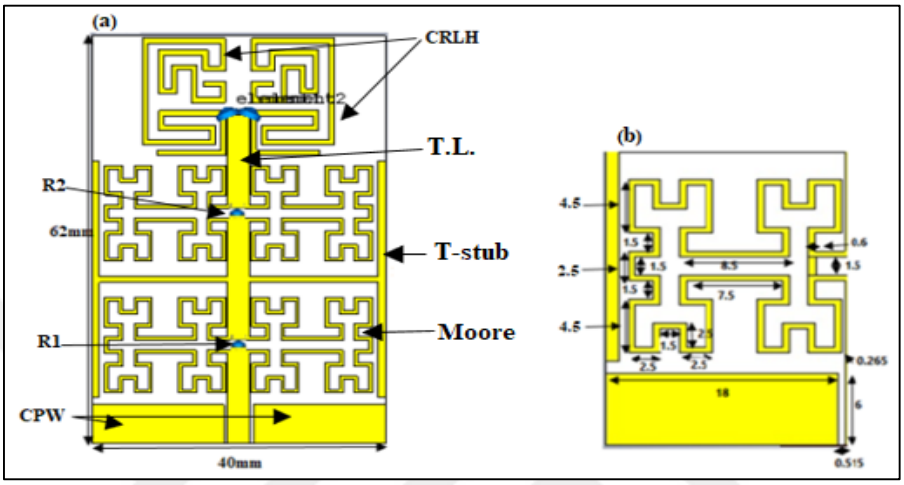

Figure 4.1: Single microstrip antenna element (a) antenna element front side (b) moore fractal unit cell.

4.2 UNIT ELEMENT DESIGN METHODOLOGY

In this section, the authors studied and analyzed each part of proposed antenna structure based on parameters analyses of antenna design simulation. also, this analysis is considered the effect of varying parts of antenna into the performance. We focused on effects of antenna parts on antenna-parameters such as antenna return loss (S_{11}) and gain spectra. (3.6, 3.9GHz and 4.9GHz) are a considered as operating frequencies in our design due to they are very suitable and applicable for 5G frequency band [37]. The simulation analysis is done by utilizing CST microwave studio software package [130]. Below we list the antenna parts which analysis and discusses to arrive to optimal design:

4.2.1 Transmission Line

In order to parametric analysis, we changed length of transmission line from (40mm into 60mm) by step 10mm with monitoring S_{11} and gain. Such analysis is an important to prove effect of transmission line length changing.

Figure (4.2) clarified (S_{11}) for three varying lengths of transmission line as (40,50,60) mm we choice (50mm) as a length of transmission line which located (3.8 GHz) as operating frequency where this frequency achieved (-24.89) as S_{11} and a good gain of (3.09).

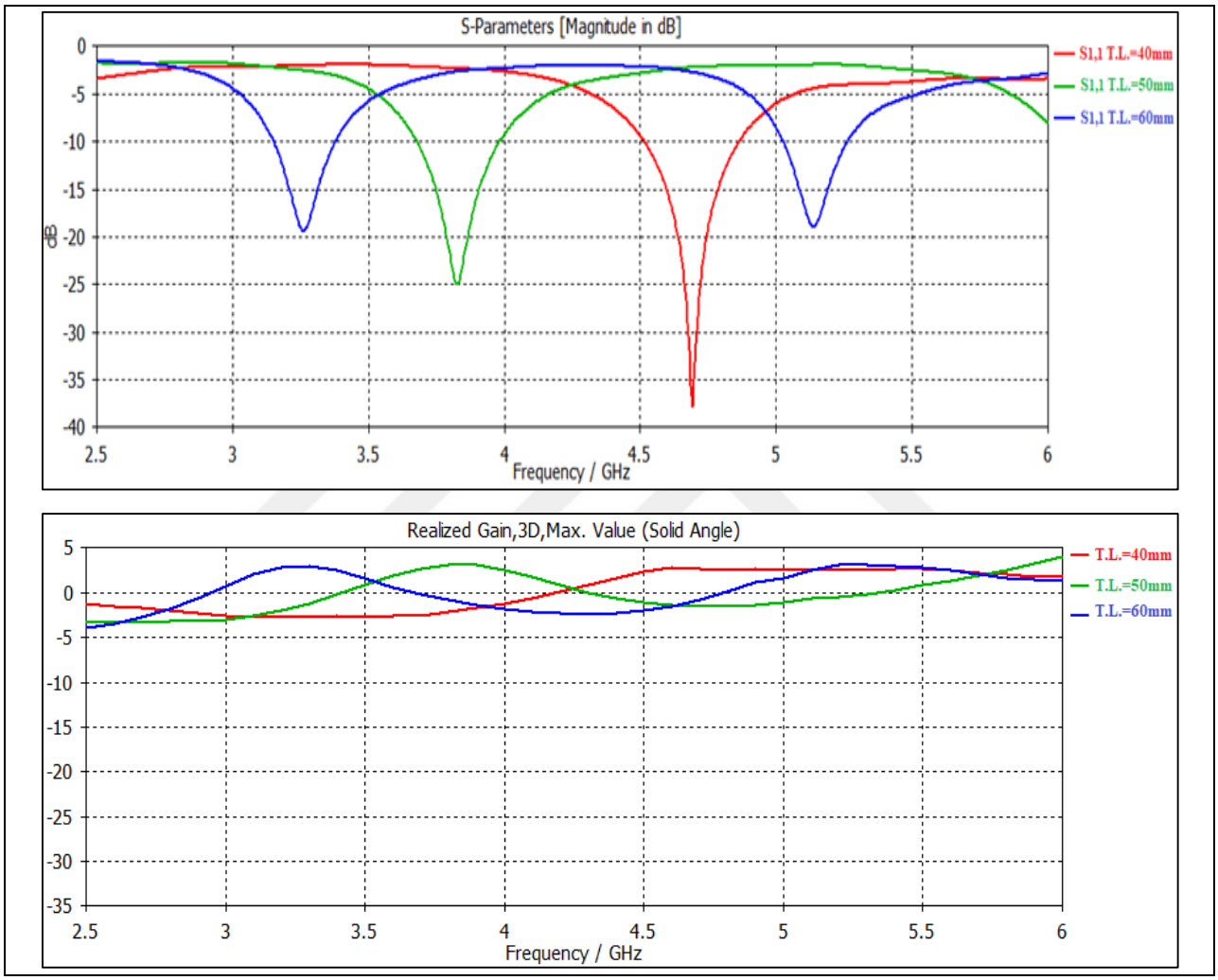

Figure 4.2: S11and gain spectra at different T.L. length.

4.2.2 Unit Cell Effects

This work design contained four (4) Moore fractal geometry which collected in two Moore cells are upper and lower cell. so, to study these cells effects on antenna performance, we used the parametric-analysis based (CST MW) simulation. firstly, we used only one Moore- unit cell in proposed design then compared the obtain results with another design that has two Moore cells. We found and observed when used the first case, antenna grants multiple frequency bands during

interest frequency range. In second scenario, after introduced other Moore-cell to be two cells, antenna generated vary frequency bands within interested frequency range. It is achieved because connection type between Moore cells on (T.L) is a series connection. In this connection, current flow in same direction through unit cells. Result of series cells combination adding their effects to each other. Due to Moore-unit cell is capacitive implication, collecting them lead to increase their number that achieve an important reduction for equivalent-capacitor that in turn increasing the operating frequency [8].

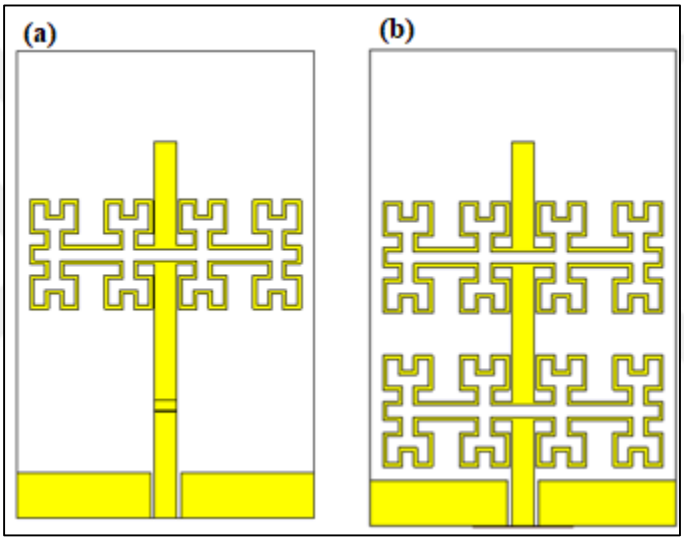

Figure 4.3: Moore fractal effect: (a) one moore unit cell (b) two moore unit cell.

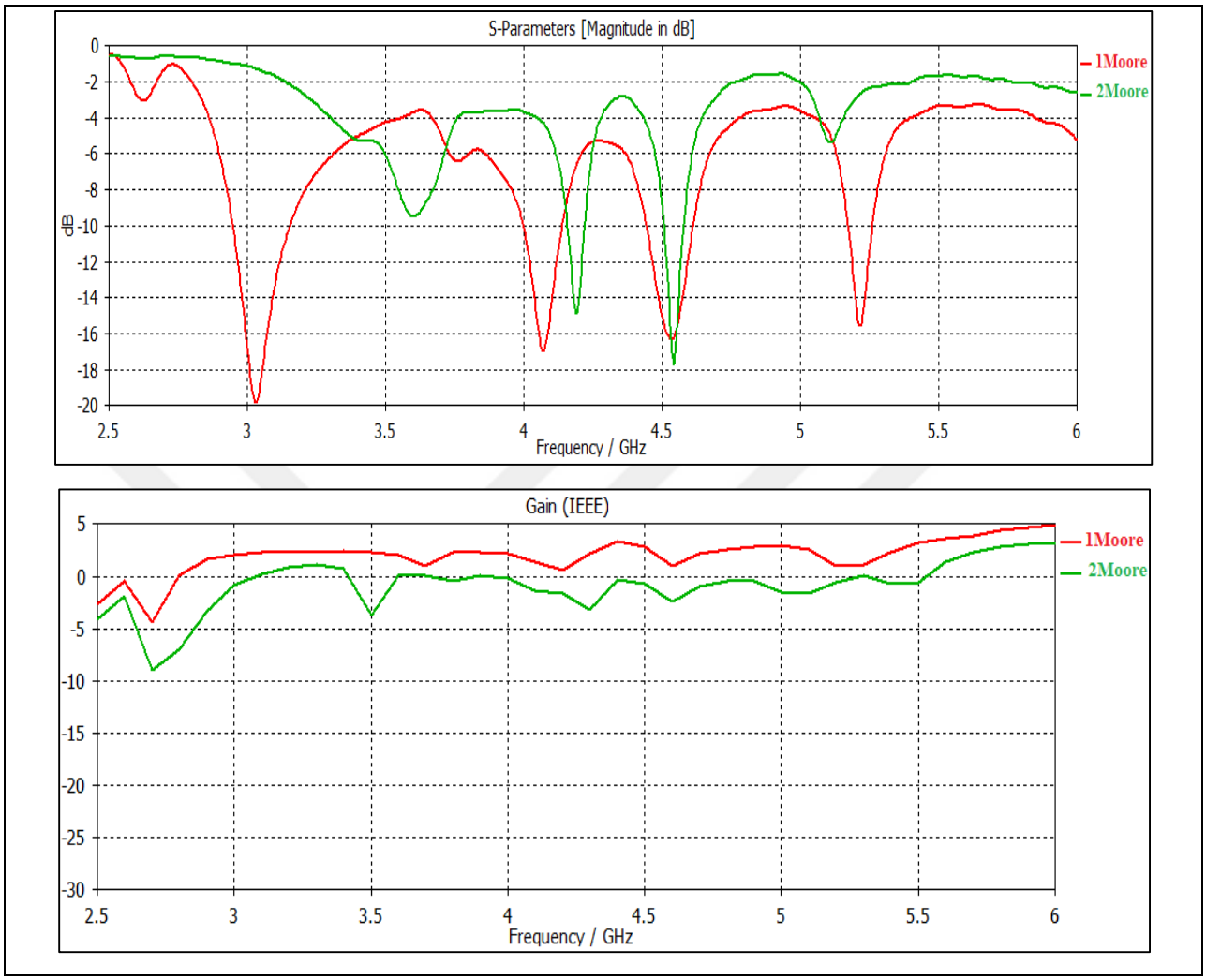

Figure 4.4: S11and gain spectra at one and two moore unit cells.

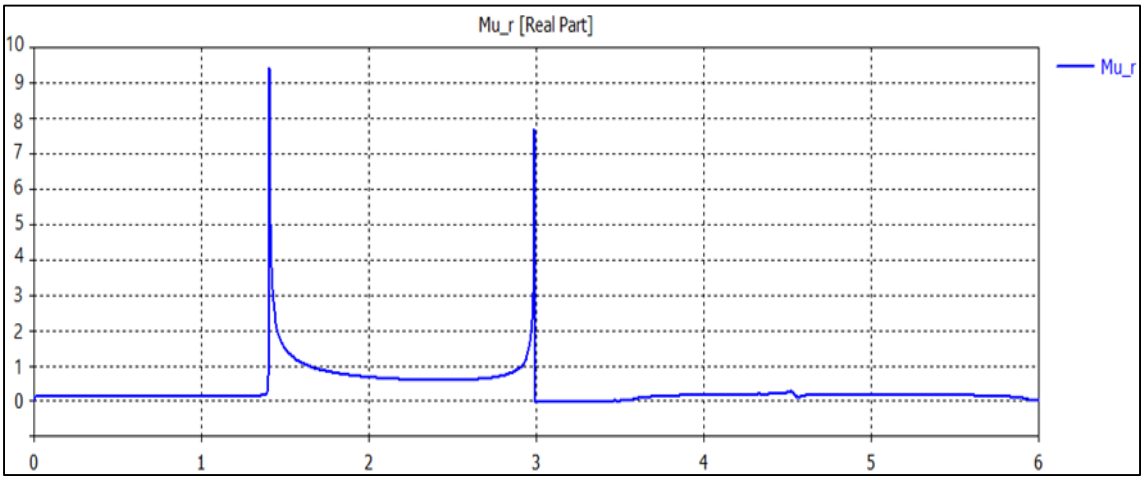

Figure 4.5: Relative permeability of the unity cell.

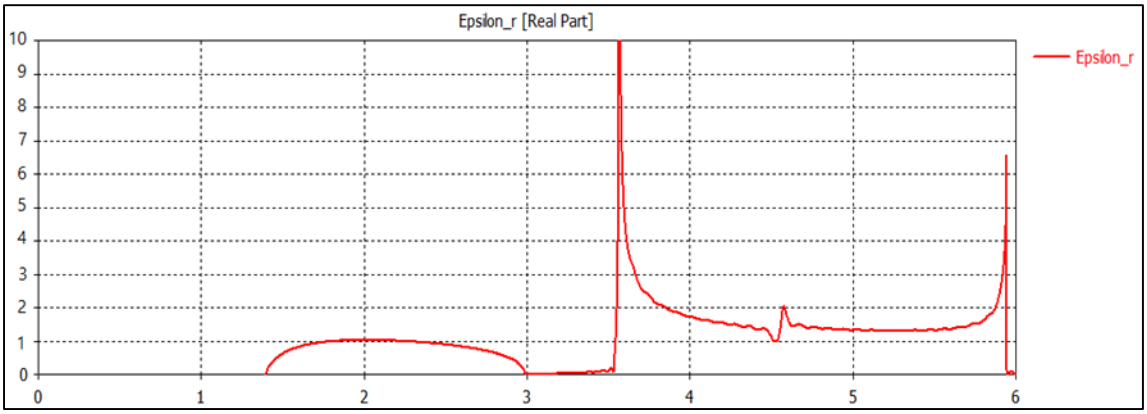

Figure 4.6: Relative permittivity of the unity cell.

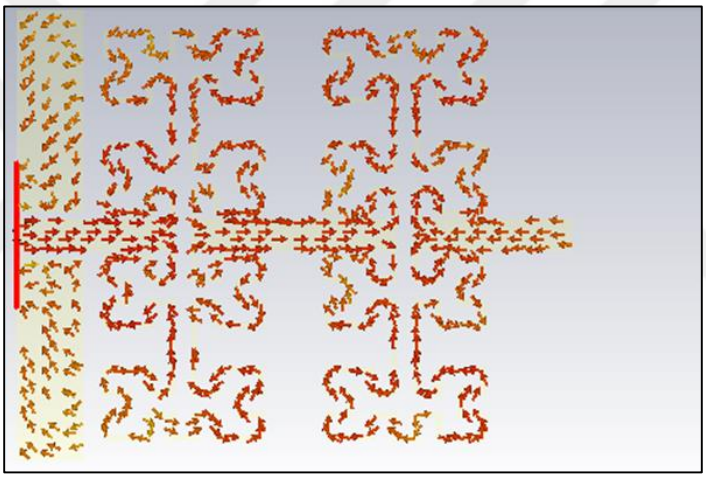

Figure 4.7: The motion current of MTM antenna element (2 moore cells).

So, to get the benefits of the two cases in single antenna element design, we introduced the (T-junction) structure as will be shown in the next section.

4.2.3 T- Junction Effects

T-junction effect on antenna parameters is discussed in this section. It utilized to repress the surface-waves from antenna ages which effects badly on radiation efficiency .T-stub is working to major-radiation beam splitting to rise number of received users from selfsame antenna within same operating-frequency [37], this feature achieves the main feature of radiation beam formation on 5G. We can observe, after added (T-stub) to MTM antenna structure the values of S11 are (-23.6 and-15.84 dB) at 3.55GHz and 3.8GHz respectively and the gain values are -0.897 at 3.55GHz

and 3.48 at 3.8 GHz operating frequency. Figure (4.9) is clarified the S11 and gain after adding T-stub.

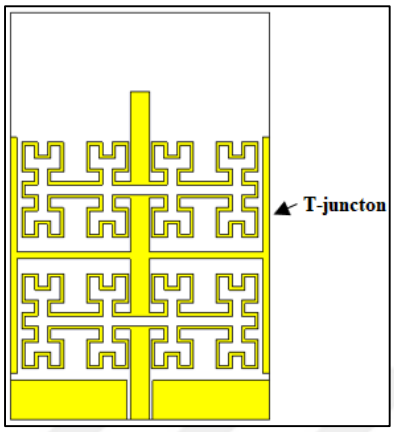

Figure 4.8: MTM antenna after adding T-stub.

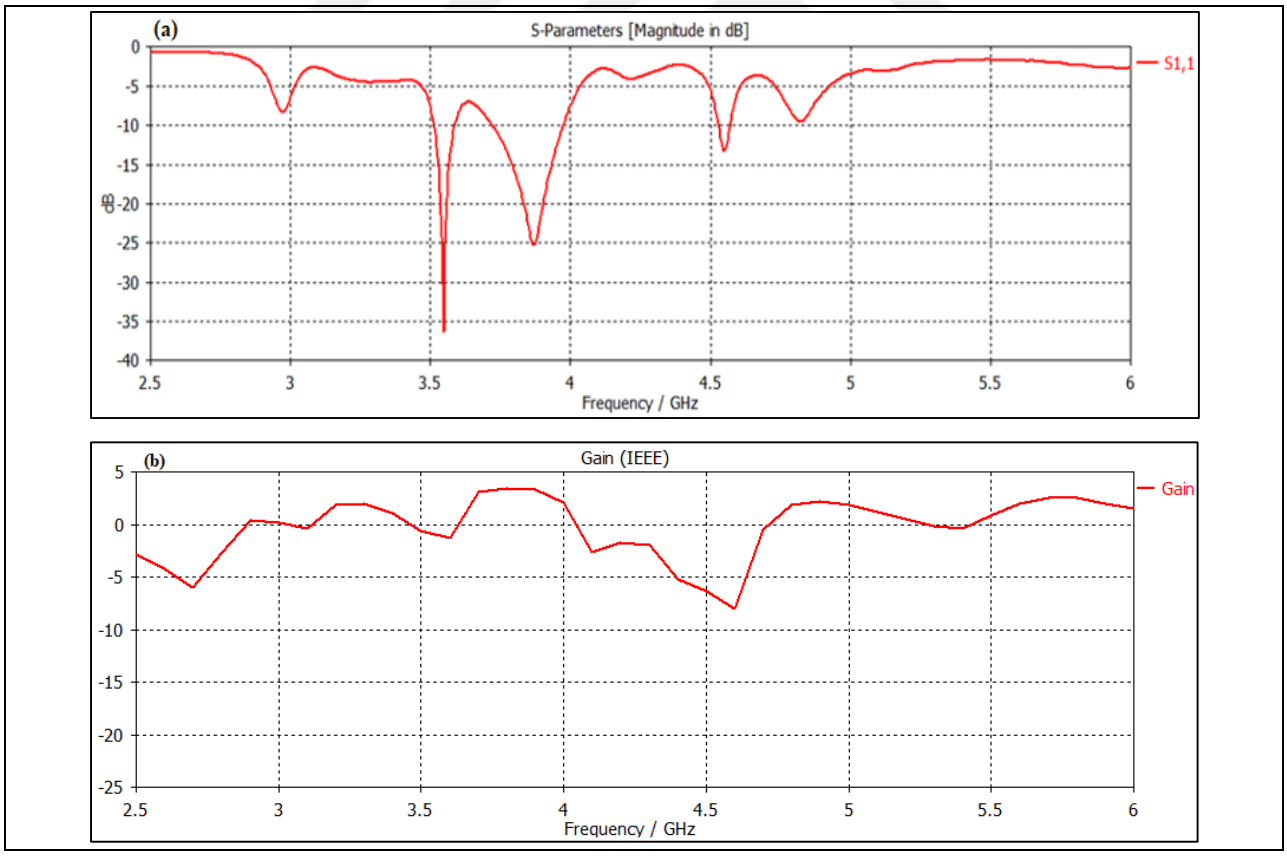

Figure 4.9: S11and gain spectra after adding T-stub.

4.2.4 Gap Effects

Gaps on (T.L.) are introduced for paid the current toward fractal cells. Gaps effect on the antenna characteristics as (resonate frequency, gain and radiation pattern) is described in this section, were these characteristics were analyzed numerically via controlling that based four states (00,01,10,11) of photo resistances (LDRs) [37], [43]. As be clarified in table (4.1).

Table 4.1: Antenna performance respect to varying of photo resistors states.

case	R1	R2	Frequency	Gain	Main lope direction	Angular beam width
1	0	0	3.87	3.36	162°	61.2°
2	0	1	3.86	2.88	150°	52.3°
3	1	0	3.72	3.43	167°	68.1°
4	1	1	3.78	2.9	149°	53.1°

Below, figure (6.10) is shown the S11 parameter with different cases conditions of LDRs.

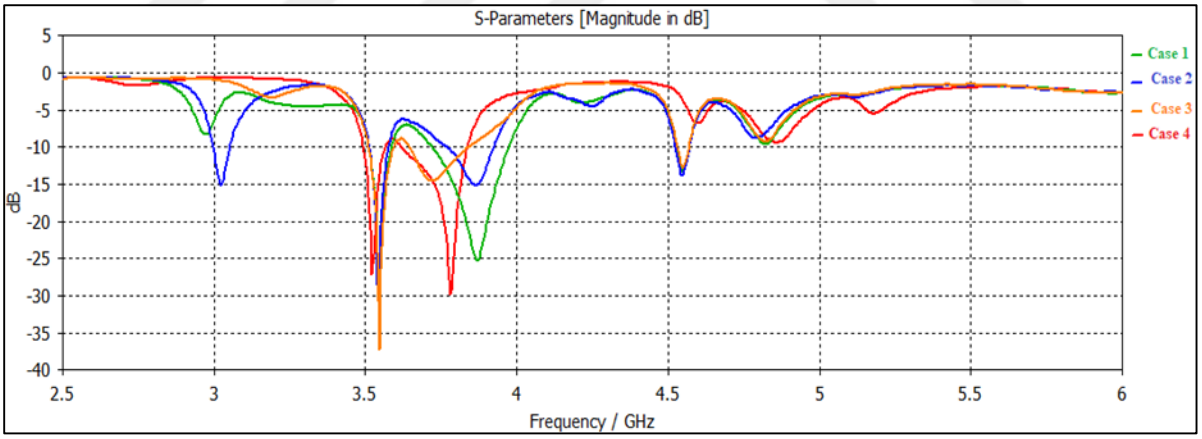

Figure 4.10: S11 parameter with varying photo resistors conditions.

4.2.5 Matching Circuit Effects

CRLH-circuit is added to avert the surface waves retardation which creates in opposite interference and an inductive loss where it can be removed via using capacitive effect of (CRLH)-circuit [43].

It works to Guide the radiation main lobe to desirable direction through controlling of patch surface current flow, due to it contains a variable capacitor load as (varactor diodes) which increases the

current magnitude in appointed direction [37]. Where the antenna side that contains less value of capacitance need less time to radiation than the other side which has higher capacitance. The second advantage of this circuit is relieving the radiation side lobes as well as rise the gain on (4.9) GHz. Now, after adding the matching circuit, the design of antenna is completed, the antenna characteristics were analyzed based four states (00,01,10,11) of photo resistances (LDRs) and without using the varactor diodes (capacitors) as be clarified in table (4.2).

Table 4.2: Antenna performance with different cases of photo resistors.

case	R1	R2	Resonate Frequency	S11	Gain (Max.)	Main lope direction	Angular beam width
1	OFF	OFF	3.75-3.9,4.9	-19.5 -10.2	3.1, 3.5	156º -5º	57.7º 54º
2	OFF	ON	4.9	-10	2.84	-179º	39º
3	ON	OFF	3.6-3.9 ,4.9	-10	0.7,3.16 3.19,2.7 2.8	172º 166º 161º -14º	78º 69º 63.4º 68.6º
4	ON	ON	3.6-3.8	-10 -20	3.3	168º 160º 149º	75.5º 64º 53º

These two varactor-diodes used to control the antenna radiation at (3.6,3.9 and 4.9GHz) and guide the main lobe to the desired location at varying the cases of (LDRs), as shown in Table (4.3), (4.4), (4.5) respectively. For mention, this phenomenon is called (beam steering) [37].

Table 4.3: Antenna main lobe direction with varying the varactor diodes at 3.6GHz.

Varactor Diodes		Main Lobe Direction (Photo Resistance)			
D1	D2	Case1 (00)	Case2 (01)	Case3 (10)	Case4 (11)
1 pF	1 pF	174	173	172	167
1 pF	5 pF	174	173	173	167
1 pF	10 pF	174	173	173	167

Table 4.4: Antenna main lobe direction with varying the varactor diodes at 3.9GHz.

Varactor Diodes		Main Lobe Direction (Photo Resistance)			
D1	D2	Case1 (00)	Case2 (01)	Case3 (10)	Case4 (11)
1 pF	1 pF	148	29	147	25
1 pF	5 pF	148	156	32	159
1 pF	10 pF	149	157	31	159

Table 4.5: Antenna main lobe direction with varying the varactor diodes at 4.9GHz.

Varactor Diodes		Main Lobe Direction (Photo Resistance)			
D1	D2	Case1 (00)	Case2 (01)	Case3 (10)	Case4 (11)
1 pF	1 pF	-2	1	-141	130
1 pF	5 pF	-176	-179	-147	128
1 pF	10 pF	-175	-178	-150	127

Below, figure (4.11) is shown S11 parameter of suggested antenna design on different cases of LDRs and without varactor diodes.

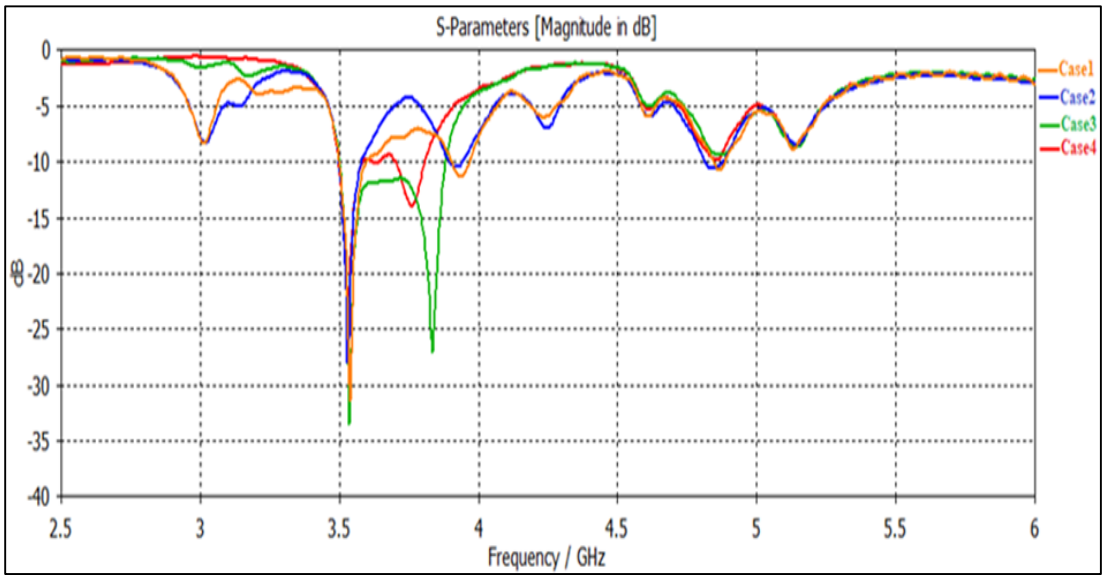

Figure 4.11: S11 parameter for proposed antenna design with varying photo resistors conditions (with matching circuit).

4.3 RADIATION PATTERN (MAIN LOBE DIRECTION AND BEAM SPLITTING)

This section displayed the Radiation pattern or is called (Main lobe Direction). It is changing by using the varactor diode in matching circuit [42],[108] to guide antenna radiation to desired location at different states of LDRs that used to reconfigurable antenna [37]. In this section we used (D1=1PF and D2=10PF) as varactor diodes at four states of LDR, due to, these diode values realized best results for antenna parameters. Figures (4.12), (4.13), (4.14) are showed the radiation patterns at resonate frequencies (3.6,3.9,4.9) GHz respectively as be clarified in tables (4.3, 4.4, 4.5) respectively too.

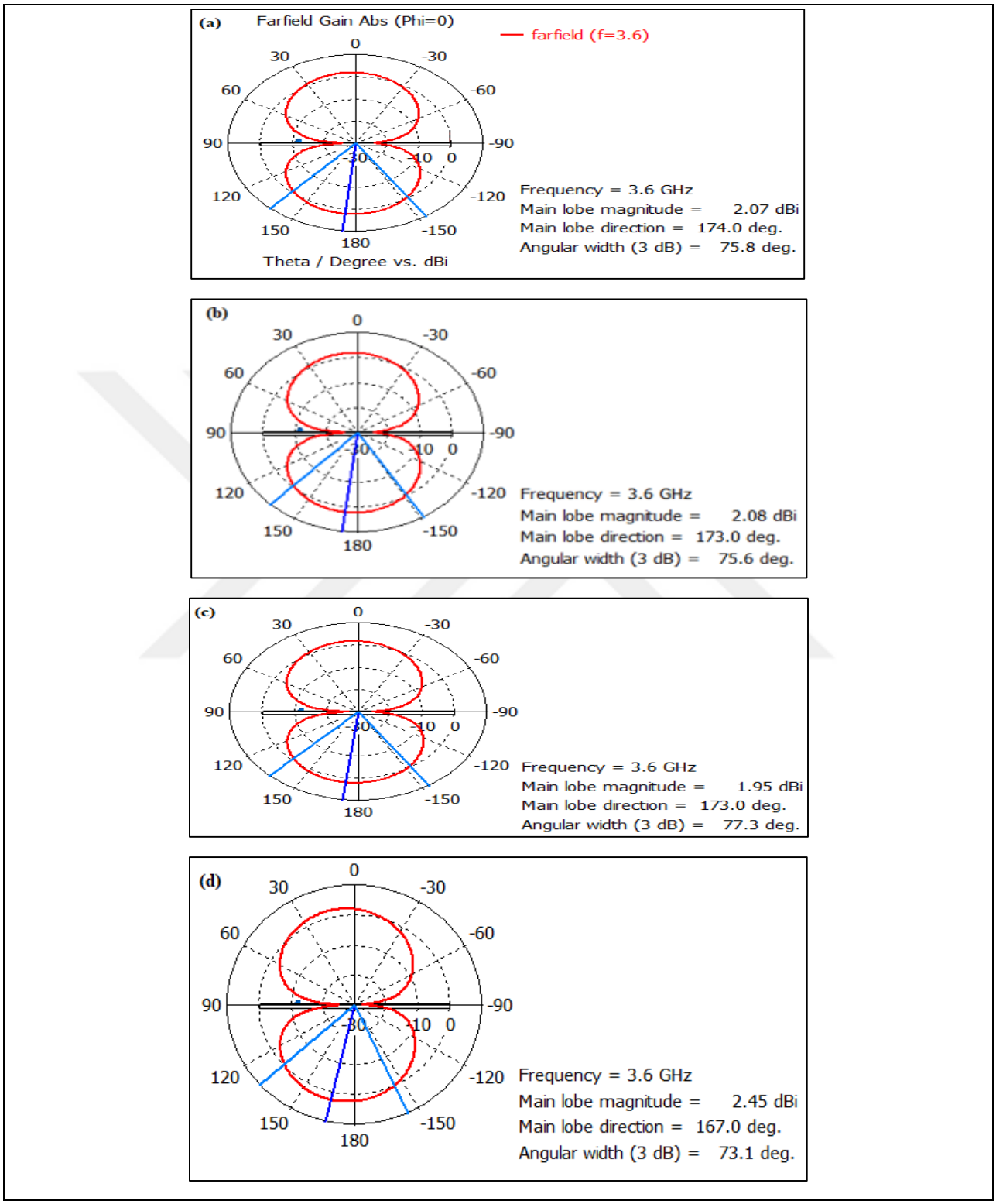

Figure 4.12: Radiation pattern of 3.6GHz cases. “figures continued” (a to d); (a)00 (b)01 (c)10 (d)11.

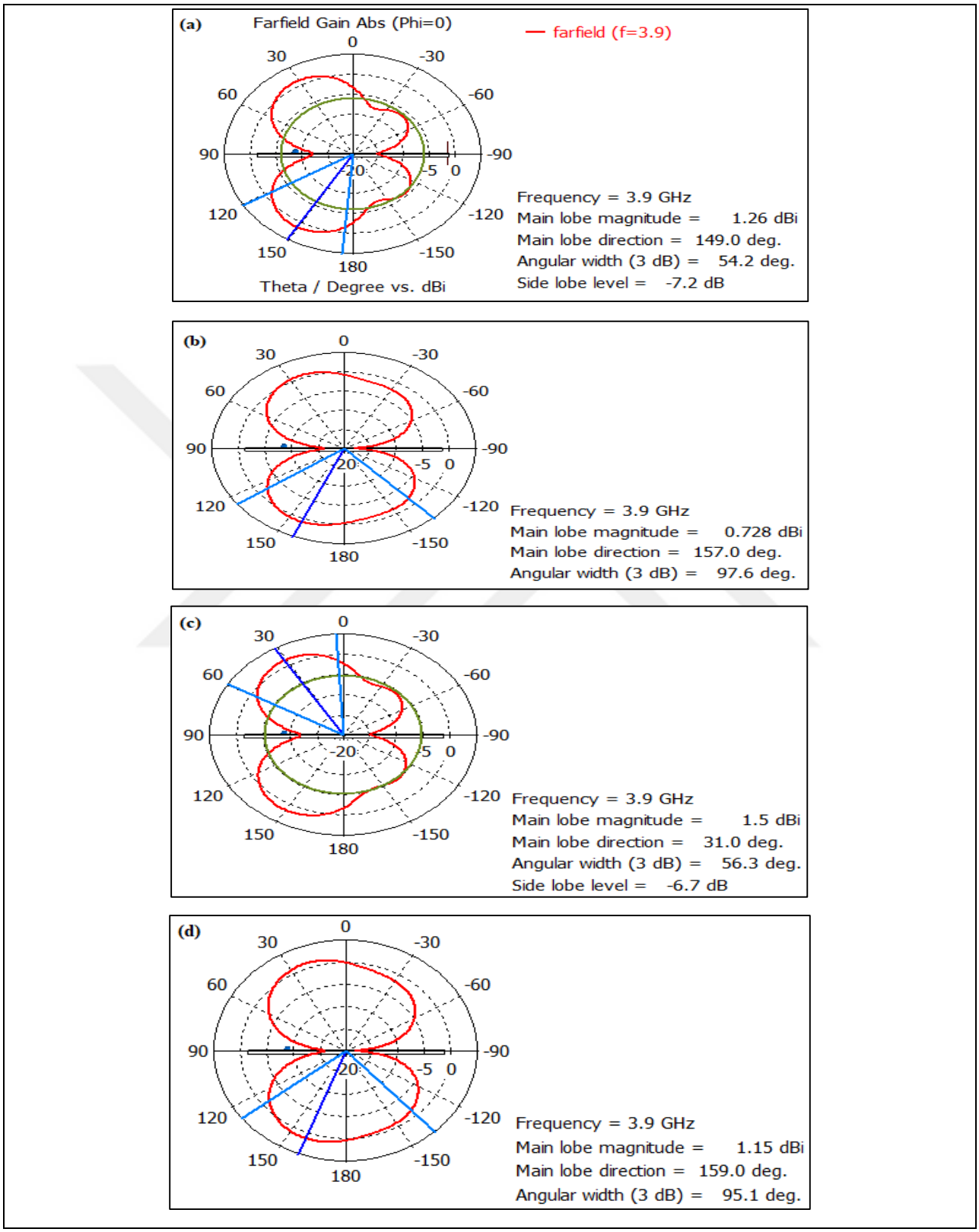

Figure 4.13: Radiation pattern of 3.9GHz cases. "figures continued" (a to d) ; (a)00 (b) 01 (c)10 (d)11.

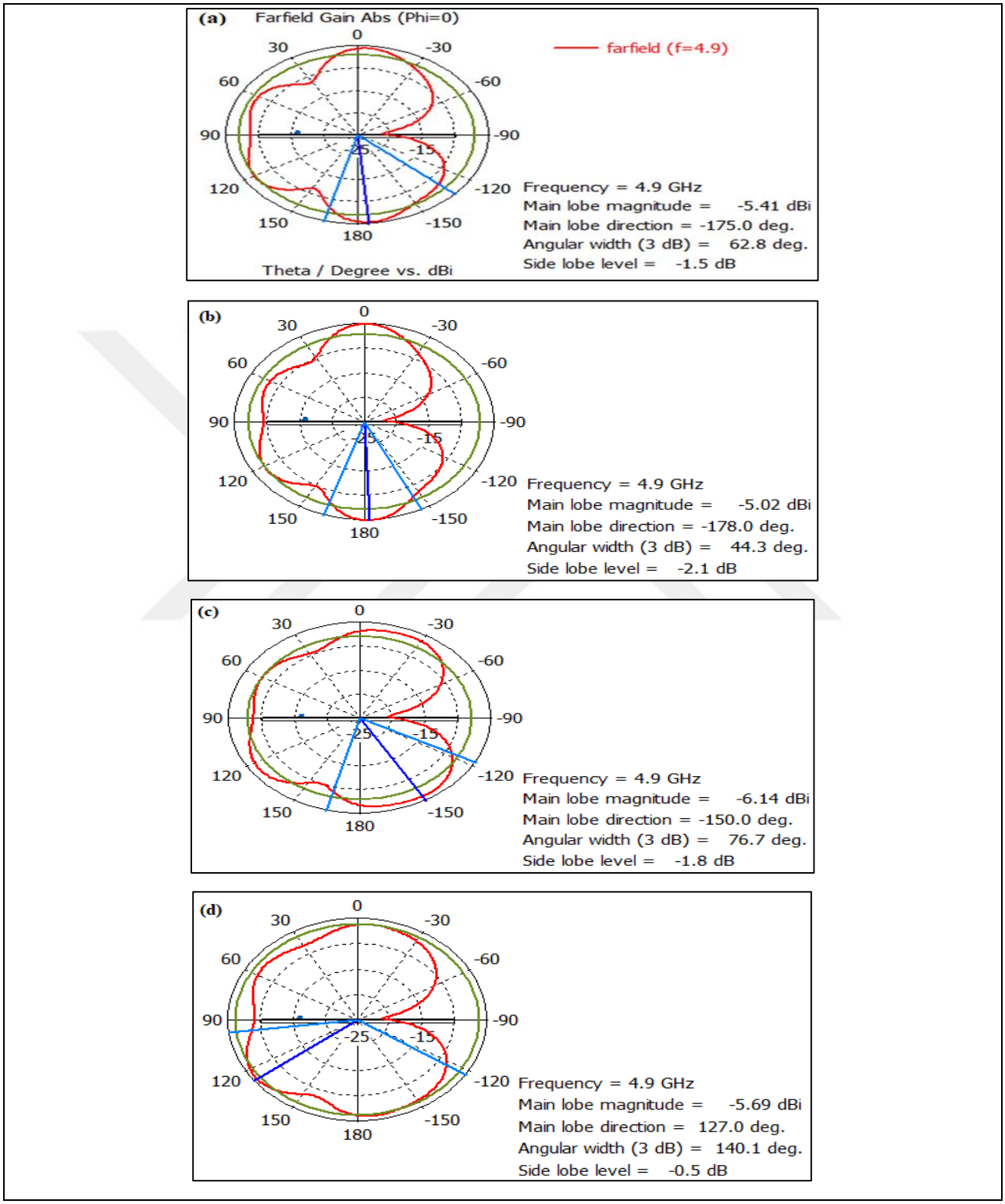

Figure 4.14: Radiation pattern of 4.9GHz cases. "figures continued" (a to d); (a)00 (b) 01 (c)10 (d)11.

The current distribution on radiated patch and the (T- junction) in antenna structure that presented in section (4.2.3) are working to split the major beam to increase the receiving users number from same antenna on same resonate frequency. This property considered as a novelty of our proposed antenna at the antenna resonate frequencies. Figure (4.15) showed, example of the beam splitting, that occurs at (4.9GHz resonate frequency, in Case2 (01) of LDRs and at the varactor diodes (D1=1 Pf, D2=10Pf) [37].

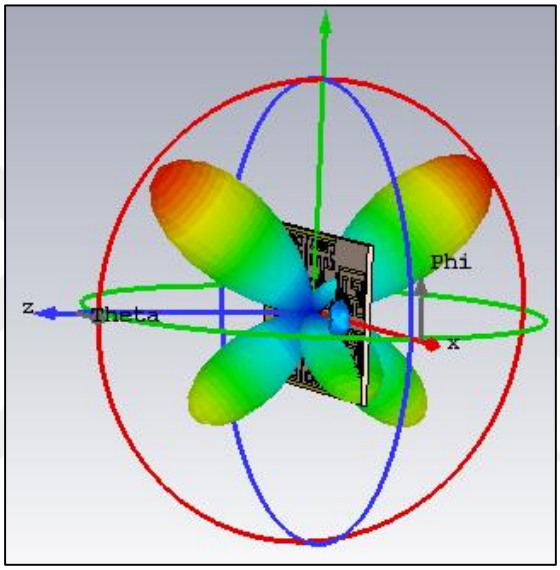

Figure 4.15: Antenna beam splitting.

4.4 ANTENNA EQUIVALENT CIRCUIT MODEL

Antenna circuit model is clarified in figure (4.16). Where the suggested structure is built utilizing Richard-model [109], that is based lumped-elements notion. The structure-based (Moore) shape, it is considered the fractal segment which could be calculated [110]:

$$N_n = nN_1 \tag{4.1}$$

Where, (n) a fractal iteration, ($N_{1)}$ a fractal segment number, (N_n) the fractal order. This revised that total fractal length (L^n) could be determined as:

$$\mathbf{L^n = \frac{8n}{2n+3} L_0^n} \tag{4.2}$$

where (L_0^n) acts perimeter of traditional rectangle which occupies by fractal. Therefore, that total perimeter length is increasing with increase an external side edge as:

$$L(n) = (2^n + 1)S \tag{4.3}$$

From equation (4.3), it is found the perimeter is increasing exponentially with (n) rise. In figure (4.16) can be seen the suggested circuit model. it is considered via connecting (50 Ω) as input-impedance of RF source series of (R-L-C) parallel branch called as (L_m=1.1nH, R_m=21Ω, and C_m=0.1pF) for Moore-structure cell. (T.L.) was characterized as inductive part (L_T=2nH) and capacitive air-gaps (C_{gap}=1.3pF). open (T-stub) that connected to the (T.L.) center is defined as ($L_{T\text{-}stub}$=1.6nH) in parallel with capacitor ($C_{T\text{-}stub}$=2.3pF), this branch is connected with ($R_{T\text{-}stub}$=30Ω) serially. While each of (R_p=22Ω and C_p=2.3pF) are represented the substrate equivalent effects and it connected in parallel with proposed model. For mention, the lumped elements in figure (4.16) are designed by (Advanced Design System ADS) software package.

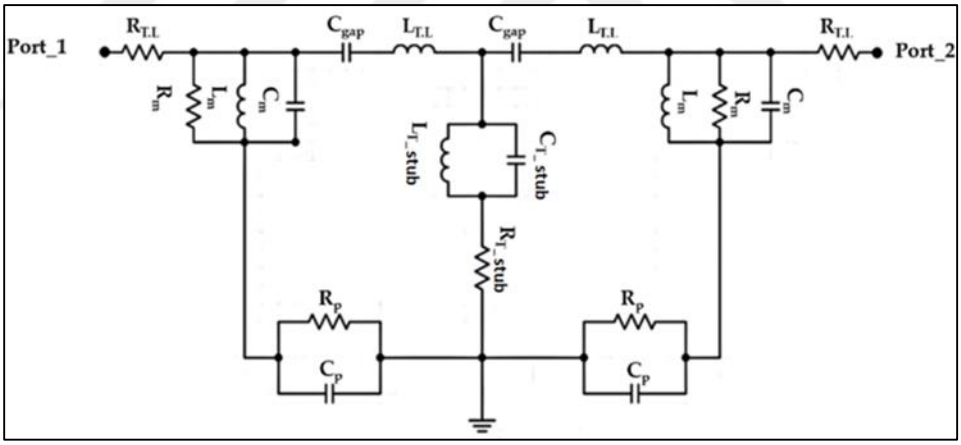

Figure 4.16: Equivalent circuit model.

4.5 EXPERIMENTAL VALIDATION

Before immediate the antenna fabrication, we implemented a numerical simulation based (HFSS) simulation [123], for more validation. we found that acquired results by both (CST and HFSS) software packages are concurrence very well. Then, suggested antenna design is fabricated utilized (chemical deposition) process as clarified in figure (4.17) (a). In this section, antenna prototype is tested experimentally by utilizing (VNA) vector network analyzer (37347A) and MW chamber. We assessed the antenna performance by expressions of (S_{11}) and gain spectrum as clarified in figure (4.17) (b). It is found the antenna provides more operating frequencies (f_r) for example, it

gives (3.9GHz and 4.9GHz) as the resonate frequencies with gain (G) of (3) and (3.5) respectively, at case1 (00) ,meaning without photo resistors and varactor diodes effects.

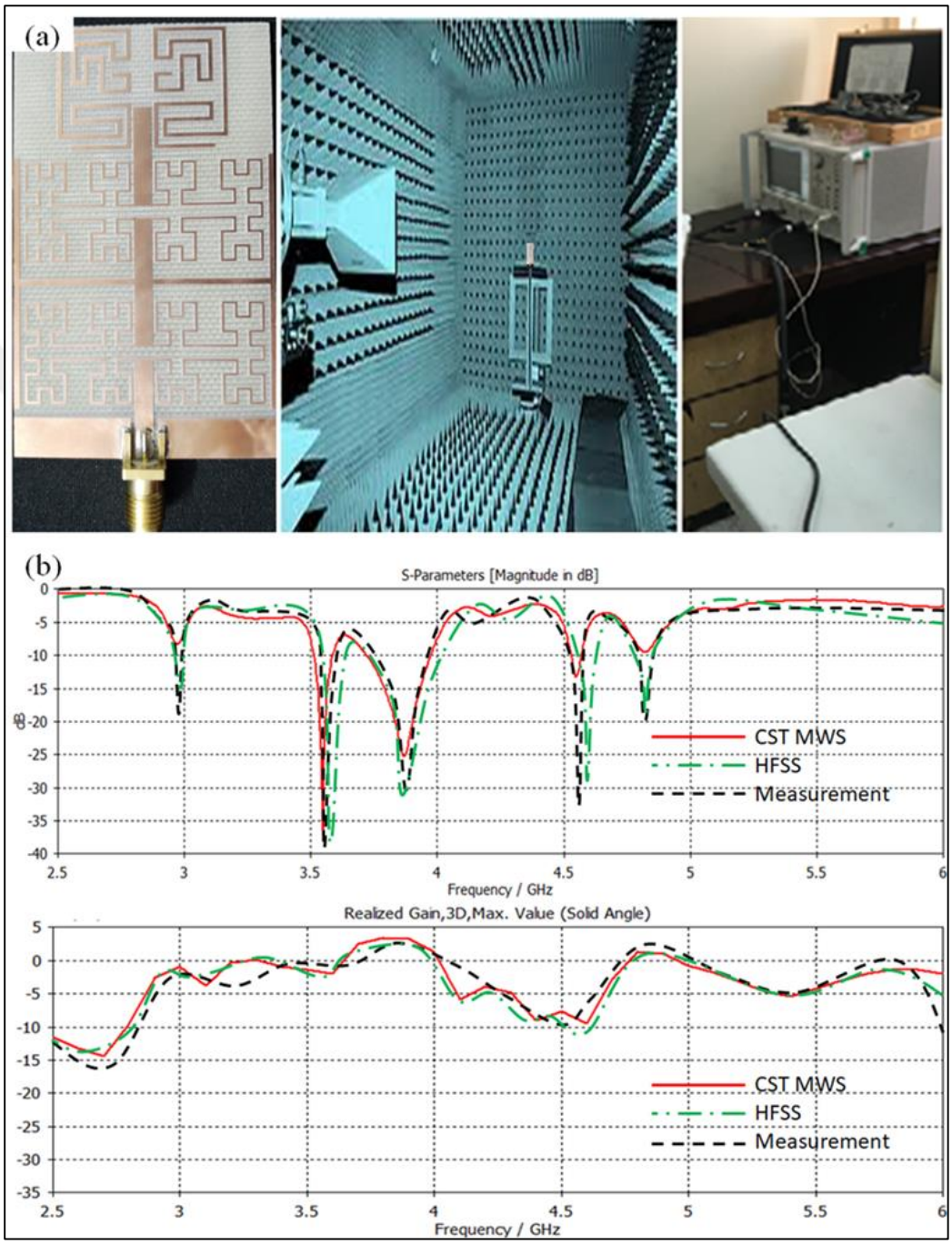

Figure 4.17: Antenna performance validation (a) fabricated-prototype and measurement process (b) S11 and gain results.

Finally, the measured and simulated results of radiation patterns on (3.6GHz, 3.9 GHz and 4.9 GHz) are clarified in figure (4.18). Measurement results were done in RF anechoic chamber. From

these measurements, we found a significant change in width and directivity of major lobe according to varying states of switching (LDRs) as (00, 01, 10, 11) and without using the varactor diodes in matching circuit load. Also, it can be shown good matching between simulated and measured results.

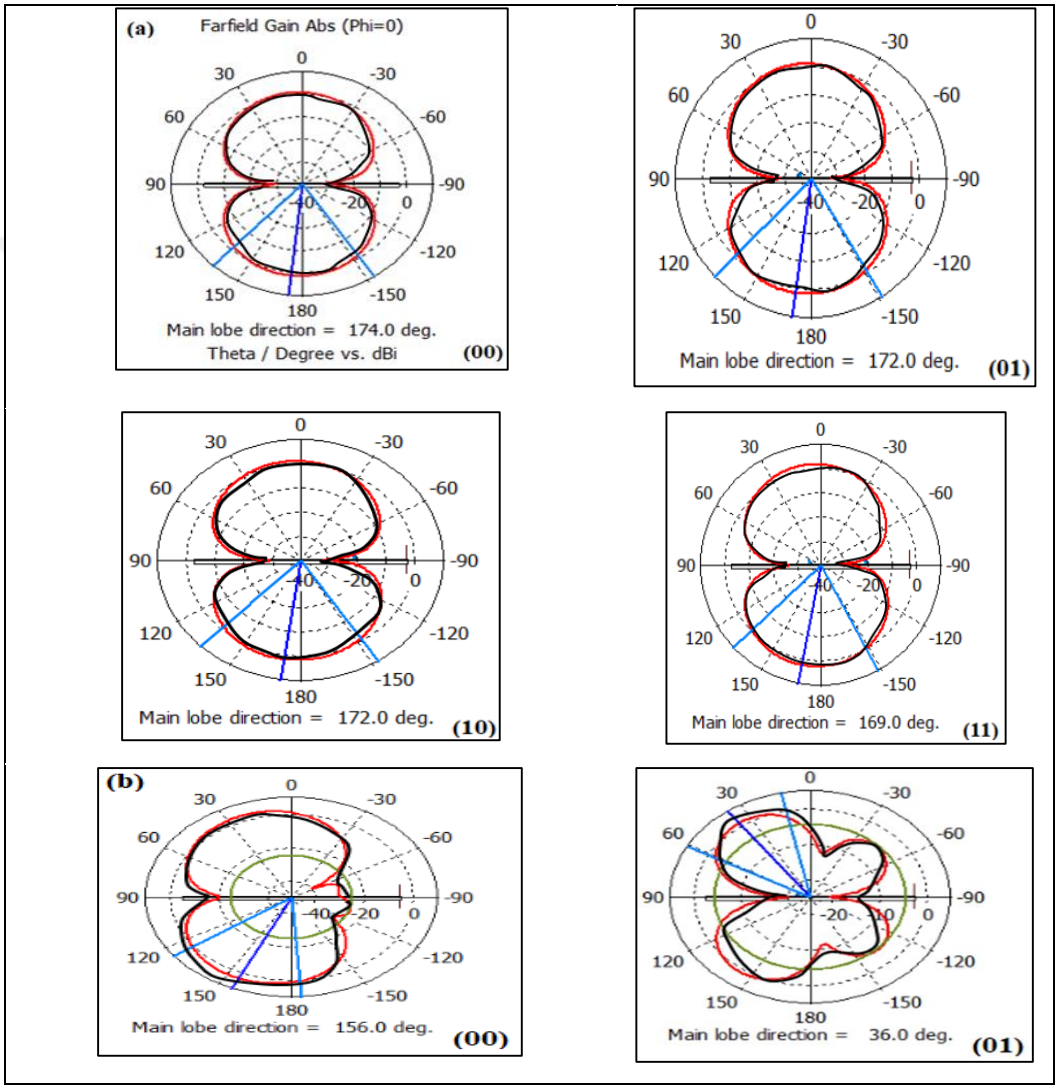

Figure 4.18: Radiation-pattern of single element (a to c) on (a) 3.6 GHz, (b) 3.9 GHz and (c) 4.9 GHz, note: back solid line is a simulation and red solid line is measured results.

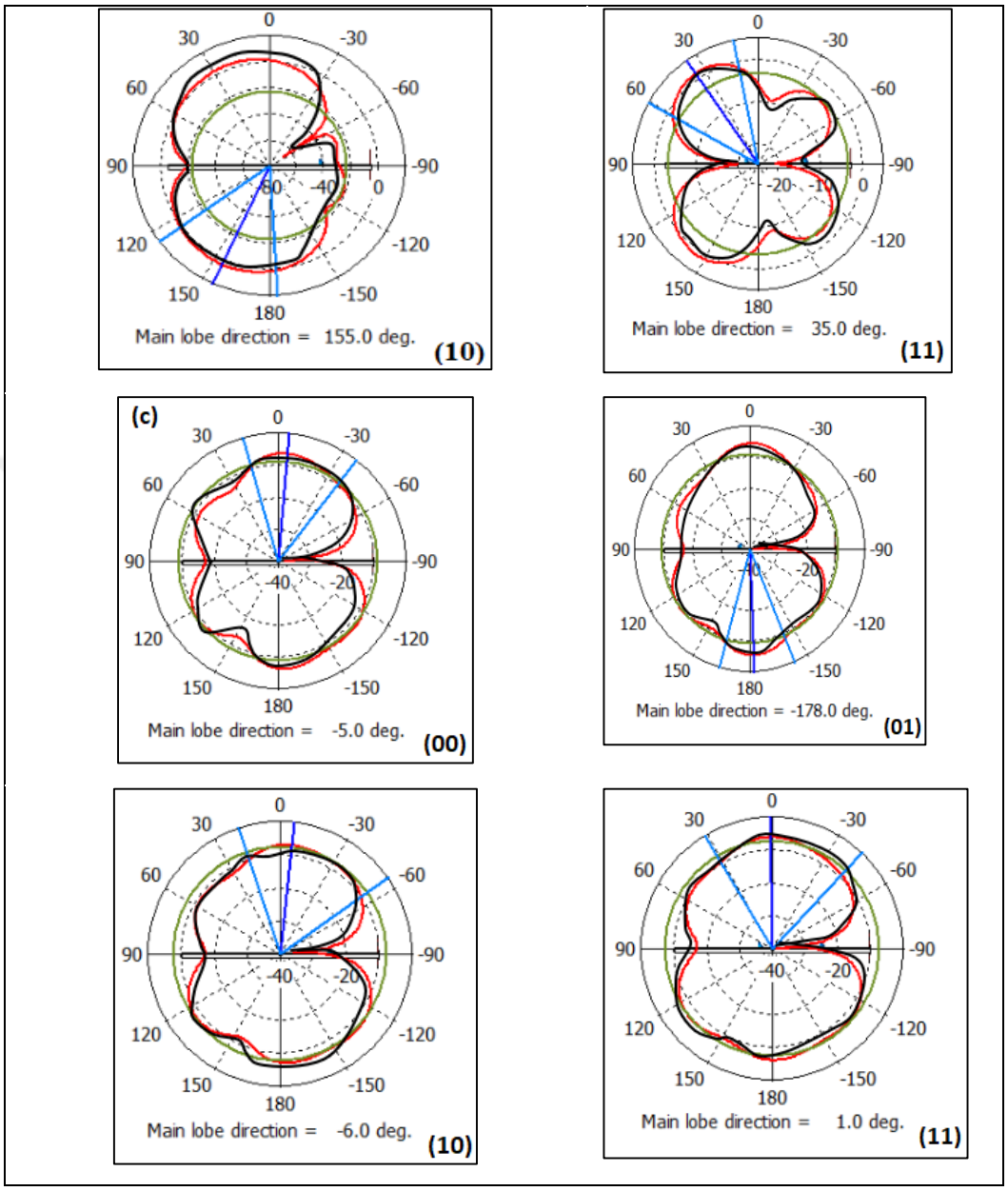

Figure 4.18: Radiation-pattern of single element (a to c) on (a) 3.6 GHz, (b) 3.9 GHz and (c) 4.9 GHz, note: back solid line is a simulation and red solid line is measured results 'Figures Continued'.

4.6 COMPARISON WITH OTHER REFERENCES

The antenna performance is compared with the other antennas that studies in previous published papers. The comparison including more terms such as (substrate type, operating frequency, antenna size dimension, gain and reconfigurable process. We found that our antenna achieves excellent design for radiate beam forming and frequency-reconfiguration. Subsequently, our antenna achieves three operating frequencies, as be list in comparison table (4.6).

Table 4.6: Comparison between this work performance with other published results.

Ref.	f_r/GHz	Substrate	G_o/dBi	Size/mm	Reconfiguration process	Diodes No.
1	3.5,3.8	FR4	2.3	10.7×22.5×1.6	No	uncontrolled
111	3.5	FR4 epoxy	5	25.2×48×1.6	No	uncontrolled
112	2.45, 3.5, 5.2	FR4	3.4	39 x 37×1.6	Frequency	1
113	2, 3.4, 2.4, 3.1	FR4	1.98	37×35×1.6	Frequency	2
114	2.1, 2.45, 3.2, 3.5	FR4	2.2	37×35×1.6	Frequency	2
115	2.55,3.5, 4.75	Teflon	3	47×19	No	uncontrolled
116	3.31,6.	Glass epoxy	2	25×25×1	Frequency	3
This work	3.6,3.9,4.9	FR4	3, 3.5	62×40×1.6	Beam forming and frequency	2

4.7 ARRAY DESIGN AND GEOMETRICAL DETAILS

In this section a novel 3D MIMO reconfigurable antenna array design is proposed for 5G applications [43]. This array structure consists of four Microstrip patch antenna which arranged as a cubic array, each cubic side has one antenna element as be clarified in figure (4.19) (a). This array provides broadside-radiation pattern in order to coverage the tangent radiation, this property as the result of add the fractal geometry, high mutual coupling reduction was realized [37].

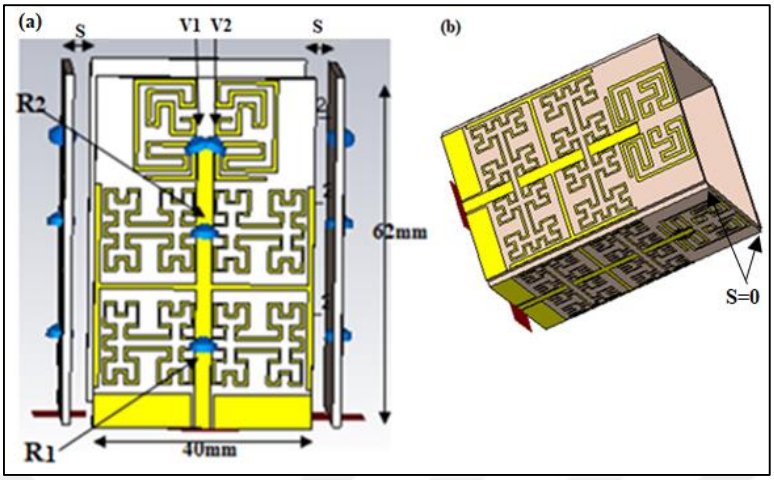

Figure 4.19: Cubic antenna array (a) front side (b) antenna array at S=0

4.7.1 Antenna Array Parametric Study

This section showed results analysis antenna array parameters such as the Return loss S_{11}, Mutual Coupling and spectral Gain.

4.7.1.1 Return loss and mutual coupling

In this section we study the S-parameter in terms of S_{11}, S_{12}, S_{13}, and S_{14}. we study these terms in three states dependent on the distance (S) that separated between Antennas in Cubic Sides, these distance represented as (0 ,3and 6) mm. (S11) is represent the return loss, (S12) and (S14) represented the mutual coupling between adjacent elements and that occurs between radial elements (between opposite side antennas) is S13 [117]-[118] .From figure (4.20), it is found the best result at the distance between adjusting elements (S= 6mm), where the ($S11 \leq -10$) and the mutual coupling is ($\leq$-20dB) for most (S12, S13, and S14) at the interest frequency band. Figure (4.20) is clarified the S-parameters at different value of S distance.

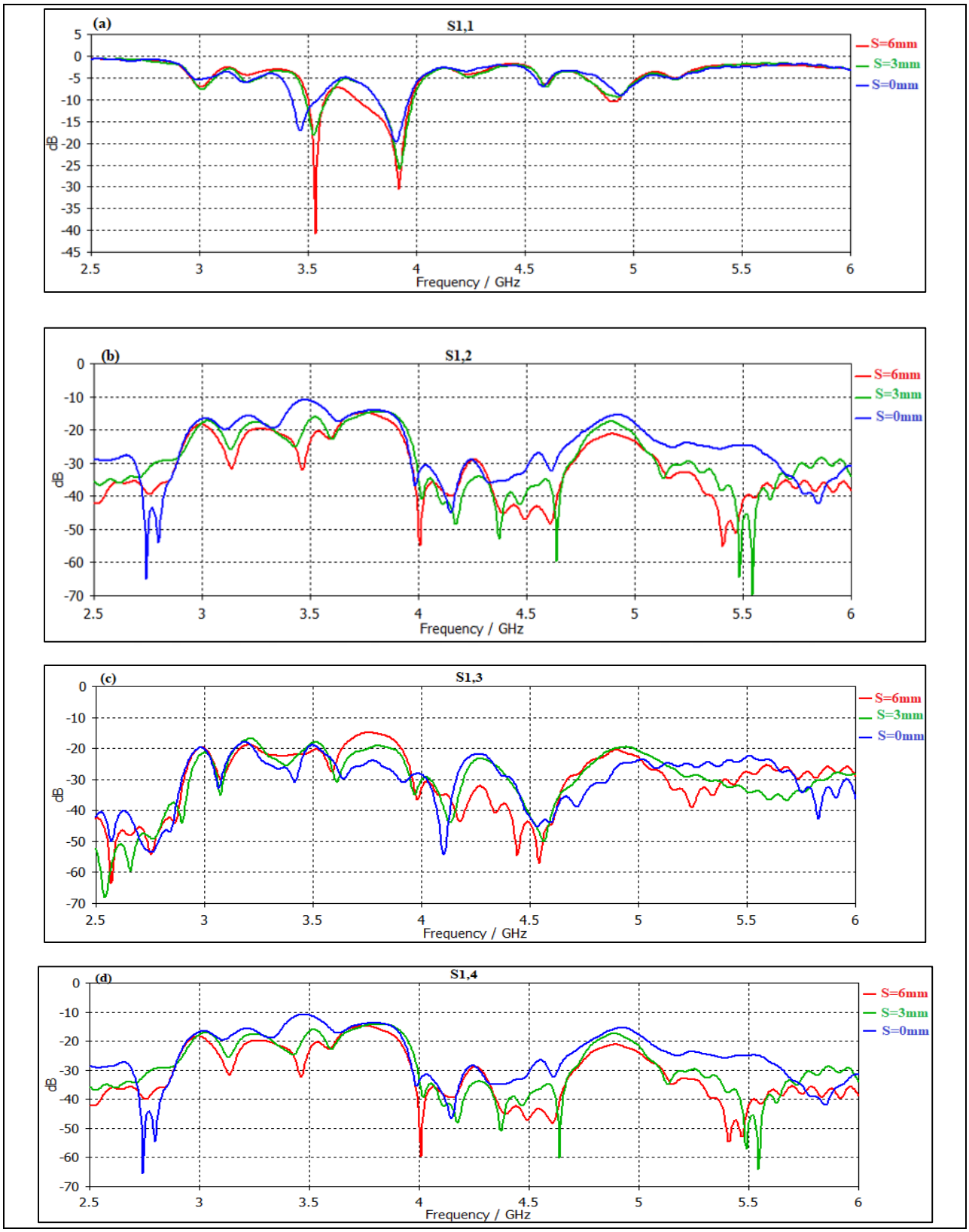

Figure 4.20: S-parameters in different value of (S) (a to d) (a) return-loss (b) and (d) the mutual coupling of adjacent elements (c) radial mutual coupling.

4.7.1.2 Gain spectra

This section clarified the Gain of Antenna Array, each Antenna generate moderate gain that suitable for 5G and other modern applications [107]. The maximum gain at (S=6mm) measured 4.4 and 4.2 at 3.9GHz and 4.9GHz respectively. Figure (4.21) is clarified the array gain at different value of S.

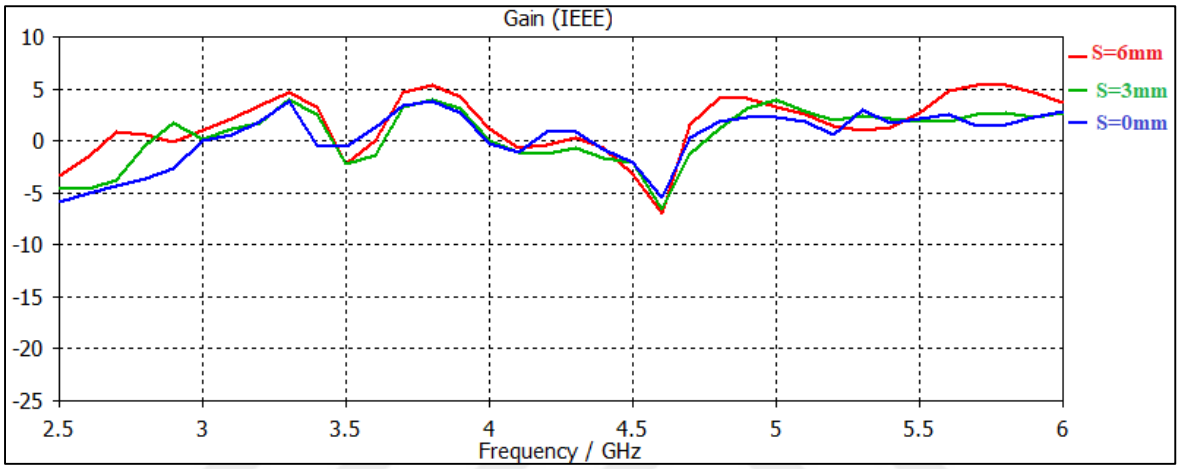

Figure 4.21: Gain of antenna array in various value of S.

4.7.2 Antenna Array Correlation and Diversity

Antenna correlation coefficient (ACC) is one of an important antenna parameter, it is measured of antenna independence respect to adjacent antennas. lower value of (ACC) is realize better independence to antennas from other.

antenna diversity or (a space diversity or spatial diversity) is a diversity scheme which utilizes two or more antennas to enhance the wireless quality and reliability. There are many types of antenna diversity such as (space, frequency, time, polarization, directional and pattern diversity) [72],[119] In this section, we focused on correlation and diversity. The correlation and diversity are measured and clarified for suggested antenna array in figure (4.22). It is found that the correlation factor at 3.6,3.9 and 4.9GHz below 0.5% as be displayed on figure (4.22) (a); while, a diversity is found nearly of 99.8% as displayed on figure (4.22) (b) [43].

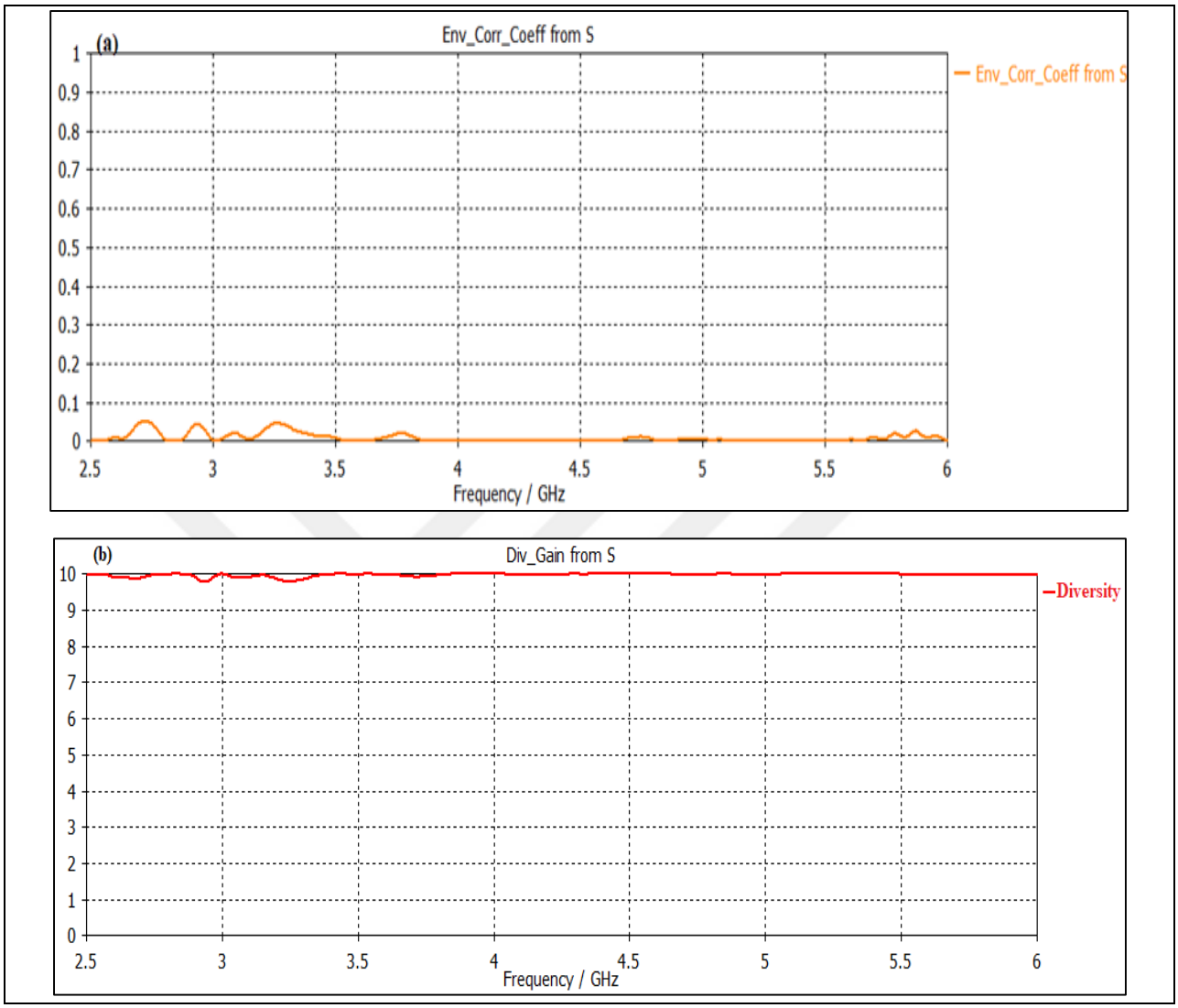

Figure 4.22: MIMO correlation and diversity (a) correlation (b) diversity.

4.7.3 Results Validation

In this section, we showed the simulated and measured results. MIMO antenna prototype is fabricated by using (FR4) substrate. S- Permeameters and the radiation patterns at the space between adjusts antennas (S=6mm) are measured. It is found, the measured result clarifies agreement with the simulated result of S- parameter by (CSTMWS) spectra with insignificant variance. So, the S-parameter and radiation patterns of antenna is measured via a (PNA) - Professional Network Analyzer (Agilent PNA 8720).

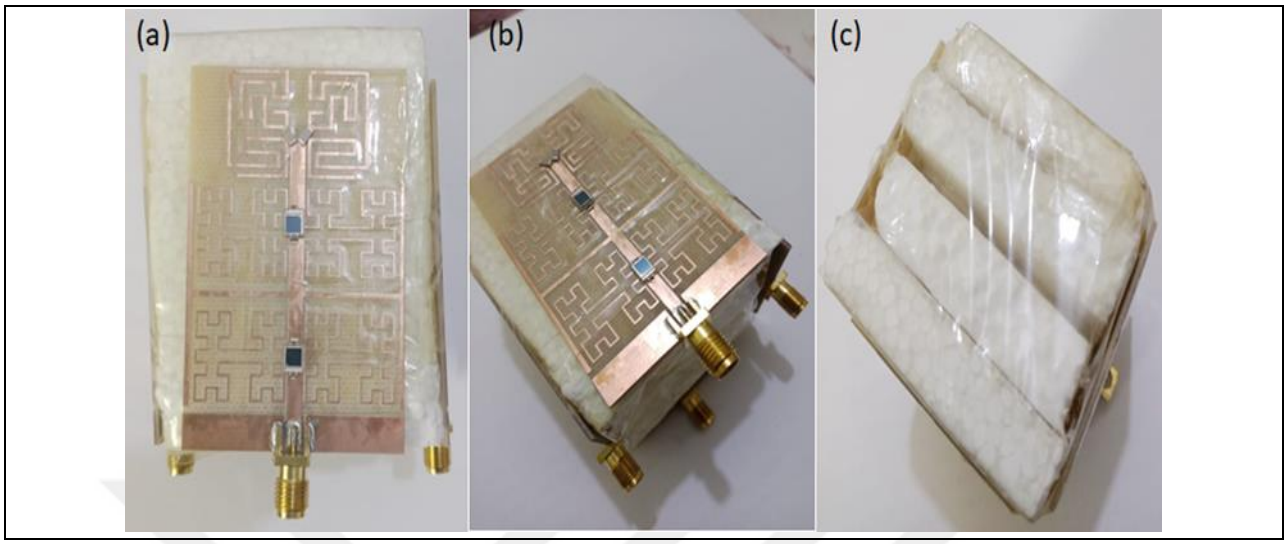

Figure 4.23: Fabricated prototype of (MIMO) antenna: (a) front view (b) cubic array (c) top view.

This section showed antenna result measurement in expressions of (S- parameters) and radiation pattern at first state, when all (LDRs) are OFF and in fourth state in other word, in case of (0,0) and (1,1). It is found, the measured results that represents by black curve is introduced an excellent agreement with simulated curve (red curve). But it is observed some of Insignificant between them, because the cables losses and the (SMA) soldering impacts.

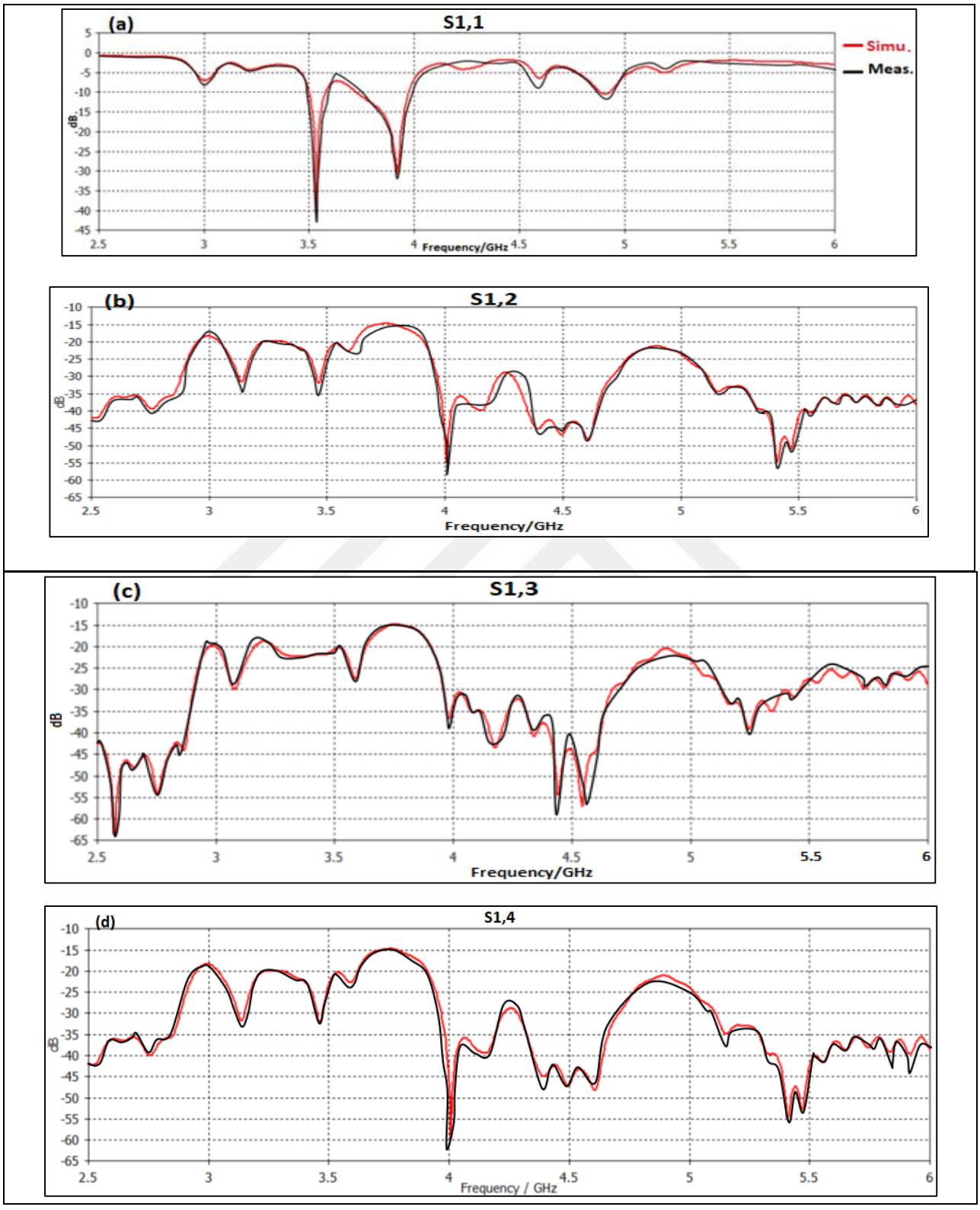

Figure 4.24: S-parameter for simulated and measured antenna when all LDRs are off.

Measured and simulated results of radiation-patterns on (3.6 GHz, 3.9 GHz and 4.9 GHz) are clarified in figure (4.25). The measurements process was done inside RF anechoic chamber in both (*Ø*-plane) and (*θ*-plane.)

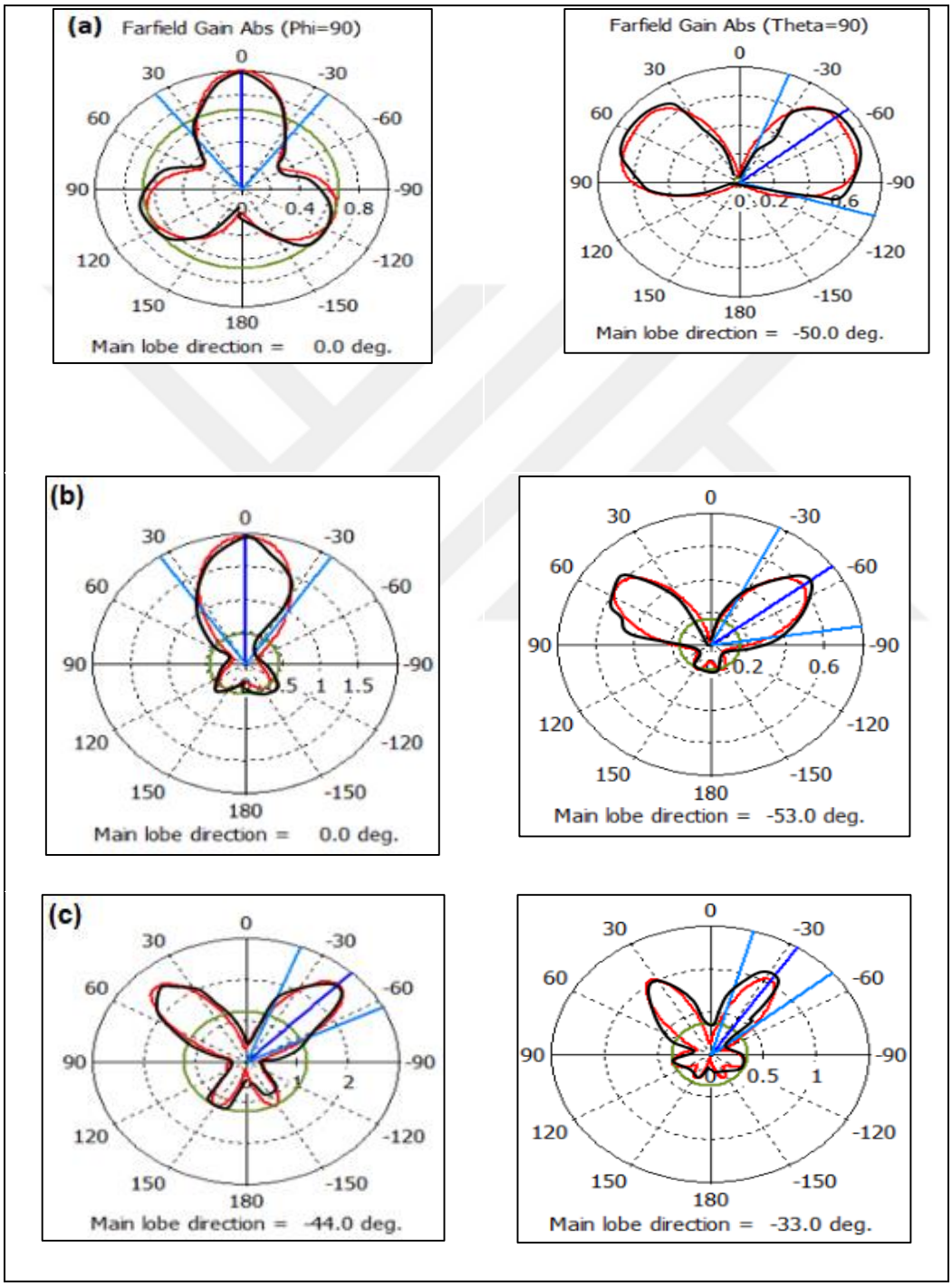

Figure 4.25: Measured and simulated results of radiation-patterns when all LDRs are off at (a) 3.6 GHz, (b) 3.9 GHz (c) 4.9GHz.

Next, it can be shown the simulated and measured result of (S-parameters) and radiation-pattern at state of all (LDRs) are ON in other word, case of (1,1).

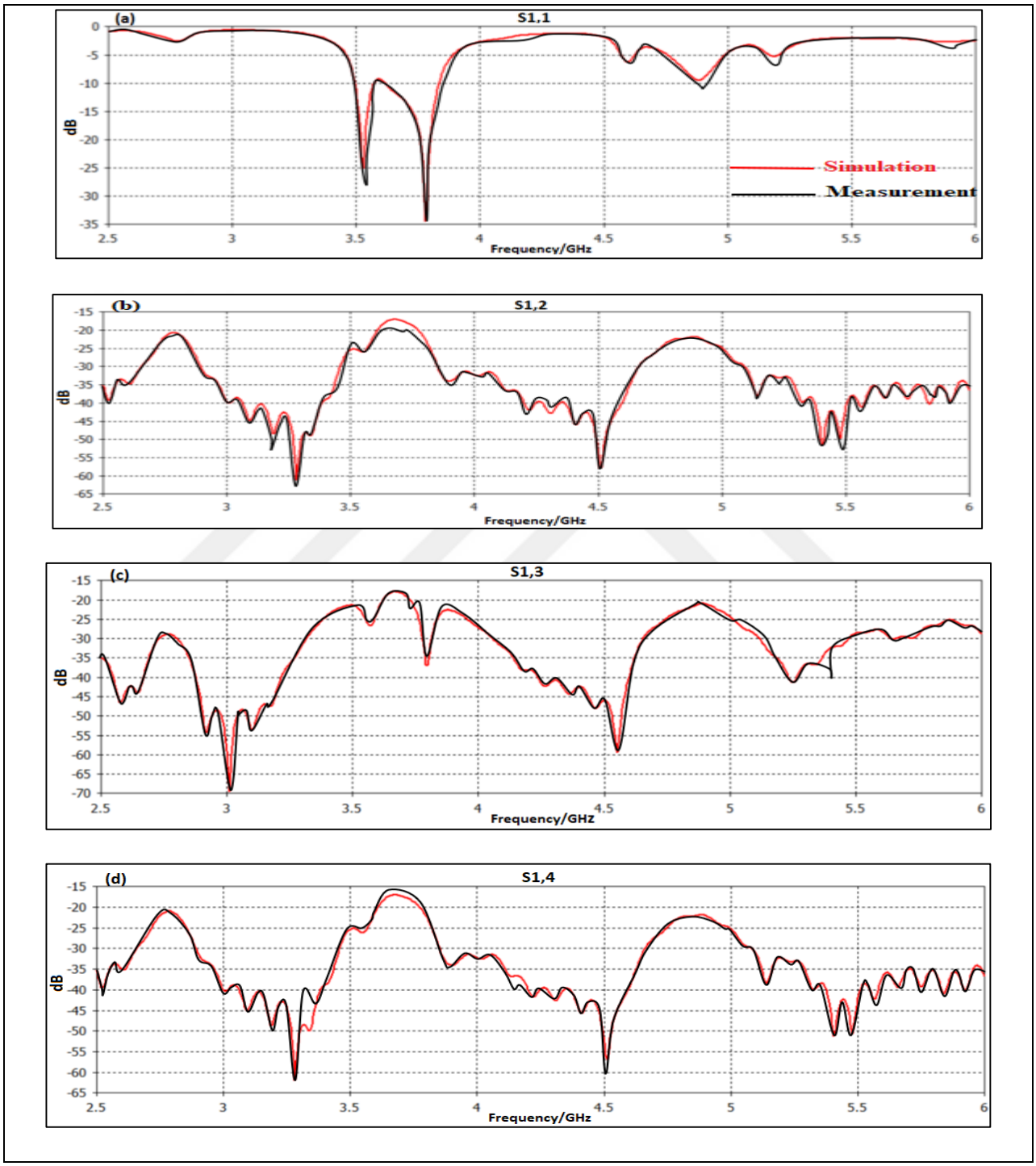

Figure 4.26: S-parameter for simulated and measured antenna when all LDRs are on.

Where, the radiation pattern measurement in both (*Ø*-plane) and (*θ*-plane.) at interested frequencies at (3.6 GHz, 3.9 GHz and 4.9 GHz) as be clarified on figure (4.27).

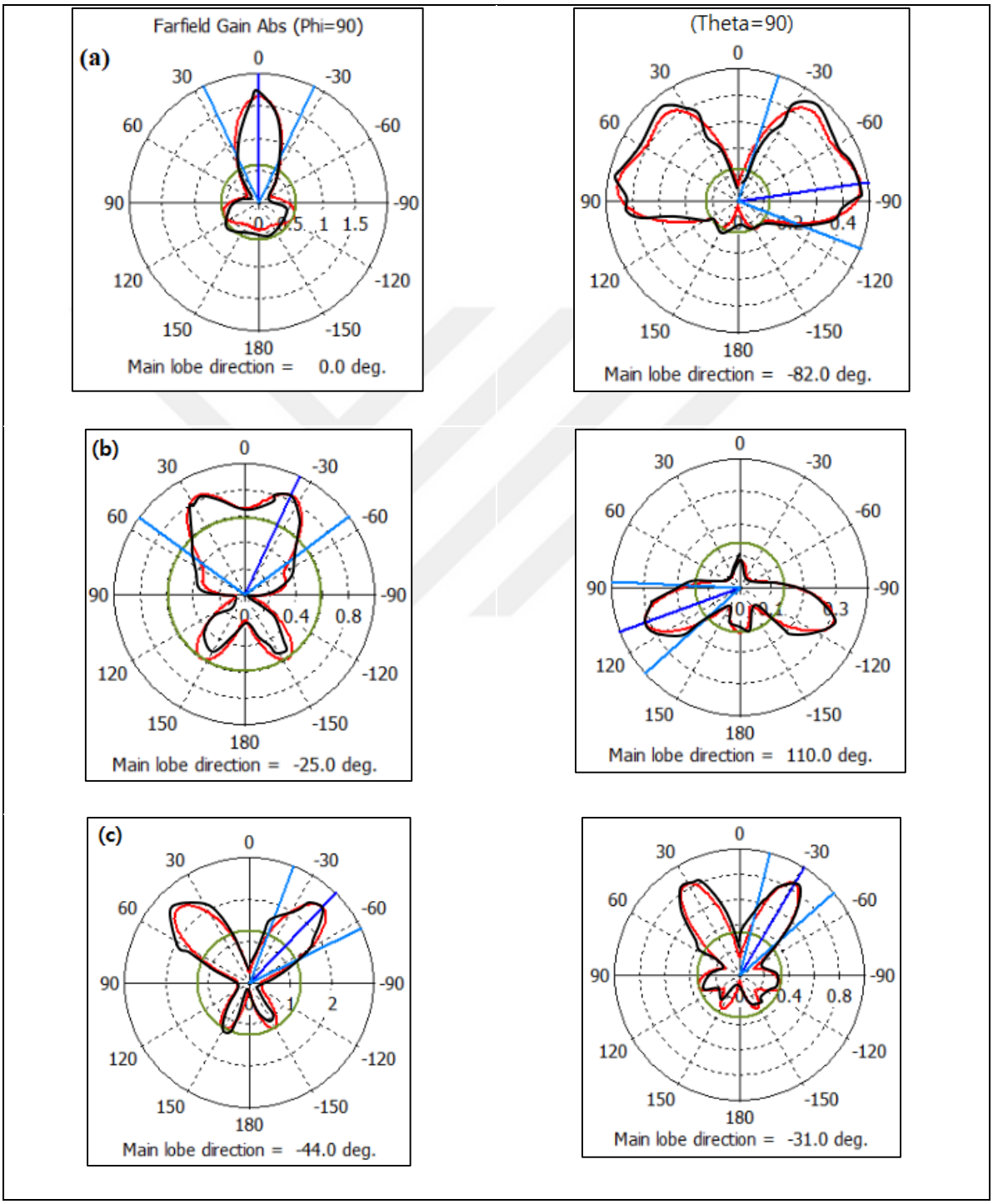

Figure 4.27: Measured and simulated radiation patterns in state of all LDRs are on at (a) 3.6 GHz (b) 3.9 GHz (c) 4.9GHz, note: the red curve represents the simulate results and the black curve is a measured.

4.8 SOLAR CELL EFFECT

In this section, it can be shown the solar (PV) cell effect on performances of proposed antenna-array in expressions of (S-parameters) and (Gain) as be shown in figure (4.28). It is found to be insignificantly affected when the solar panel introduced. In fact, the array gain is enhanced slightly at interested frequency bands, this is achieved by suppressed the surface wave effects through introduced the solar panel normally to antenna array [121].

Figure (4.28) is clarified the (S-Parameters: S11, S12, S13 and S14) and (Gain spectra) curves of antenna array with and without solar panel integrated. In figure (4.28) (b), it is found the (S11) is matching (S11≤-10dB) where is insignificantly affected at added solar panel and from figure (4.28): (c), (d) and (e) we observed the (S12, S13 and S14) are insignificantly affected also. In figure (4.28) (f), it is observed the antenna array gain is insignificantly affected at the operating frequencies, where it is found the antenna gain value is (4.3,4.2) at 3.9GHz and 4.9GHz respectively without adding the solar panel and it is measured of (4.32) at 3.9GHz and (4.1) at 4.9GHz after introducing the solar panel.

In general, it is found the solar panel is not affect negatively on antenna parameters (S-Parameters, gain and radiation pattern) when attached it on antenna array perpendicularly. This section proves that the novelty of this work to generate self-power wireless communication system without impact negatively on wireless characteristics.

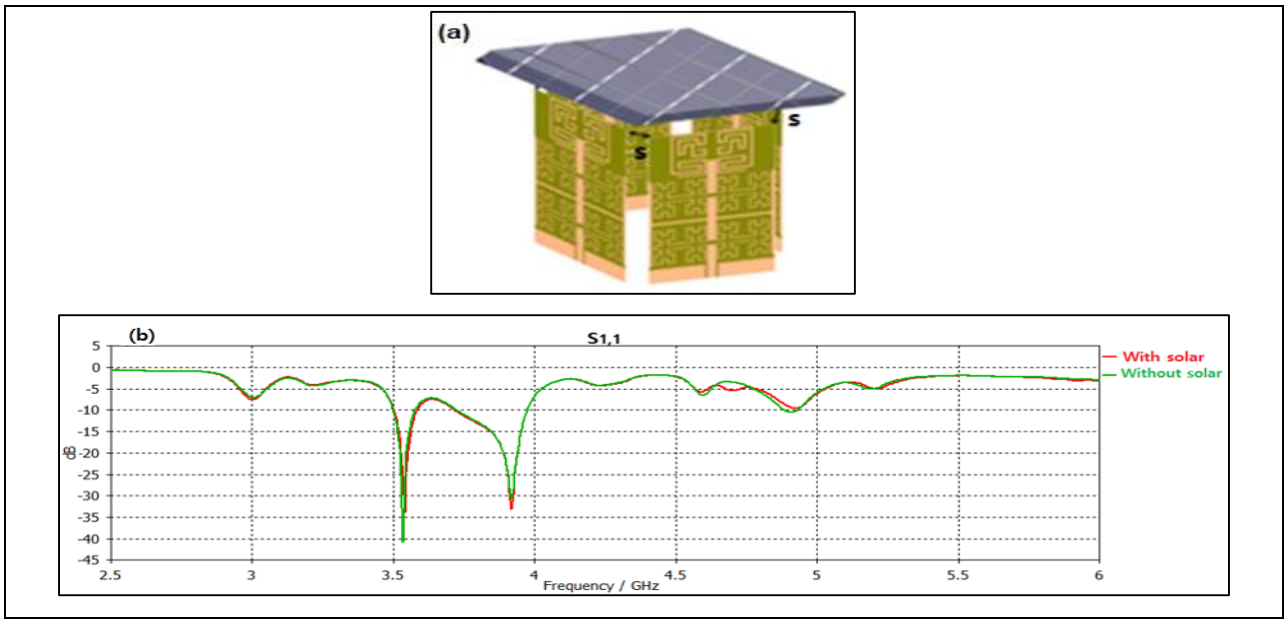

Figure 4.28: Array performance with and without solar panel instillation (a to f) ; (a) system design (b) S11 (c) S12 (d) S13 (e) S14 (f) gain.

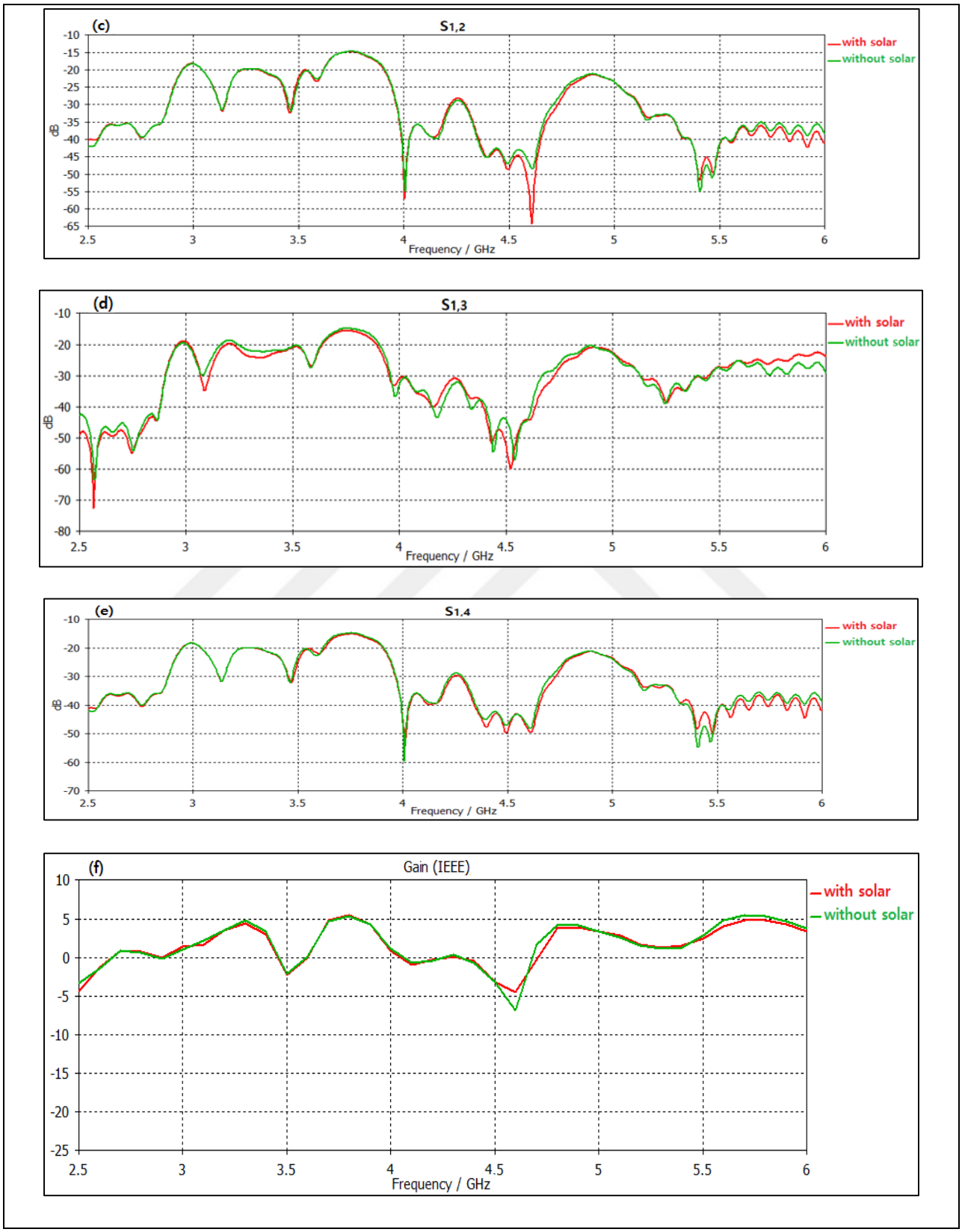

Figure 4.28: Array performance with and without solar panel instillation (a to f) ; (a) system design (b) S11 (c) S12 (d) S13 (e) S14 (f) gain 'Figures Continued'.

4.8.1 Experimental Validation

This section clarified the measurement of antenna array performance by utilizing VNA (37347A) and RF chamber [121].

The antenna array is fabricated, we can clarify the prototype and the results validation experimentally as be shown in figure (4.29). The acquired results from the simulation analysis are compared with an experimental measurement, figure (4.29) (b) and (f), is displayed the measured (S11) and gain. It is found that the results of experimental and simulation are agreement very well. The other measurements of S-parameters (S12, S13, and S14) are shown in figure (4.29) (c)-(e), where the validated of the maximum coupling (S≤ -20dB) after introduced the solar panel.

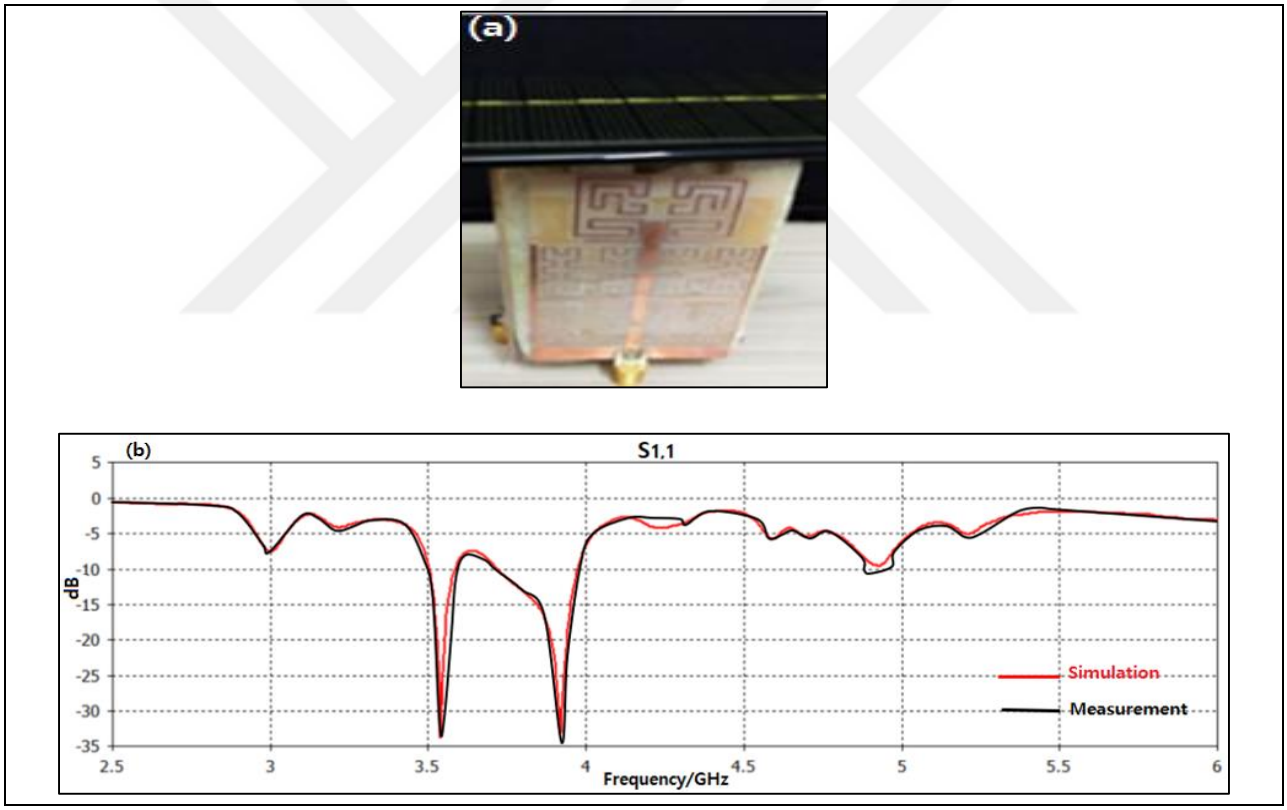

Figure 4.29: Simulated and measured results of array performance with solar panel instillation (a to f); (a) system design (b) S11 (c) S12 (d) S13 (e) S14 spectra (f) gain.

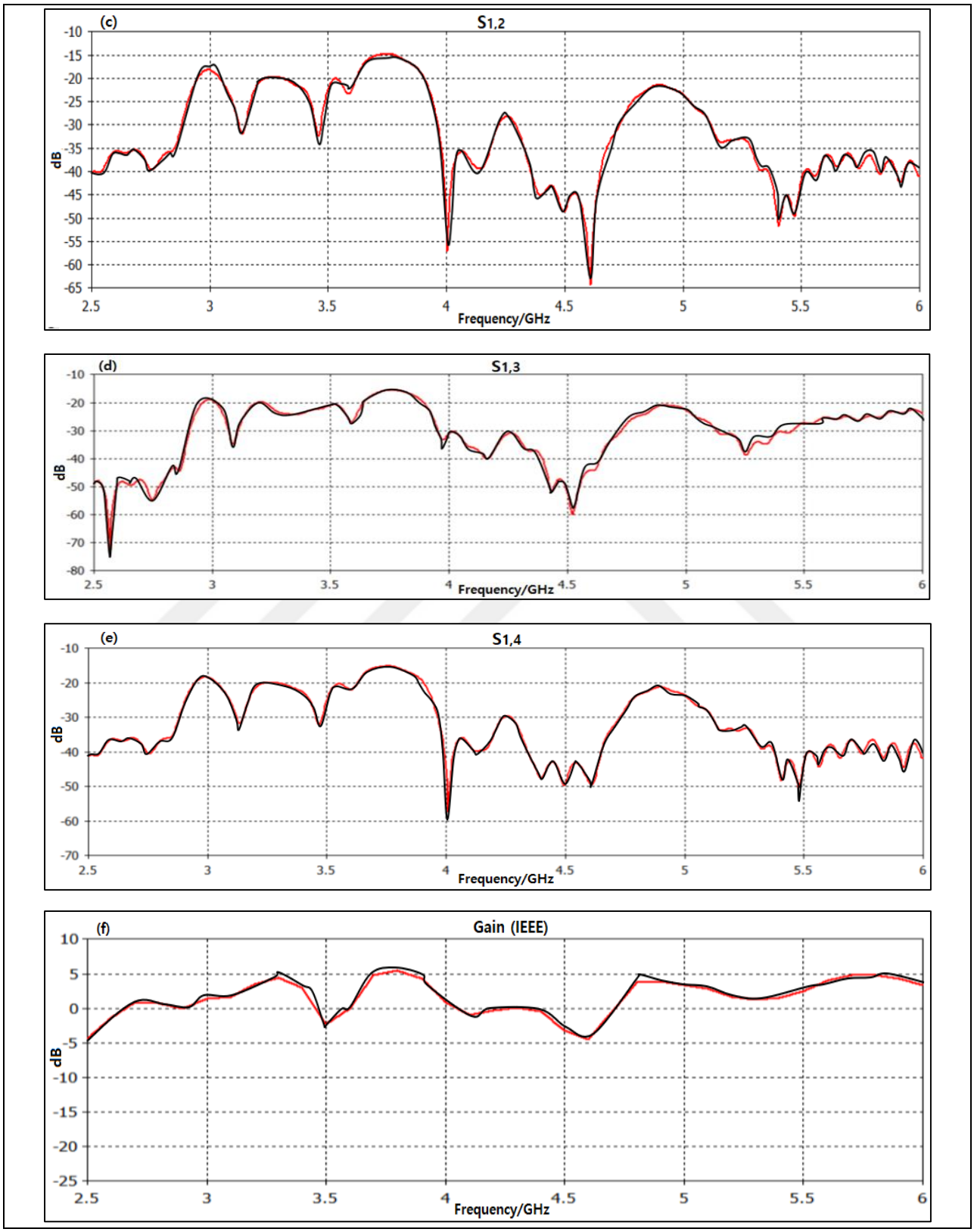

Figure 4.29: Simulated and measured results of array performance with solar panel instillation (a to f); (a) system design (b) S11 (c) S12 (d) S13 (e) S14 spectra (f) gain 'Figures Continued'.

Next, array radiation-patterns are measured on resonate frequencies of (3.6GHz, 3.9GHz, and 4.9GHz) as shown in figure (4.30) and figure (4.31). where it is observed, improving the radiate directivity of suggested antenna. The measured and simulated results are agreeing to each other well. The radiation pattern of figure (4.30) is measured at (Ø=0) and (Ø=90) in case of all RDLs are OFF (00) and without using the varactor diodes as be shown.

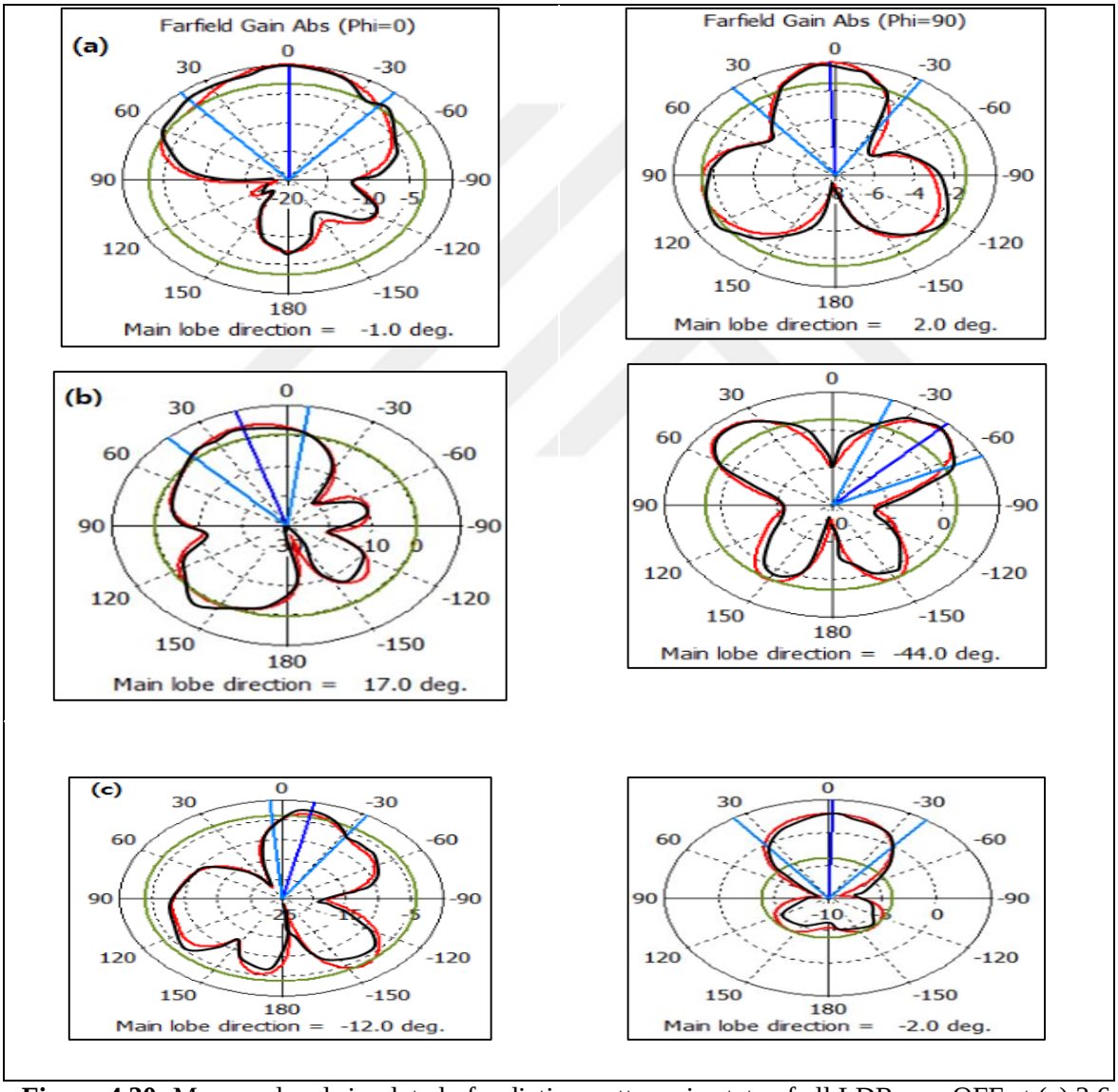

Figure 4.30: Measured and simulated of radiation patterns in state of all LDRs are OFF at (a) 3.6 GHz (b) 3.9 GHz (c) 4.9GHz, note: the red curve represents the simulate results and the black curve is a measured.

And the radiation pattern is measured also at (Ø=0) and (Ø=90) in case of all RDLs are ON (11) and without using the varactor diodes as shown below in figure (4.31).

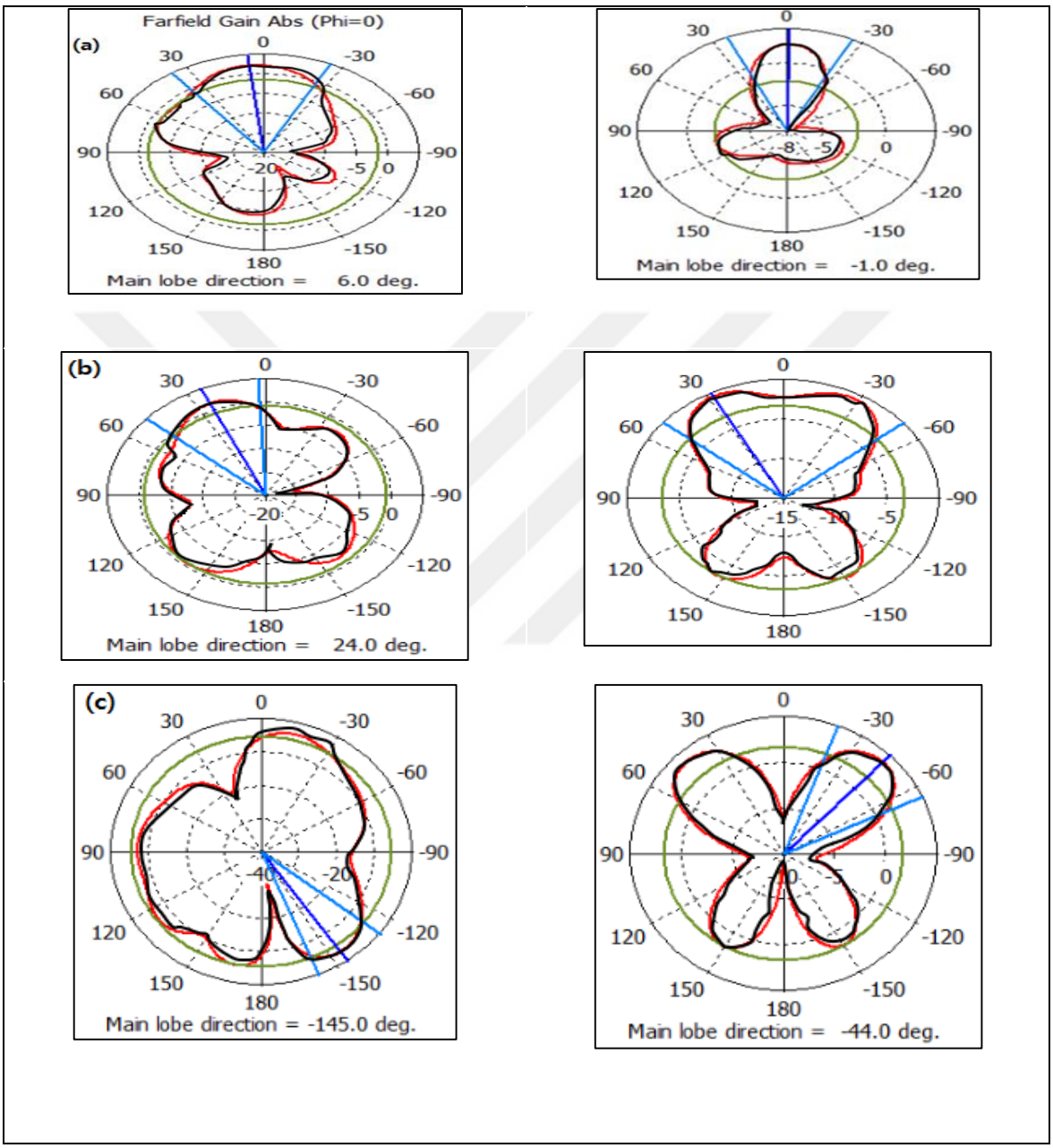

Figure 4.31: Measured and simulated of radiation patterns in state of all LDRs are on at (a) 3.6 GHz (b) 3.9 GHz (c) 4.9GHz, note: the red curve represents the simulate results and the black curve is a measured.

4.9 SOLAR CELL HARVESTING

This section focuses on study the solar cell properties and solar energy harvesting.

4.9.1 Properties

This work uses the solar cell that has some features such as [121]:

a. High rate of conversion.
b. High output efficiency.
c. It could be Work weak light effect.
d. Working voltage (6V)
e. (1W) as output power
f. Working current about (0-200 mA)

4.9.2 Solar Energy Harvesting

Antenna-array was integrated with a solar panel and introduced to the test. As the result, before and after integrated the solar PV panel, measured (I-V) characteristics are displayed in figure (4.32) [98]. (I-V) characteristics are not affected before and after integrated solar panel, due to a solar panel are placed properly (perpendicular) on the antenna-array.

After install the panel on the proposed antenna array, the (I-V) characteristics of solar PV panel are measured. figure (4.32) showed (I-V) characteristics after antenna integration, where the solar energy is defined as (photo-current) and (photo-voltage) axis at different light intensity curves by setting the value from ($500W/m^2$ to $1000W/m^2$) as clarified in figure (7.5).

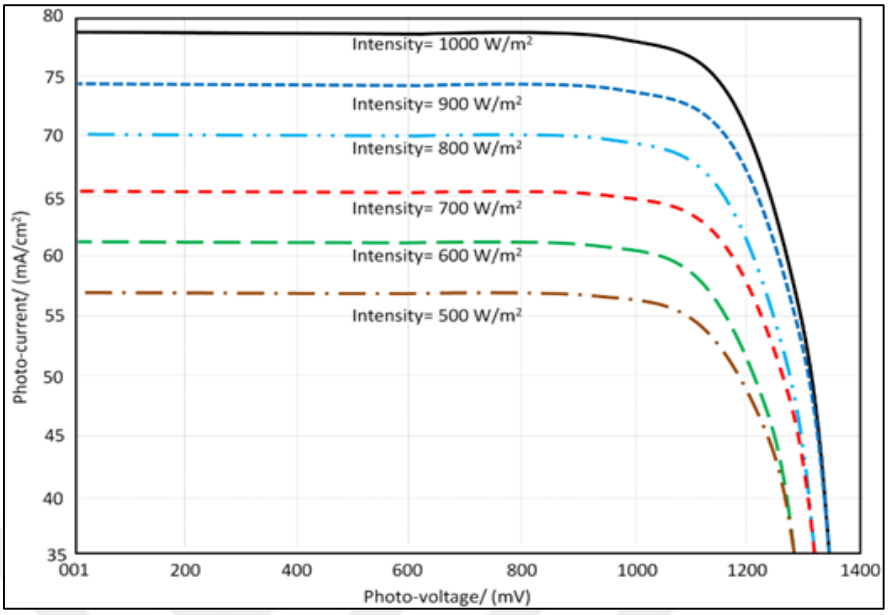

Figure 4.32: Solar PV panel performance after mounted on suggested array structure.

4.10 RECTENNA-ARRAY STRUCTRE

The proposed work is extended to evaluate the ability of the proposed antenna array of energy harvesting. Therefore, the author applied an experimental technique to collect the RF energy from the rounding environments. In this work, the antenna array is connected through a 50Ω input port with a commercial RF rectifier. As clarified in figure (4.33), the proposed system is projected by applying RF signal away from the proposed antenna to cover the frequency bands from 0.3GHz up to 6GHz. The proposed antenna located in front of the transmitter antenna and connected to the commercial module RFD102A as an RF rectifier. The energy is changed from -20dBm to 20dBm to monitor the output voltage from the used rectifier terminals. The collected voltage is obtained in DC form output. The rest of the proposed systems is explained as following:

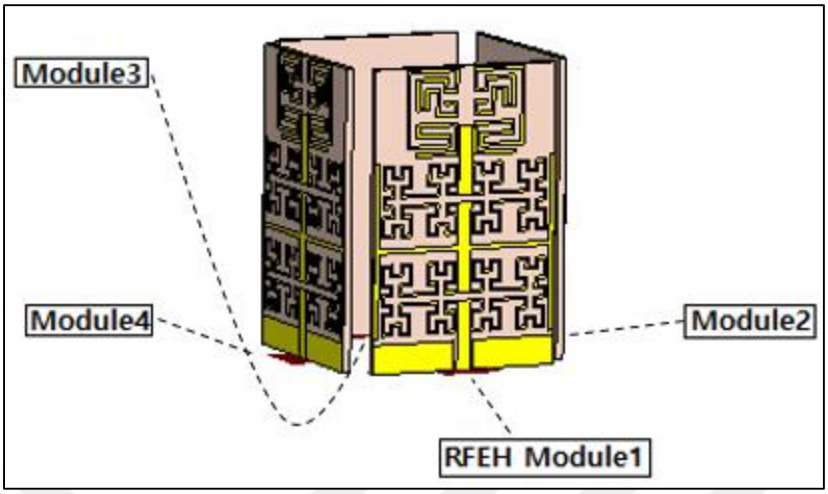

Figure 4.33: Rectenna array structure (antenna+RFEH module).

4.11 PROJECT RFEH MODULE (RFD102A)

In this work a (RFD102A) module is proposed for RFEH, where this compact module is considered an excellent device for convert the alternating wireless power to constant DC- voltage. It can operate on wide-range frequency; it operates during (60Hz to 6GHz) band. When it connects to antenna, it can get the power from wireless sources and can be utilized as sensor to low-power signals. It structured of dimension (5mm x 7mm x 1.8mm) [87].

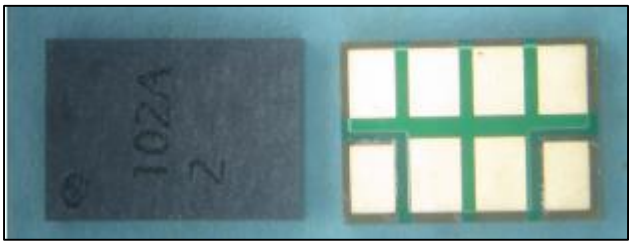

Figure 4.34: RFD102A-RFEH module.

4.11.1 Electrical Properties

This section lists the electrical properties of (RFD102A) that used to RF energy harvesting system.

a. Output voltage

As listed in table (7.1), the proposed module provides an output voltage within the range of 0.4V to 34V in maximum. Such variation is relative to the input power variation. Therefore, these values could be much greater than the output voltage when is connected to the practical wireless system as will be seen later.

Table 4.7: Output voltage of RFD102A module.

-13 dBm	0.4V
0 dBm	2.9V
10 dBm	10.4V
20 dBm	30V
30 dBm	34V

b. Range of operating frequency

The range of operating frequencies is between (60 Hz to 6GHz).

c. Modula pins

It contains eight Pins, Pin (1) is acts Dc output voltage , Pin (4) is the RF Input source and Pins (2,3,5,6,7,8) are represented the Ground as be clarified in figure (4.35) and (4.36), The module dimensions of (5mm x 7mm x 1.8mm) .

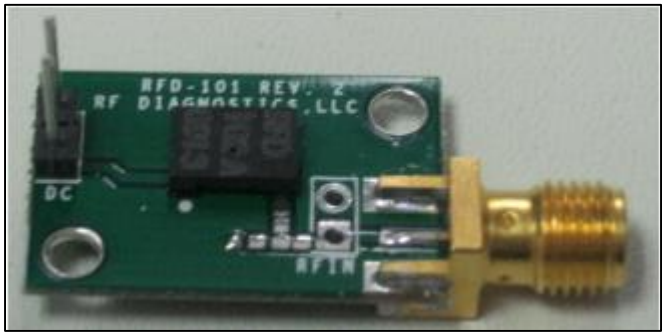

Figure 4.35: RFD102A-RFEH board.

The module board connects with match impedance placed on (RFIN) and optional (pin) header to connect antenna by hole antenna.

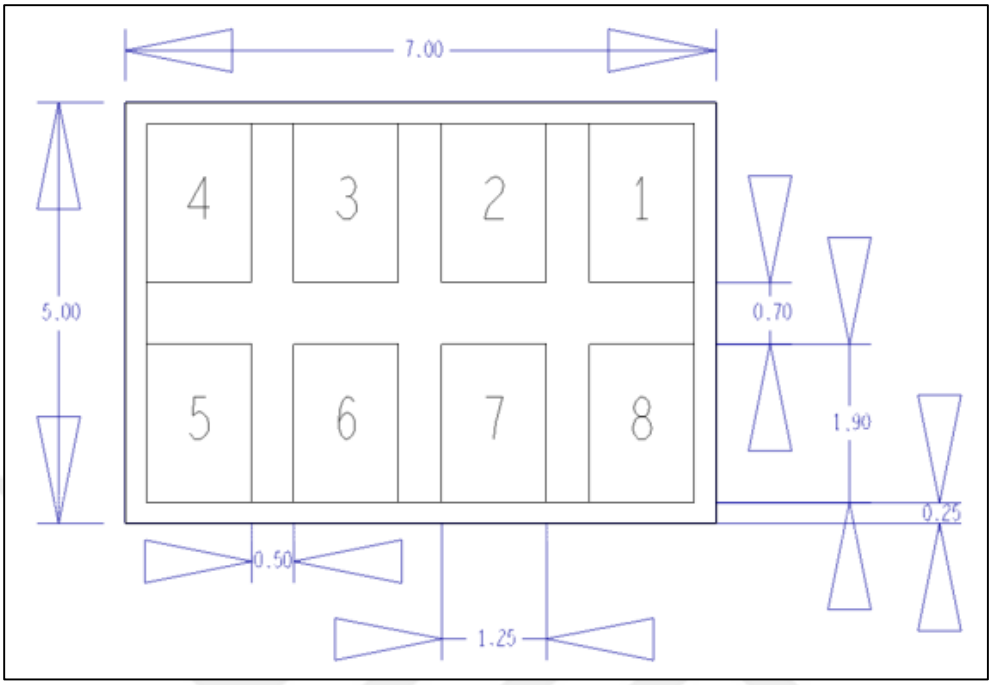

Figure 4.36: Top view of RFD102A module.

d. Maximum ratings and output voltage protection

RFD102A has some feature as be listed below:

a. ESD protection to (8 kV) pulse protection of RF input-line
b. +, -10V peak voltage of RF input-line.
c. +33dBm as max RF input power on RF input-pin.
d. It can use an external zener diode with module to avert the device failure.
e. -0.5V, +40V max DC output-pin.
f. 18mA max output-current.
g. Module may be partial or permanent damage when exceeding above limits.

The load value is (1-10 kohm) on DC output for transfer maximum efficiency power. Some input impedance tuning need certain frequency to design working. Module able to produce (18mA) as maximum DC current in (50ohm) load under stressed condition. Better design offer between (1-10mA) for energy harvesting system. S-parameters of (RFD102A-TB) module are available on different input powers from (-20dBm to +20dBm). Matching is required to realize the best results; the user needs to choose between matching circuit to get better sensitivity within low input power

and matching for ameliorate power transfer within high input powers due to it is a nonlinear device. The matching must be achieved experimentally to locate the best configuration [87]. In Table (4.8), the collected output DC voltage values are listed respect to input power changing. These values are found to be vary with input power variation; it can be clarified in figure (7.10).

Table 4.8: Measured of DC output voltage of RFD102A module.

-13 dBm	0.4V
0 dBm	2.9V
10 dBm	10.4V
20 dBm	30V
30 dBm	34V

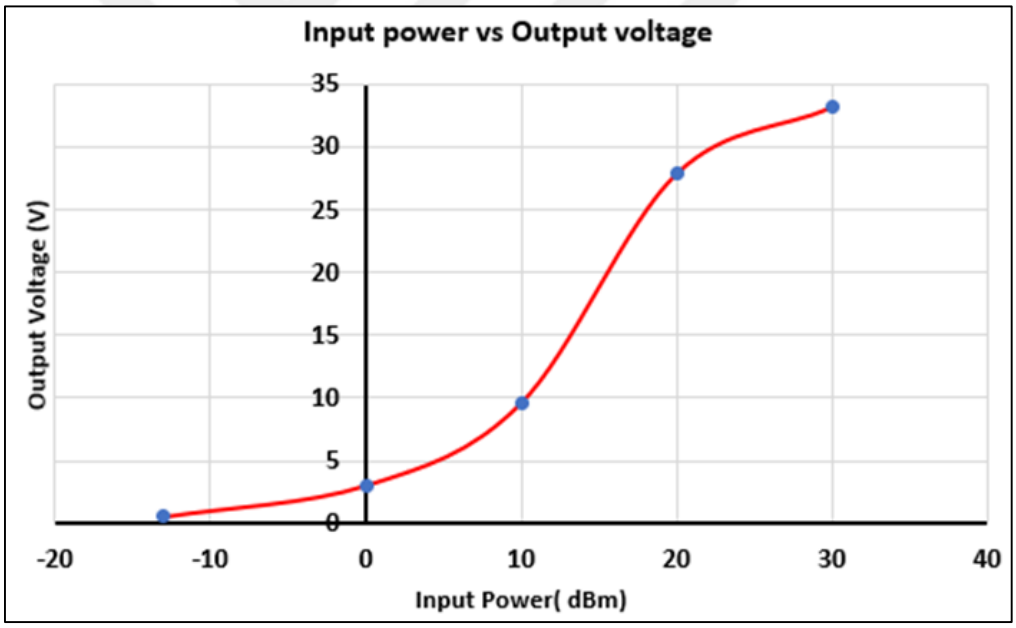

Figure 4.37: Input power vs output voltage of RFD102A.

4.12 PROCEDURE OF INTEGRATED SYSTEM STRUCTURE

In this section, we described the final structure design, this integrated system structured by integrated sub-6 GHz microstrip antenna array with solar cell and Radio Frequency Energy Harvesting system. Where the solar PV panel would be located as perpendicular (vertical) to array axis (as separated part) to avoid shadowing effect of rectenna array and to allow about (100%) of sunlight to arrive directly to solar (PV) cell without obstacles and to avoid the negative

effect of solar (PV) cell on antenna radiation characteristics due to it material nature if it located in parallel as part of antenna array. This integrated system has ability to power generation for rectenna array ,power is represents the collection of (RFEH) low power and good amount of power that produced by solar (PV) cell as well as is supporting a good radiation performance, gain and efficiency with low cross polarization levels ,where it realized balance between electromagnetic radiation and the power generated.

The final structure of this work is completed by five steps:

a. First step, design single antenna element as be shown in chapter six.
b. Second step, design 3D cubic antenna array as be clarified in chapter six.
c. Third step, integrated antenna array with solar PV cell as be shown in chapter seven.
d. Four step, integrated antenna array with RFEH system as be shown in chapter seven.
e. Finally, integrated the antenna array with solar cell and RFEH system as be shown in figure (4.38) (e).

All these steps are done experimentally in Al-Ma'moon University College, engineering labs as be shown in figure (4.38).

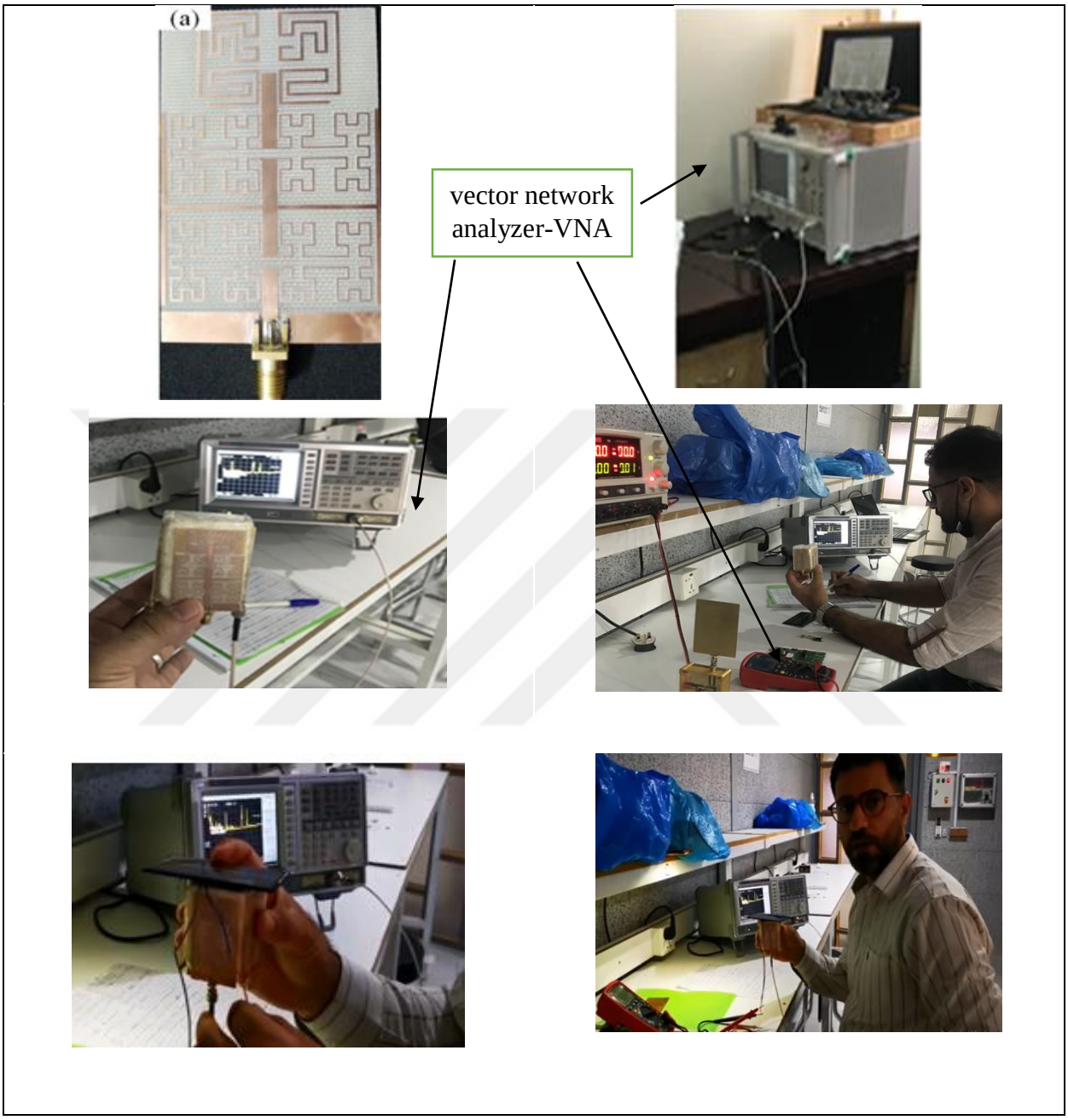

Figure 4.38: Steps of measurement results of proposed work (a to e); (a) single antenna element (b) 3D antenna array (c) integrated antenna array with solar PV cell (d) integrated antenna array with RFEH system (e) self-powered system (integrated the antenna array with solar cell and RFEH system).

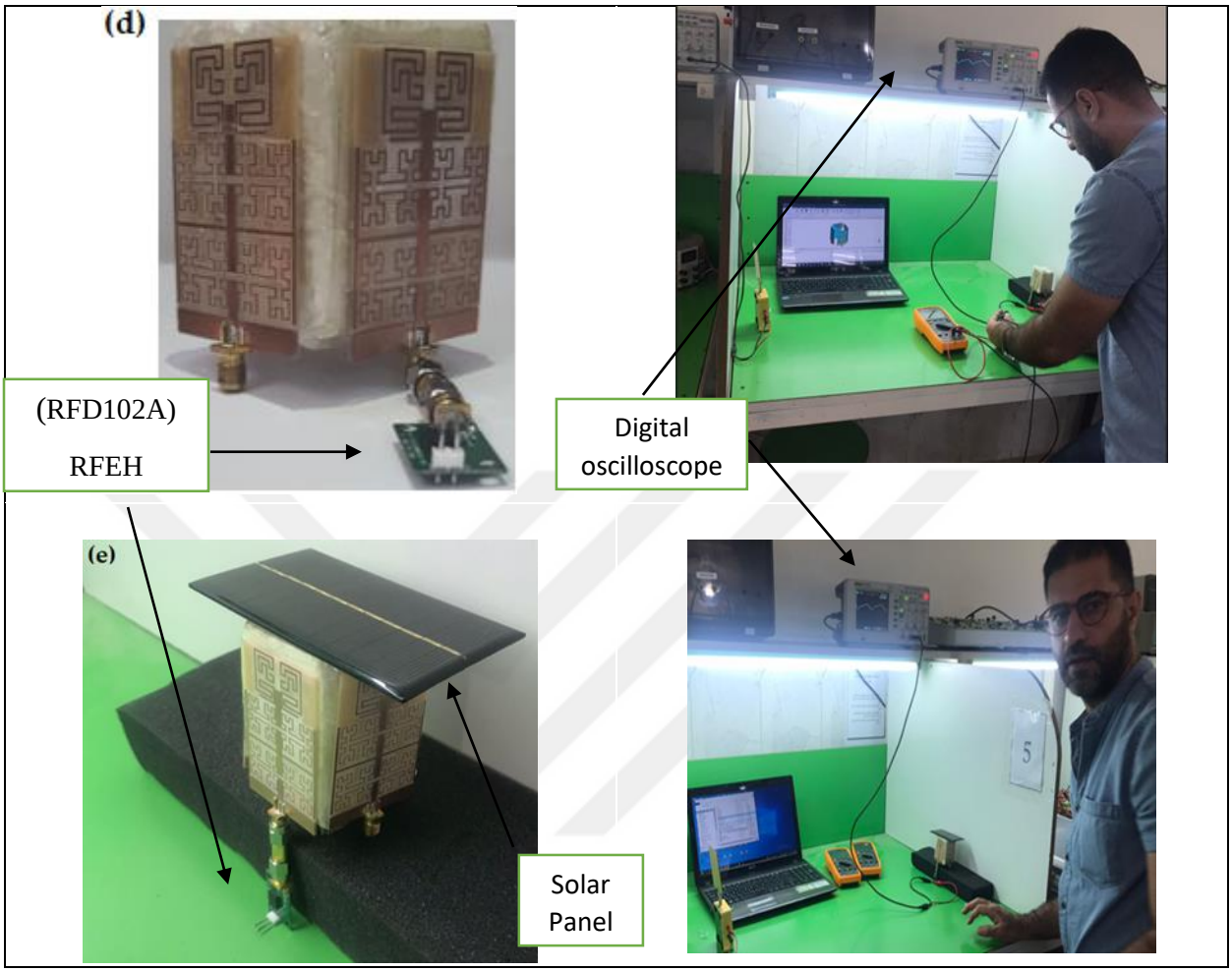

Figure 4.38: Steps of measurement results of proposed work (a to e); (a) single antenna element (b) 3D antenna array (c) integrated antenna array with solar PV cell (d) integrated antenna array with RFEH system (e) self-powered system (integrated the antenna array with solar cell and RFEH system) 'Figures Continued'

4.13 SUMMARY

In this chapter we could be focused on frequency and radiation patterns of a reconfigurable antenna for 5G applications. Antenna array based (MIMO) system of a reconfigurable antenna which is proposed, designed, fabricated and measured in this research. The antenna structure is very suitable for 5G network and modern wireless systems. This structure is proposed for 5G reconfigurable (MIMO) antenna array. However, the technique has been utilized to realize radiation pattern configuration by used (LDRs) and varactor diodes in different resonant frequencies for sub-6 GHz 5G. In conclusion, in this chapter we found our suggested antenna operates at 3.6GHz and 4.9 GHz

when all LDR are ON. Where, the antenna is providing gain of (2.2) at 3.6 GHz and (4) at 4.9 GHz. And When LDRs are OFF the antenna produced gain of (4.3) at 3.9GHz and (4.2) at 4.9GHz as the operating frequencies. Therefore, such antenna is suitable for short and medium range of 5G modern applications. Finally, we are found the (MIMO) antenna operates in range of sub-6GHz at resonant frequencies of (3.6GHz, 3.9GHz and 4.9GHz).

Next, we could be focused on two scenarios for build self-powered system, first scenario, introduced integrated the antenna array with solar PV cell to generate efficient power for antenna array operating and studied the effect of solar panel on antenna parameters in term of (S- parameter , gain and radiation pattern). Second scenario, introduced the integrate antenna array with RFEH system (RFD102A module) to generate amount of power for antenna array operating. In conclusion, the final proposed integrated system is very suitable for 5G network and modern wireless systems where it can provide the efficient amount of power to antenna array by collects the power that generated by solar panel and RFEH system**.**

5. CHAPTER FIVE

5.1 CONCLUSION

This thesis proposed novel antennas for modern applications including 5G communication networks at sub-6GHz frequency bands. The proposed work is oriented to the following sections: In the first section, an antenna configuration is suggested to design reconfigurable antenna in terms of radiation pattern and frequency bandwidth for 5G applications. Reconfiguration process is applied utilizing two varactor diodes to steer the antenna radiation pattern to desired direction. However, the antenna frequency reconfiguration is achieved utilizing two LDRs to control the antenna bands. We found that suggested antenna provides an excellent matching on frequency bands of 3.6, 3.9 GHz and 4.9 GHz.

This work is extended to design novel antenna array based on a 3D structure with a steerable radiation pattern for 5G communication networks. Therefore, a novel technique is invoked based on optical switches by using LDR switches to control the antenna beam direction. The proposed antenna system is introduced as a MIMO array with insignificant mutual coupling of a cubical geometry. The suggested array is structured from four antennas based on CRLH and T-stub to keep low coupling effects between adjacent antennas. Therefore, it is found the greatest coupling not more than -20dB during operating frequency band. The proposed antenna radiation pattern is controlled with two LDRs to be changed from $\pm 30^{o}$, $\pm 40^{o}$, and $\pm 45^{o}$ at 3.6GHz, 3.9GHz, and 4.9GHz, respectively. The antenna gain is found be moderate with the range of 3.2dBi to 4.2dBi. The antenna provides low correlation factor due to the high radiation diversity which is achieved from the CRLH and open T-stub introductions.

Finally, the suggested antenna array is integrated with solar panel and RFEH system. Such integration is employed to realize self-powered node, the solar panel would be located perpendicular to the antenna array axis to avoid it effects on array electromagnetic radiation. Where this integrated system achieves a balance between electromagnetic radiation and power generation. The antenna array is designed and fabricated, the simulation is done by using CST software, the energy harvesting system circuits is designed using Agilent Advanced Design System 2020 (ADS 2020) software and it is found that the experimental results of fabrication are agree very well with those obtained from CST MWS.

5.2 FUTURE WORK

This work is conducted to a design of 3D antenna array-based MIMO networks of self-powered communication systems. The proposed antenna systems can be extended in the future to the following aspects:

a. The channel performance ibn terms of bit error rate and channel capacity can be extended for this work to be calculated in the future to characterize the transmitter and receiver in the form of a certain modulation process.
b. The proposed work can be extended to cubic sat technology by collecting the solar energy from the space and converted to microwave energy to be transmitted to a ground station.
c. The proposed work is introduced to Moore fractal geometry and can conducted to consider more different fractal geometries to increase the antenna bandwidth and systems performance.
d. The use other configuration arrays based on 3D structures can be used for such design to realize an excellent antenna array performance and characterizations.
e. The use of a transmission network between the antenna elements can be an excellent option to realize a single feed technology to the antenna array.
f. The use of direct antenna modulation and coding process could a further step to develop smart antenna technology for modern wireless communication networks.

.

REFERENCES

[1] M. Yerlikaya , S. S. Gültekin and D. Uzer b "A novel design of a compact wideband patch antenna for sub-6 GHz fifth-generation mobile systems," Int. Adv. Res. Eng. J., vol. 04, no. 02, pp. 129–133, 2020, doi: 10.35860/iarej.688973.

[2] S. Kumar , A. S. Dixit , R. R. Malekar , H. D. Raut and L. K. Shevada, "Fifth Generation Antennas: A Comprehensive Review of Design and Performance Enhancement Techniques", Vol.4,IEEE Access.

[3] P. Kumar , T. Ali (Senior Member, IEEE), and M. M. Manohara Pai (Senior Member, IEEE) "Electromagnetic Metamaterials: A New Paradigm of Antenna Design" , Digital Object Identifier 10.1109/ACCESS.2021.3053100,vol.9,IEEE Access.

[4] P. S Manage , U. Naik , S. Nargundkar , V. Rayar "A Survey on applications of Metamaterials in Antenna Design," Proceedings of the Third International Conference on Smart Systems and Inventive Technology (ICSSIT 2020) IEEE Xplore Part Number: CFP20P17-ART; ISBN: 978-1-7281-5821-1.

[5] Deepa Pattar, Preeti Dongaokar, "Design of Metamaterial Based Patch Antenna for Gain Enhancement" IEEE International Conference for Innovation in Technology (INOCON) Bengaluru, India. Nov 6-8, 2020.

[6] Z. Al-dulaimi, T., A. Elwi ,D. C. Atilla, C.Aydin "Design of Fractal based Monopole Antenna Array with Ultra-Mutual Coupling Reduction for MIMO Applications", 978-1-5386-7132-0/18, IEEE, 2018.

[7] Praveena A, V A Sankar Ponnapalli ," A Review on Design Aspects of Fractal Antenna Arrays", International Conference on Computer Communication and Informatics (ICCCI -2019), Jan. 23 – 25, 2019, Coimbatore, INDIA.

[8] R. Verma, S. Kumar," Design and Analysis of Fractal Geometry Loaded Microstrip Patch Antenna" 2020 IEEE 5th International Conference on Computing Communication and Automation (ICCCA) Galgotias University, Greater Noida, UP, India. Oct 30-31, 2020.

[9] H. Dildar , F. Althobiani and I. Ahmad et al, "Design and Experimental Analysis of Multiband Frequency Reconfigurable Antenna for 5G and Sub-6 GHz Wireless Communication", Micromachines 2021, 12, 32. https://doi.org/10.3390/mi12010032.

[10] Nimisha Sharma, Asmita Rajawat, Sindhu Hak Gupta, “Design and Performance Analysis of Reconfigurable Antenna in WBAN Applications”, Proceedings of the International Conference on Intelligent Computing and Control Systems (ICICCS 2020) IEEE Xplore Part Number:CFP20K74-ART; ISBN: 978-1-7281-4876-2.

[11] B. Xi , X. Liang et al, “Optical Transparent Antenna Array Integrated With Solar Cell” , IEEE ANTENNAS AND WIRELESS PROPAGATION LETTERS, VOL. 19, NO. 3, MARCH 2020.

[12] O. R. Alobaidi, Md. Akhtaruzzaman, V. S., N.Amin, “Koch Fractal Loop Circular Polarization (CP) Antenna Integrated with Solar Cells”, Proceeding of the 2019 6th International Conference on Space Science and Communication (IconSpace), 28-30 July 2019, Johor Bahru, Malaysia1.

[13] SYMON K. Podilchak, David Comite, “Solar-Panel Integrated Circularly Polarized Meshed Patch for CubeSats and Other Small Satellites”, IEEE Access, DOI: 10.1109/ACCESS.2019.2928993, 2019.

[14] Eduardo Vicente Valdés Cambero, Humberto Pereira da Paz ,“A 2.4 GHz Rectenna based on a Solar Cell Antenna Array”, IEEE ANTENNAS AND WIRELESS PROPAGATION LETTERS, 2019.

[15] Q. H. Dao, T. J. Cherogony, B. Geck,“ Optically Transparent and Circularly Polarized Patch Antenna for K-Band Applications”, GeMiC , IMATech e.V. Ratingen, Bochum, Germany.

[16] T. A. Elwi, “A Further Realization of a Flexible Metamaterial-Based Antenna on Nickel Oxide Polymerized Palm Fiber Substrates for RF Energy Harvesting”, Wireless Personal Communications, Volume 10, no. 12, pp.1-15, August 2020.

[17] T. A. Elwi, D. A. Jassim and H. H. Mohammed, “Novel miniaturized folded UWB microstrip antenna-based metamaterial for RF energy harvesting,” International Journal of Communication Systems, Volume 1, issue 2, January 2020.

[18] S. K. Divakaran , D. D. Krishna , Nasimuddin, “RF energy harvesting systems: An overview and design issues”, int. journal RF and Microwave Computer Aided Engneering 2019.

[19] H. Abbasizadeh, and A. Hejazi, et al, “High-Efficiency and Wide-Input Range RF Energy Harvester Using Multiple Rectenna and Adaptive Matching”, Energies, MDPI ,2020, 13, 1023; doi:10.3390/en13051023.

[20] Anand Trikolikar, Swapnil Lahudkar, “A Review on Design of Compact Rectenna for RF

[21] Energy Harvesting,” Proceedings of the International Conference on Electronics and Sustainable Communication Systems (ICESC 2020) IEEE Xplore Part Number: CFP20V66-ART; ISBN: 978-1-7281-4108-4.

[22] H. Nakano, “Low-profile Natural and Metamaterial Antennas: Analysis Methods and Applications”, handbook, John Wiley & Sons, 2016.

[23] R. Kumara,ManojKumarbJasgurpreet SinghChohanbSantoshKumarc, “ Overview on metamaterial: History, types and applications ,materials today”, Volume 56, Part 5, 2022, Pages 3016-3024.

[24] N. Engheta and R. W. Ziolkowski , “Metamaterials: physics and engineering explorations”, Third Edition,3rd Ed., John Wiley & Sons, 2006.

[25] T. A. Elwi, “A Further Realization of a Flexible Metamaterial-Based Antenna on Nickel Oxide Polymerized Palm Fiber Substrates for RF Energy Harvesting”, Wireless Personal Communications, Volume 10, no. 12, pp.1-15, August 2020.

[26] K. Sun, A. Fan et al, “ An overview of metamaterials and their achievements in wireless power transfer”, Journal of Material Chemistry C ,2018.

[27] D. Ali, T. A. Elwi, S. Ozbay, “Metamaterial-based Printed Circuit Antenna for Biomedical Applications”, European Journal of Science and Technology, (26), 12-15, (2021).

[28] Y. Alnaiemy, T. A. Elwi, L. Nagy, “Mutual Coupling Reduction in Patch Antenna Array Based on EBG Structure for MIMO Applications”, Periodica Polytechnica Electrical Engineering and Computer Science, Volume 1, number 4, pp.1-11, September 2019.

[29] IEEE standard definitions of terms for antennas, IEEE Transactions on Antennas and Propagation (Volume: 17, Issue: 3, May 1969), https://doi.org/10.1109/TAP.1969.1139442

[30] C. Balanis, “Antenna Theory Analysis and Design”, Third Edition, 3rd Ed. 2005.

[31] Y.Huang and K. Boyle , “ ANTENNAS FROM THEORY TO PRACTICE”, First Edition,1st Ed.,2008 by wiley and sons.

[32] D. M. POZAR "Microwave Engineering ", Fourth Edition,4TH Ed.,2012.

[33] S. T. Al-hadeethi, T. A. Elwi , A. A. Ibrahim and H. H. Al-khaylani, "A New Meta Material Based Monopole Antenna For 5G Mobile Communication Networks" , Eurasiaweb International Conference, Baghdad, Iraq, 20th – 21st February, 2022.

[34] S. M. Obaid, T. A. Elwi, and M. Ilyas, "Fractal Minkowski-Shaped Resonator for Noninvasive Biomedical Measurements Blood Glucose Test," Progress in Electromagnetics Research c, Volume 107, pp. 143-156, December 2020..

[35] M. Ikram, N. Nguyen-trong and A. M. Abbosh, "Common-Aperture Sub-6 GHz and Millimeter-Wave 5G Antenna System", IEEE Access,2020, Digital Object Identifier 10.1109/ACCESS.2020.3034887.

[36] A. Gupt and R. Jha, "A Survey of 5G Network: Architecture and Emerging Technologies", DOI: 10.1109/ACCESS.2015.2461602, IEEE Access 2020.

[37] T. A. Elwi, "Remotely Controlled Reconfigurable Antenna for Modern Applications", Microwave and optical letters, Volume 6, issue 1, pp. 1-19, April 2020.

[38] H. H. Al-khaylani, T. A. Elwi and A. A. Ibrahim, "A Novel Miniaturized Reconfigurable Microstrip Antenna Based Printed Metamaterial Circuitries for 5G Applications" , Progress In Electromagnetics Research C, Vol. 120, 1–10, 2022.

[39] K. Li, L. Li , Cheng Zhu, and C. Liang, "A New Polarization Reconfigurable Microstrip Antenna Based on Complementary Split Ring Resonator", Progress In Electromagnetics Research Letters, Vol. 46, 119–125, 2014.

[40] A. Ghaffar1, X. Li et al , "Flexible Frequency and Radiation Pattern Reconfigurable Antenna for Multi-band Applications", 4th Australian Microwave Symposium, Sydney, Australia, 13 – 14 February 2020.

[41] I. Ahmad and W. Rehman Khan et al , "A Pentaband Compound Reconfigurable Antenna for 5G and Multi-Standard Sub-6GHz Wireless Applications", Electronics 2021, 10, 2526. https://doi.org/10.3390/electronics10202526.

[42] Y. TAWK , J. Costantine , F. Makhlouf, at el , "Wirelessly Automated Reconfigurable Antenna With Directional Selectivity" , IEEE Access Digital Object Identifier 10.1109/ACCESS.2019.2650203. 2019.

[43] M. Ahmad,| S. Kabeer , et al , "Compact single-varactor diode frequency-reconfigurable microstrip patch antenna" , IET Microwaves, Antennas & Propagation, DOI: 10.1049/mia2.12119 ,2019.

[44] H. H. Alkhaylani, T. A. Elwi, A. A. Ibrahim, “Optical remote-controlled miniaturized 3D reconfigurable acrlh-printed MIMO antenna array for 5G applications”, Microwave and Optical Letters,2022, DOI:10.1002/mop.33504.

[45] H. Abu Bakar, R. Abd Rahim, “ Liquid-Based Reconfigurable Antenna Technology: Recent Developments, Challenges and Future”, Sensors 2021, 21, 827. https://doi.org/10.3390/s21030827 .

[46] R. Mishra, “An Overview of Microstrip Antenna”, HCTL Open International Journal of Technology Innovations and Research (IJTIR),2018.

[47] J. R. JAMES, P. S. HALL and C. WOOD, “Microstrip Antenna Theory and Design”, Twelfth Edition,12th Ed., IEE Electromagnetic Waves Series 12.

[48] A. S. Kamel, “Design and implementation of an antenna for 5G application”, master thesis College of Information Engineering at Al-Nahrain University, 2021.

[49] K. Jain and K. Gupta, “Different Substrates Use in Microstrip Patch Antenna-A Survey”, International Journal of Science and Research (IJSR), p:1802-1803,2018.

[50] A. A. Qureshi and M. U. Afzal, “Performance Analysis of FR-4 Substrate for High Frequency Microstrip Antennas”, CJMW2011 Proceeding.

[51] B. Taha and T. AlSharabati, “Performance Comparison between the FR4 Substrate and the Rogers Kappa-438 Substrate for Microstrip Patch Antennas”, International Journal of Computer Science and Mobile Computing, Vol.9 Issue.2, February- 2020, pg. 1-12.

[52] C. P. WEN, “Coplanar Waveguide: A Surface Strip Transmission Line Suitable for Nonreciprocal Gyromagnetic Device Applications”, IEEE Transactions on Microwave Theory and Techniques, VOL. MTT-17, NO. 12, December 11969.

[53] Z. AL-Dulaimi and T.A. Elwi et al, “Design of Fractal based Monopole Antenna Array with Ultra-Mutual Coupling Reduction for MIMO Applications”, IEEE Xplore ,978-1-5386-7132-0/18,2018.

[54] B. S. Dhaliwal, A. Kaur, S. Pattnaik, “Optimization of Hybrid Fractal Antenna Using Curve Fitting and GA Approach for RF Energy Harvesting Application”, IEEE Xplore ,978-1-7281-2577-0/19,2019.

[55] A. I. Imran, T. A. Elwi, and Ali J. Salim, "On the Distortion less of UWB Wearable Hilbert-Shaped Metamaterial Antenna for Low Energy Applications," Progress In Electromagnetics Research M, Volume 101, pp. 219-239, March 2021.

[56] T. A. Elwi, Z. A. AL-Hussain, O. Tawfeeq, “Hilbert Metamaterial Printed Antenna based on Organic Substrates for Energy Harvesting”, IET Microwaves, Antennas & Propagation, volume 12, number 4, pp.1-8, June 2019.

[57] S. Akkole and N. Vasudevan, “Compact Multiband Microstrip Fractal Antenna Design for Wireless Applications –An Overview”, Fourth International Conference on Electronics, Communication and Aerospace Technology (ICECA-2020) IEEE Xplore Part Number: CFP20J88-ART; ISBN: 978-1-7281-6387-1.

[58] R. K. Abdulsattar, T. A. Elwi, Z. A. Abdul Hassain, “A New Microwave Sensor Based on the Moore Fractal Structure to Detect Water Content in Crude Oil”, MDPI Sensors, Vol. 21, pp. 7143.

[59] R Rashmitha, N Niran et al, “Microstrip Patch Antenna Design for Fixed Mobile and Satellite 5G Communications”, Third International Conference on Computing and Network Communications ,2020.

[60] A. J. Lozada and S. Donglin, “MICROSTRIP ANTENNA FOR SATELLITE COMMUNICATIONS”, IEEE, 2008, 978-1-4244-2193-0/08,

[61] S. S. Kashyap and V. Dwivedi, “Stacked Swastika Shape Microstrip Patch Antenna for Terahertz Applications”, IEEE©2014 , DOI:978-1-4799-6986-9/14.

[62] M. J. Hakeem and M. Nahas , “Improving the Performance of a Microstrip Antenna by Adding a Slot into Different Patch Designs”, Engineering, Technology & Applied Science Research,2021.

[63] Y. Alnaiemy, T. A. Elwi, L. Nagy, and T. Zwick, “A systematic analysis and design of a high gain microstrip antenna based on a single EBG layer,” Infocommunications Journal, vol. 10, no. 4, pp. 22–30, 2018.

[64] Y. Alnaiemy, T. A. Elwi, and N. Lajos, “Enhancing the microstrip antenna gain using a novel EBG lens based on a single layer,” in 2018 11th International Symposium on Communication Systems, Networks & Digital Signal Processing (CSNDSP). IEEE, 2018, pp. 1–4.

[65] Y. Alnaiemy, T. A. Elwi, L. Nagy, “Mutual Coupling Reduction in Patch Antenna Array Based on EBG Structure for MIMO Applications”, Periodica Polytechnica Electrical Engineering and Computer Science, Volume 1, number 4, pp.1-11, September 2019.

[66] M. A. Jawad, M. A. Elwi, E. Y. Salih, T. A. Elwi, and Zulkifly Abbas, “Monitoring the Dielectric Properties and Propagation Conditions of Mortar for Modern Wireless Mobile Networks,” Progress in Electromagnetic Research Letters, Volume 89, pp. 91-97, January 2020.

[67] S. N. Mahmood and A. J. Ishak , “Full Ground Ultra-Wideband Wearable Textile Antenna for Breast Cancer and Wireless Body Area Network Applications”, Micromachines,12,322,2021.

[68] M. B. Kakhki, M. Mantash and T.A. Denidni, “Gain Enhancement of Colinear Antenna-Array Using a Frequency Selective Surface”, IEEE©2018, 978-1-5386-1338-2/18.

[69] Z. Al-Dulaimi, T. A. Elwi, and D. C. Atilla, “Design of a meander line monopole antenna array based hilbert-shaped reject band structure for MIMO applications,” IETE Journal of Research, pp. 1–10, 2020.

[70] https://amiestudycircle.com/free-samples/amie/chapters/arrays.pdf.

[71] Y. Al Naiemy, T. A. Elwi, and L. Nagy, “An end fire printed monopole antenna based on electromagnetic band gap structure,” Automatika, vol. 61, no. 3, pp. 482–495, 2020.

[72] Y. Cho, J. Kim et al , “MIMO-OFDM Communication with Matlab”, Handbook, wiely.

[73] A.Borja , J. Kelly and P. Xiao, “technique for MIMO antenna design with flexible element number and pattern diversity”, IEEE Acess,2019.

[74] I. Watanabe and K. Nishimori et al , “Effectiveness of the virtual massive MIMO in 5G with OFDM”, Proceedings of ISAP2020, Osaka, Japan, IEEE Xplore,2020.

[75] A. Abdulmjeed, T. A. Elwi, and S. Kurnaz, “Metamaterial Vivaldi Printed Circuit Antenna Based Solar Panel for Self-Powered Wireless Systems" , Progress In Electromagnetics Research M, Vol. 102, 181-192, 2021.

[76] A. Sokolov ,D. Galayko and M. P. Kennedy, “Near-Limit Kinetic Energy Harvesting From Arbitrary Acceleration Waveforms: Feasibility Study by the Example of Human Motion”, IEEE Access, Digital Object Identifier 10.1109/ACCESS.2020.3042388, 2020.

[77] M. H. Alsharif , S. Kim and N. Kuruoglu,“Energy Harvesting Techniques for Wireless Sensor Networks/Radio-Frequency Identification: A Review”, Symmetry,MDPI,2019.

[78] S. Muhammad and J. J. Tiang, “Harvesting Systems for RF Energy: Trends, Challenges, Techniques, and Tradeoffs”, Electronics MDPI, 2022.

[79] L. Ramalingam and S. Mariappan et al, “The Advancement of Radio Frequency Energy Harvesters (RFEHs) as a Revolutionary Approach for Solving Energy Crisis in Wireless Communication Devices: A Review”, Digital Object Identifier 10.1109/ACCESS.2021.3098895, IEEE Access, 2021.

[80] S. Y. Mansour, “Design of Multi-Band RF Energy Harvesting System”, Master thesis, March 2018.

[81] I. K. Ivanov, "Radio frequency energy harvesting for autonomous systems", University of Bedfordshire, PhD. Thesis, April 2018.

[82] R. L. Boylested and L. Nashelsky “Electronic Devices and Circuit Theory”,book hand Ninth Edition.

[83] W. F. Waller , "Rectifier Circuit Electronic Engineering Series", Macmillan engineering evaluation,2017.

[84] U. Fulari and S. B. Lande et al, "Battery Life Improvement Technique for Electric Vehicle", Journal of Seybold Report , Vol. 15, ISSUE 7, 2020.

[85] Z. Chen, Q. Zhang , and Q. Liang, "Carbon-Coatings Improve Performance of Li-Ion Battery", Nanomaterials 2022, Vol:12, Issue: 36. https://doi.org/10.3390/nano12111936

[86] T. Yongguang, W. Jiang, X. Guoning et al,"Perovskite Solar Cells for Space Applications: Progress and Challenges", Advance Materials , 2006545 p:1-22, 2021.

[87] M. Amanath and R. Keshavarz et al, "A Review on Antenna Technologies for Ambient RF Energy Harvesting and Wireless Power Transfer: Designs, Challenges and Applications", IEEE Access , Digital Object Identifier 10.1109/ACCESS.2022.3149276, 2022.

[88] L. Manh , P. Bich et al, "A Concurrent Triple-band RF Energy Harvesting Circuit for IoT Sensor Networks", IEIE Transactions on Smart Processing and Computing, vol. 10, no. 2, April 2021.

[89] H. Fouad and H. Farouk , "Power Management of RF Energy Harvesting for Healthcare Communication System", International Journal of Scientific & Engineering Research Volume 8, Issue 3, March-2017.

[90] T. Soyata , L. Copeland and W. Heinzelman, "RF Energy Harvesting for Embedded Systems: A Survey of Tradeoffs and Methodology", IEEE circuits and systems magazine,2016.

[91] O. Blaise, A. D. Olujimi , "A Comparative Review of Emerging Wireless Technology", International Journal of Scientific Research in Computer Science, Engineering and Information Technology ISSN : 2456-3307 (www.ijsrcseit.com) doi : https://doi.org/10.32628/CSEIT206536 163 .

[92] R. Sivapriyan and D. Elangovan et al, "Recent Research Trends in Solar Photovoltaic System", 2020 5th International Conference on Devices, Circuits and Systems (ICDCS),IEEE Xplore.

[93] A. Luque and A. Hegedus, "Handbook of Photovoltaic Science and Engineering", Second Edition,2nd Ed., Wiley and sons 2003.

[94] L.A. Dobrzański and M. Szczęsna et al, "Electrical properties mono- and polycrystalline silicon solar cells", Journal of achievements in materials and manufacturing engineering ,Vol:59,Issue 2,2013.

[95] L.A. Dobrzański and A. Drygała et al, "Monocrystalline silicon solar cells applied in photovoltaic system", Journal of achievements in materials and manufacturing engineering, Vol:53, Issue 1,2012.

[96] I. Cappelli, A. Fort et al ,"Polycrystalline silicon photovoltaic harvesting for indoor IoT systems under red- far red artificial light", 2021 IEEE Sensors Applications Symposium (SAS), Sundsvall, Sweden, Doi:10.1109/SAS51076.2021.9530063.

[97] Elieser Tarigan, "Hybrid PV-T Solar Collector using Amorphous Type of Solar Cells for Solar Dryer", 2020 International Seminar on Intelligent Technology and Its Applications (ISITIA), 978-1-7281-7413-6/20/$31.00 IEEE Xplore 2020.

[98] https://energyeducation.ca/encyclopedia/Photovoltaic_cell

[99] P. Singh and V. TR et al, "P-V and I-V Characteristics of Solar Cell", Design Engineering conference paper June 2021.

[100] M. Drapalik and J. Schmid et al, "A Study of the Antenna Effect of Photovoltaic Modules ", International Conference on Renewable Energies and Power Quality (ICREPQ'10) Granada (Spain), 23rd to 25th March, 2010.

[101] Y. Chen , Y. Wu and C. Chung , "Solar-Powered Active Integrated Antennas Backed by a Transparent Reflect array for CubeSat Applications", Digital Object Identifier 10.1109/ACCESS.2020.3012133,IEEE Access,2020.

[102] Y. Chen, Y. Wu and C. Chung , "A Wireless Sensor Network Based Solar Powered Harvesting System for Aquaculture ", Journal of Information Sciences and Computing Technologies(JISCT),Vol:7 ,Issue:2,2018.

[103] A. Bagher, M. Vahid and M. Mohsen, "Types of Solar Cells and Application", American Journal of Optics and Photonics, Vol:3, Issue:5,p:94-113,2015.

[104] J. Zhao and R. Ghannam ,"Photovoltaic Power Harvesting Technologies in Biomedical Implantable Devices Considering the Optimal Location", IEEE Journal of Electromagnetics, RF and Microwaves in Medicine and Biology,2019.

[105] A. Govind, "Antenna Impedance Matching – Simplified ", White paper, Abracon LLC, www.abracon.com.

[106] M. R. Jena, G. P. Mishra," Fractal Geometry and Its Application to Antenna Designs", International Journal of Engineering and Advanced Technology (IJEAT),Vol:9,Issue:1,2019.

[107] A. A. Al-shaikhli, "Reconfigurable Miniaturized Microstrip Antenna Based Metamaterials for Portable Wireless Biomedical Applications", Master Thesis, ECE Dept., Altinbas University, Turkey,2022.

[108] H. H. Al-khaylani, T. A. Elwi , A. A. Ibrahim and S. T. Al-hadeethi, "Microstrip Antenna Design for sub-6 GHZ Fifth Generation (5G) Mobile Communication" , International Journal of Electrical, Electronics and Data Communication, Volume-10, Issue-3, Mar.-2022.

[109] P. Mishra and S. S. Pattnaik, "Metamaterial loaded fractal based interdigital capacitor antenna for communication systems," Progress In Electromagnetics Research, vol. 70, pp. 127–134, 2018.

[110] R. W. Ziolkowski and C.Cheng, " Lumped element models of double negative metamaterial-based transmission lines", RADIO SCIENCE, VOL. 39, RS2017, doi:10.1029/2003RS002995, 2004.

[111] Y. Chen, "Fractal Modeling and Fractal Dimension Description of Urban Morphology", MDPI, Entropy 2020, 22, 961; doi:10.3390/e22090961.

[112] N. Ferdous, G. C. Hock et al, " DESIGN OF A SMALL PATCH ANTENNA AT 3.5 GHZ FOR 5G APPLICATION", International Conference on Sustainable Energy and Green Technology 2018.

[113] A. Iqbal and U. Naeem et al, " Design, Fabrication and Measurement of a Compact, Frequency Reconfigurable, Modified T-shape Planar Antenna for Portable Applications", Journal of Electrical Engineering and Technology , May 2017.

[114] I. Ahmad and U. Habib et al, "Hexagonal shaped CPW Feed based Frequency Reconfigurable Antenna for WLAN and Sub-6 GHz 5G applications", IEEE Xplore,2020.

[115] Shakir Ullah and Sadiq Ullah et al, "Frequency Reconfigurable Antenna for Portable Wireless Applications", Journal of Computers, Materials & Continua, DOI:10.32604/cmc.2021.015549,2021.

[116] X. Tang and Y. Li et al, "Ultra-Wideband Patch Antenna for Sub-6 GHz 5G Communications", IEEE, 978-1-7281-5006-2 / 19 , 2019.

[117] A. Iqbal and U. Naeem et al," Sub-6 GHz Quad-Band Reconfigurable Antenna for 5G Cognitive Radio Applications ", Access Journal,Vol:36,Issue:8 , 2021.

[118] M. Li and X. Chen et al, "Mutual Coupling Reduction in Sub-6 GHz Antenna Array Using Defected Walls",020 International Conference on Microwave and Millimeter Wave Technology (ICMMT), IEEE,DOI: 10.1109/ICMMT49418.2020.9386361, 2020.

[119] H. S. Ahmed and T. A. Elwi, "On the design of a reject band filter for antennas mutual coupling reduction", International Journal of RF and Microwave Computer-Aided Engineering, volume 11, number 3, pp.1-11, April 2019.

[120] W. Yadum and N. Nakajima, "The correlation of diversity/MIMO antenna for portable terminals", Wireless Communications and Mobile Computing, https://onlinelibrary.wiley.com/doi/epdf/10.1002/wcm.510,2007.

[121] A. Iqbal and U. Naeem et al, " Sub-6 GHz Quad-Band Reconfigurable Antenna for 5G Cognitive Radio Applications ", Access Journal, Vol:36, Issue:8, 2021.

[122] H. H. Al-khaylani, T. A. Elwi, A. A. Ibrahim, "Optically Remote Controlled of Miniaturized 3D Reconfigurable CRLH Printed Self-Powered MIMO Antenna Array for 5G Applications", Micromachines, MDPI,2022.

[123] Computer Simulation Technology (CSTMW2020) [Online]. Available: www.cst.com.

[124] Advance Design System (ADS2020) [Online]. Available: www.ansoft.com.